Shale Gas Reservoirs of Utah:

Survey of an Unexploited Potential Energy Resource

Steven Schamel
GeoX Consulting Inc
Salt Lake City, UT

Prepared for the Utah Geological Survey

State of Utah Contract #051845

OPEN-FILE REPORT 461 September 2005
Utah Geological Survey
a division of
Utah Department of Natural Resources

Disclaimers

Table of Contents

Executive Summary

Given the very limited amount and scope of information in the literature relevant to Utah's black shales, the 'screening criteria' that could be applied in this project, in most instances, was limited to just (1) organic richness and maturity of the black shale, (2) thickness of the kerogen-rich interval, (3) likelihood of natural and induced fracturing, determined subjectively, and (4) potential barriers to hydraulic fracturing, or water-saturated zones, in adjacent strata. As a consequence, the assessments presented herein are subjective and should be considered preliminary, pending further data gathering and analysis.

This project has recognized five kerogen-rich shale units as having reasonable potential for commercial development as shale gas reservoirs. These are four members of the Mancos Shale in northeast Utah - the Prairie Canyon, the Juana Lopez, the Lower Blue Gate, and the Tununk. The fifth is the black shale facies within the Hermosa Group in southeast Utah.

The Prairie Canyon and Juana Lopez Members are both detached mudstone-siltstone-sandstone successions embedded within the Mancos Shale in northeast Utah. The Prairie Canyon Member is up to 1,200 ft thick, but the stratigraphically deeper Juana Lopez Member is less than 100 ft. Both are similar in lithology and basinal setting to the gas-productive Lewis Shale in the San Juan basin. As in the Lewis Shale, the lean, dominantly humic, kerogen is contained in the shale interlaminated with the siltstone-sandstone. The high quartz content is likely to result in a higher degree of natural fracturing than the enclosing claystone-mudstone rocks. Thus, they may respond well to hydraulic fracturing. Also the porosity of the sandstone interbeds averaging 5.4% can enhance gas storage. Both units extend beneath the southeast Uinta basin reaching depths sufficient for gas generation and retention from the gas-prone kerogen. Although not known to be producing natural gas at present, both units are worthy of testing for add-on gas, especially in wells that are programmed to target Lower Cretaceous or Jurassic objectives.

The Lower Blue Gate and Tropic-Tununk shales generally lack the abundant siltstone-sandstone interbeds that would promote natural and induced fracturing, but they do have zones of observed organic richness in excess of 2.0% that might prove to be 'sweet spots' for shale gas where the rocks are sufficiently buried beneath the southern Uinta basin and perhaps parts of the Wasatch Plateau.

The black shale facies in the Hermosa Group of the Paradox basin is enigmatic. These shales contain mixed type II-III kerogen that should favor gas generation, yet oil with associated gas dominate current production. They are relatively thin, just a few tens of feet thick on average, yet they are encased in excellent sealing rocks, salt and anhydrite. In the salt walls (anticlines) the shales are complexly deformed making them difficult to develop even with directional drilling methods, but where they are likely less deformed in the interdome areas (synclines) they are very deep. Yet in these deep areas one can expect peak gas generation. The shales are overpressured, which suggests generation currently or in the recent past. Prospects are good that shale gas reservoirs can be developed in the Paradox basin, but it may prove to be technically and economically challenging.

Introduction

General Statement

Shale gas reservoirs (Curtis, 2002) are organic-rich and self-sourcing, fine-grained rocks that owe their very low permeability to both very small grain-size and clay content. Many, but not all, are true clay shales and high-TOC hydrocarbon source rocks with high log resistivity values, gamma-ray (GR) intensity in the range 150-400 API units, and mean bulk density of about 2.50 g/cc. The high resistivities are attributed to the generation and retention of hydrocarbons within the shale. The high GR and low bulk density correlate with relatively high organic content. Organic-rich shales characteristically are storage sites for adsorbed gas. The organic matter in the shale may contain as much as 60 scf of natural gas per ton of rock. Methane and associated natural gas liquids are stored primarily within three sites: the shale matrix pore space, adsorbed on organic matter, and within the network of natural fractures, both micro- and macro-fractures. Where water saturations and ambient pressures are high, significant quantities of natural gas also may be dissolved in the formation water.

The generation of oil and/or natural gas in such very tight fine-grained rocks initally results in increased fluid pressures (Osborne and Swarbrick, 1997) leading to internal fracturing that in turn facilitates primary migration of the hydrocarbons (Capuano, 1993: Berg and Gangi, 1999). Eventually, at higher levels of thermal maturity or with low-temperature biogenic gas generation, the macro- and micro-fracture network so developed enhances the gas storage and deliverability of the kerogen-rich shales.

Well documented gas production comes from the Devonian shales of the Appalachian basin (Ryder and others, 1998; Milici and Ryder, 2004), the Devonian Antrum Shale of the Michigan basin (Martini and others, 1998), the Devonian New Albany Shale of the Illinois basin (Walter and others, 2000), Mississippian Woodford Shale of the Anadarko basin (Lee and Deming, 2002), and the Mississippian Barnett Shale in the Fort Worth (East Newark) basin (Kuuskraa and others, 1998; Bowker, 2002; Petzet, 2002). All of these Paleozoic shales are organic-rich. Consequently a large portion of the natural gas is stored within the organic matter. In contrast, the Cretaceous gas "shales" of the Rocky Mountain basins are organically lean (1-2% TOC) and much siltier. They are not true shales. The organic matter is the source of the natural gas, but most of it is stored within the low permeability rock matrix and natural fracture system. As with all other continuous-gas reservoirs, a well-developed natural fracture system appears to be essential for drainage of the gas from the rock matrix.

The Rocky Mountain region is suspected to contain most of the undiscovered unconventional gas resources of the Lower 48 (Fletcher, 2005). In recent years the gas production and transport infrastructure has grown in Utah (Isaacson, 2003) such that the time is right to examine closely the potential for commercial exploitation of that most unconventional type of unconventional gas resource, namely *shale gas*.

Project Objectives and Methods

This project has identified several shale reservoirs within Utah that have potential of producing commercial quantities of methane and associated natural gas liquids. This was accomplished by comparing the known sedimentologic and geochemical, and where possible petrophysical and/or rheologic, characteristics of candidate shales against established properties of actual producing shale gas reservoirs outside of Utah. When possible, this report describes the potential shale gas reservoirs in sufficient detail as to define specific possible natural gas plays. A set of recommendations lays out strategies for exploration and possible exploitation of this potentially new natural gas resource in Utah. The purpose of the study is to encourage industry to develop this energy resource to the fullest extend.

The project has advanced in three phases. The initial phase established a set of screening criteria for identifying potential shale gas reservoirs. This was done through a critical examination of the known characteristics of shales that are currently producing commercial quantities of methane and natural gas liquids. These criteria were then used to screen Phanerozoic organic-rich shales in Utah (Table 1). The shales having moderate or good potential of being shale gas reservoirs are herein described in terms of those properties that indicate a probable natural gas play. At least five strongly potential shale gas plays have been recognized through this study. Finally, a strategy for developing future shale gas reservoirs of Utah is set out in a series of recommendations to the UGS and to industry.

Table 1: The initial candidate Phanerozoic shale units investigated for shale gas potential.

Potential Utah Shale Gas Reservoirs		
Tertiary	Green River	Black shale facies
Cretaceous	Mancos Shale	Prairie Canyon Member (Mancos B) Lower Bluegate Member Juana Lopez Member Tropic Shale-Tununk Member Mowry Shale
Permian	Phosphoria-Park City (Meade Peake Member)	
Pennsylvanian	Paradox Formation (black shale lenses)	
Mississippian	Manning Canyon Shale - Doughnut Formation Delle Phosphate Shale Member	

The study has utilized public domain data sources, and any volunteered information given with the understanding that it may be entering the public domain through this project. The information has come from libraries at the University of Utah and the Utah Department of

Natural Resources, Interlibrary Loan, internet searches, and other appropriate sources. Where relevant to the project goals, knowledgeable persons named in the text and/or acknowledgements have been consulted. Given the severe temporal and financial limitations of the project, no new laboratory analyses of rock or hydrocarbon samples were undertaken.

As in integral part of the project all or selected portions of seven cores sampling potential shale gas reservoirs were examined at the USGS (Denver) and UGS Core Research Centers. The cores studied were:

- Marsing #16 (Green River Formation), Wasatch County, 16-10S-8E
- Coseka Resources 8-2-15-22 State of Utah (Prairie Canyon Member), USGS #D-333, Uintah County, 2-15S-22E
- Tenneco Brunel E 28-10 (Prairie Canyon Member), USGS #D-319, Rio Blanco Co. Colorado, 28-4S-102W
- Coseka Resources 15-29-4-103 Gentry (Prairie Canyon Member), USGS #D-351, Rio Blanco Co., Colorado, 29-4S-103W
- Coseka Resources 6-15-1S-103 Federal (Prairie Canyon Member), USGS #D-339, Rio Blanco Co., Colorado, 15-1S-103W
- River Gas of Utah #1 (Blue Gate Shale, Ferron Sandstone and Tununk Shale), Carbon County, 36-14S-9E
- USGS Escalante #1 (Straight Cliffs Formation and Tropic Shale), USGS #E-064, Garfield County, 36-35S-2E.

In the course of carrying out the study it became clear that there is a paucity of useful geochemical data on organic richness and thermal maturity of Utah black shales, let alone information on gas content, petrophysical properties, and rock mechanic properties. The studies that have been published are largely pre-1990, were carried out to support oil exploration, not gas, or were purely 'academic' research of secondary utility for hydrocarbon assessment. This was a serious limitation for this project, and it presents a data barrier that must be overcome before serious shale gas exploration and development work can proceed.

Geochemistry and Origin of Natural Gas

The organic matter (*kerogen*) preserved in rocks is derived largely from bacteria and blue-green algae (type I kerogen), marine green-algae (type II), or higher woody plants (type III). Because of the elemental composition of their precursors, bacterial and algal *sapropelic* kerogens are rich in hydrogen, whereas woody or *humic* kerogens are hydrogen poor (Hunt, 1979). All are capable of generating methane and other natural gases, but sapropelic kerogens initially yield larger volumes of liquid hydrocarbons than humic kerogens (Fig. 1). They are considered to be *oil-prone*, whereas humic kerogens are *gas-prone* by default. Because sapropelic kerogen starts with a higher elemental concentration of hydrogen, it will have a larger yield of both oil and methane than humic kerogen (Figs. 1 and 2). Sapropelic kerogens can generate twice as much hydrocarbon gas per gram of organic matter as humic kerogen (Lewan and Henry, 2001). Carbonate source rocks (i.e., Type IIS kerogen) can generate even more methane, as much as 2.5 times as much as Type III kerogen. To a large extent the methane and related energy gases from sapropelic kerogen are generated from residual oil (*bitumen*) remaining in the source rock interval (or reservoired oil pool) as it is buried to very deep levels of the basin (Lewen, 2002). Prolific natural gas provinces are not restricted to coal-bearing basins.

Methane is formed in sedimentary basins at very shallow depths through microbial breakdown of organic matter (*methanogenesis*) and at greater depths by *thermal disaggregation* of organic molecules containing hydrogen. The microbes responsible for *biogenic* methane survive temperatures less than about 40-50º C (Hunt, 1979; Fig. 1), whereas the chemical processes leading to *thermogenic* methane become significant at temperatures greater than 135-175º C (Pepper and Corvi, 1995). There are two main sources of thermogenic gas: maturing source rocks and the *in situ* cracking of oil in reservoirs or residual in black shales (Pepper and Dodd, 1995; Schenk and Horsfield, 1998). Sweeney and Burnham (1990) calculate that source-rock gas generation occurs between 0.5 and 2.2% Ro, whereas oil-cracking gas generation occurs between 1.6 and 3.3% Ro (Fig. 3).

Natural gas of microbial origin is nearly pure methane (C_1) with virtually no other hydrocarbon gases (low *wetness* value), but with various amounts of carbon dioxide. The bulk of C_1-C_4 generation occurs after the peak of bitumen generation, but CO_2 generation occurs before, during and even after generation of liquid hydrocarbons (Seewald and others, 1998). Type I sapropelic kerogens tend to initiate generation of gas at higher stages of thermal maturity (depths of burial) than do either type II or type III kerogens (Fig. 2).

Natural gas of microbial origin (Martini et al., 2003) is nearly pure methane (C_1) with virtually no other hydrocarbon gases (low *wetness* value), but with various amounts of carbon dioxide (Fig. 2). Due to the metabolic selectiveness of the microbes, biogenic methane is isotopically lighter (larger negative ä^{13}C) than thermogenic methane (Fig. 4). The ä^{13}C of microbial methane is typically lighter than -55 $^{0}/_{00}$ (Mattavelli and Novelli, 1988; Whiticar, 1994). Also low maturity thermogenic gas produced from primary cracking of kerogen is primarily methane (Seewald and others, 1998). In contrast, mature thermogenic gas associated with the onset of bitumen generation consists of methane together with other hydrocarbon (C_{2+}) gases (high *wetness* value), ä^{13}C values only slightly lighter than the precursor organic matter, and associated non-hydrocarbon gases, such as nitrogen, helium and/or hydrogen sulfide. As the thermal maturity of the natural gas increases, the wetness value again decreases. Thus, shallow microbial *and* deep, highly mature thermogenic methane both are *dry gas*, lean in the C_{2+} fraction and distinguished only by their ä^{13}C isotopic compositions (Fig. 4).

The two principal metabolic pathways leading to methanogenesis (Schoell, 1980) are:

- CO_2 reduction: $CO_2 + 4\ H_2 \quad > CH_4 + 2\ H_2O$
- Acetate fermentation: $CH_3COO^- + H2O \quad > CH_4 + HCO_3^-$

Methane generated by the two processes can be distinguished by comparing carbon and hydrogen isotopic compositions, ä^{13}C vs. äD (Whiticar at al., 1986). Methane formed by CO_2 reduction is less depleted in deuterium (äD) and more depleted in ^{13}C than methane formed by acetate fermentation (Fig. 5). Approximately 20% of the methane in all commercial natural gas is biogenic in origin (Wiess and Kvenvolden, 1993).

The bulk of C_1-C_4 generation occurs after the peak of oil generation, but CO_2 generation occurs before, during and even after generation of liquid hydrocarbons (Seewald and others, 1998). Gas generation is not restricted to high thermal maturities representing post-oil generation (>1.2 %Ro). Significant amounts of thermogenic gas can be generated together with oil (Schenk and Horsfield, 1988). Approximately 75% of source rock gas has been generated by the end of oil generation (1.1% Ro). However, bitumen and kerogen retained in a maturing source rock that has passed through the oil window will crack to natural gas with further thermal stress (Pepper and Dodd, 1995).

Primary migration out of the source rock initially proceeds by *diffusion* through rock matrix micropores and mesopores to macropores and fractures (Mann, 1994). From there a petroleum bulk phase develops and moves by *Darcy flow* along the macropore and fracture network of the source rock. Overpressure associated with the volume expansion of newly generated hydrocarbons is widely accepted as the principal driving mechanism of expulsion (England et al., 1987; Durand, 1988), but other factors also can play a role.

Primary migration can occur only after the source rock pore space is fully saturated by newly generated hydrocarbons. Mackenzie and Quigley (1988) demonstrate a causal link between *expulsion efficiency* and initial petroleum potential of a source rock. The richer the source rock, the larger the excess volume of petroleum that is available for expulsion after the pore and fracture network in the source rock is fully saturated. In rich source rocks, those capable of generating more than 5 kg HC/ton rock, the expulsion efficiency is estimated to be on the order of 60-80%. However, in leaner source rocks the expulsion efficiency is less than 40%. Very tight source rocks with permeabilities in nanodarcies (i.e., shale gas reservoirs) also are likely to have relatively low expulsion efficiencies of liquid hydrocarbons.

To the extent that gas dissolves in kerogen and bitumen, rocks saturated in solid and liquid hydrocarbons may retain much of the gas co-generated with oil or formed by oil cracking. Also gas may migrate with difficulty from an oil-saturated tight rock due to relative permeability issues. For these reasons, oil-prone shales may not actually be the most productive shale gas reservoirs despite there inherent higher gas-generative capacity. However, over geologic time, as opposed to a production timeframe, gas expulsion efficiency is greater than 90% regardless of the source rock type (Pepper, 1991). Thus, it helps if gas generation in the shale is very recent.

In very fine-grained source rocks having matrix permeability less than a microdarcy (10^{-19} to 10^{-20} m^2), fracturing may be induced by pore-pressure buildup caused by the conversion of organic matter to less dense oil and gas (Berg and Gangi, 1999). The resulting fractures increase rock permeability by perhaps as much as six or seven orders of magnitude to 10-13 m^2 (Capuano, 1993) and provide pathways for primary migration. Pressure-induced fracturing is more likely to occur in rich source rocks capable of generating large volumes of oil or at elevated levels of maturity where gas is generated. High rates of petroleum generation and/or stress loading of the source rock (Cosgrove, 2001) will further aid this natural hydraulic fracturing process.

A necessity for microbial methane production at shallow depths in sediments is sufficient pore space for the methanogens to exist and grow (Rice, 1993). In low permeability shales, a microfracture network may be essential to provide both living space and pathways for delivery of vital nutrients.

Characteristics of Producing Shale Gas Reservoirs

The experience gained in developing shale gas reservoirs in the currently producing regions of the United States provides the best guide to exploration for and exploitation of additional shale gas resources (Hill and Nelson, 2000). The Appalachian and Illinois basins (Ohio Shale and New Albany Shale, respectively) have been producing shale gas from generally shallow, low-yield wells since the 1800's. However, shale gas development in three other basins - San Juan (Lewis Shale), Fort Worth (Barnett Shale), Michigan (Antrim) - has arisen over just the past two decades and now dominates the attention of the natural gas industry. It is the newer shale gas resources that have been exploited with the most advanced technologies and about which we have the greatest knowledge.

The Newark East (*Barnett Shale*) field in the Forth Worth basin is now the largest gas field in Texas. Although shallow gas had been produced in the area since early in the twentieth century, the Barnett discovery well was drilled only in 1982. Until 1992 only 10 wells/year on average were completed in the field, but that year there were 99 new wells. Just a decade later (2002) there were 1,870 wells producing an average of 600 MMcfd of natural gas and gas condensates (Rach, 2004). The mean EUR per well reported by Devon Resources, the largest operator in the field, is 1.25 Bcfg (Pollistrano et al., 2003). At present there are over 2.5 Tcf of booked proven gas in the field (Bowker, 2003), and exploration drilling outside of the field is rapidly increasing the reserve base for the Barnett Shale in the broader Fort Worth basin (Pezet, 2005).

The Forth Worth basin is a segment of the Ouachita foreland basin bounded on the north by the Arkoma aulacogen (Montgomery and others, 2005). At the onset of the basin subsidence in Mississippian time, kerogen-rich Barnett Shale was deposited unconformably on various Ordovician carbonate units, the tight Viola and Simpson Limestones in the deeper, easternmost part of the basin and the highly karstified Ellenburger Limestone further to the west. The 600 ft thick Barnett Shale is overlain by the Pennsylvanian Marble Falls Formation. The Marble Falls shale-limestone forms a good containment ceiling for hydrocarbon entrapment and for hydraulic fractures. Where present immediately beneath the Barnett Shale, the Viola Simpson plays a similar role, however, the karstified and porous Ellenberger does not. The Forestburg Limestone separates the Upper and Lower Barnett Shale members (Fig. 6). In the 'core area' north of Fort Worth (Wise Co.), the Lower Barnett typically delivers 75-80% of the gas, while the Upper Barnett yields just 20-25% when even completed (Johnson, 2004a).

The Barnett Shale is typically a black, organic-rich (Type II kerogen; 12% avg. TOC) siliceous shale with a mean composition of 45% quartz (possibly recrystallized radiolaria), 27% clay (illite-smectite and illite), 10% carbonate, 5% feldspar, 5% pyrite; 5% organic matter and little to no free water (Bowker, 2002). The average porosity is 5-6% and matrix permeability is extremely low, 0.0007-0.005 md.

The Barnett Shale yields a wide variety of hydrocarbons depending on the level of maturity: dry gas, high BTU-high value wet gas, condensate and 40º-50ºAPI oil. Gas occurs as free gas in the matrix and in fractures, and as absorbed gas on/in kerogen. The CO_2 content is normally very low, less than 2%. Estimated total gas content of the Barnett Shale in the high maturity (>1.1% Ro) 'core area' is 50-200 scf/ton of rock or 100-150 bcf/ mi^2, which is roughly the equivalent of 575 Mcf/ac ft (Bowker, 2002). The BTU value of the gas is directly proportional to the vitrinite maturity level of the black shale; in the East Newark field it is 1,050-1,300 BTU (Pollastrano et al., 2003). The principal source of gas in the East Newark field is from cracking of residual oil and bitumen (Jarvie et al., 2001). The fact that the shale is slightly overpressured (0.52 psi/ft) indicates that gas generation is continuing at present. The high quartz content and overpressure enhance potential for natural and induced fracturing of the shale beds.

All shale gas reservoirs require *fracture stimulation* to connect the natural fracture network to the well bore. It is in finding the fracture stimulation methods most appropriate to individual shale reservoirs that the industry has made greatest progress in recent years. Nowhere is this more evident than in the East Newark field. After many years of using relatively timid stimulation techniques to avoid "water damage" to the shale, the method now used widely in the Barnett Shale is multi-stage massive water fracture stimulation (Rach, 2004; Johnson, 2004a). A single stage will pump about a million gallons of lightly treated water carrying a low sand concentration (about 100,000 lbs) at high pump rates (Johnson, 2004b). Tilt meter surveys show that the massive frac treatments result in very large surface contact with the shale, a total of many miles of induced fracture length (Fisher et al., 2002). Both fracture recompletions (Fig. 7) and horizontal wells are increasing the per-well EUR. The widespread adoption of the plunger gas lift devices replacing down-hole electric pumps to clear the borehole of water is improving gas rates and costs of operating. These methods recently developed in the East Newark basin still need to be tested in other shale gas regions, such as the San Juan basin.

The *Lewis Shale* was deposited in a shallow, off-shore marine setting during an early Campanian transgression (Fig. 8) southwestward across shoreline deposits of the underlying progradational Cliffhouse Sandstone Member of the Mancos Formation (Nummendal and Molenaar, 1995). The gas resources of the Lewis Shale are currently being developed, principally through re-completions of existing wells targeting deeper, conventional sandstone gas reservoirs (Dube and others, 2000). This play is a possible analogue for Utah Upper Cretaceous shale-reservoired gas resources.

The 1,000 to 1,500 ft thick Lewis Shale is lowermost shoreface and 'prodelta' deposits composed of thinly laminated (locally bioturbated) siltstones, mudstones and shale. The average clay fraction is just 25%, but quartz is 56%. The rocks are very tight. Average matrix gas porosity is 1.7% and the average gas permeability is 0.0001 md. The rocks also are organically lean, with an average TOC is only 1.0%; the range is 0.5 to1.6%. The reservoir temperature is 140°F (46°C). Yet the adsorptive capacity of the rock is 13-38 scf/ton, or about 22 Bcf per 160 acres (Jennings and others, 1997). In the re-completed wells, the gas rates from the Lewis Shale range from 10 to 200 Mcf per day, averaging 60 Mcf per day. The Lewis Shale exhibits a hyperbolic decline rate of about 6.5%. Over a 30-year predicted life for the renovated wells (maintaining current 80-acre spacing), the average estimated ultimate recoveries are 300-500 MMcf (Mavor and others, 2003). The total storage capacity of the current production fairway is 24 Tcf. The USGS estimates a mean 10.2 Tcfg and 30.5 MMbngl of undiscovered resource in the Lewis Shale play (USGS FS-147-02).

A large number of different well completion and stimulation methods have been used in the Lewis Shale (Dube and others, 2000). Due to the sub-normal (0.22 psi/ft) fluid pressures and resulting high potential for formation damage by water imbibition in natural fractures, both liquid CO_2 and 70-80 quality nitrogen foam fracture treatments are considered to be the most effective. Perforations are placed preferentially in high-quartz intervals, the easiest facies to fracture, and fracturing is carried out in two stages, with 80,000 to 100,000 lbs of sand proppant per stage.

Production of natural gas from various Devonian and Mississippian black shale units is widespread in the western Appalachian basin (Roen, 1984; Milici, 1993), extending from central New York State (Van Tyne, 1993) through Pennsylvania, eastern Ohio (Broadhead, 1993), southwest West Virginia, eastern Kentucky into eastern Tennessee (Fig. 9). In fact, wherever the net thickness of Devonian-Mississippian high-GR (radioactive) black shales is greater than 100 ft gas and the average TOC greater than a few percent (Fig. 10), production is established. Most wells are very low yield, but they have continued to produce reliably for many decades supplying farms and small communities with a cheap source of energy (Pachen and Hohn, 1993). The earlier, shallower wells generally were drilled for water, not gas or oil. Prior to the rapid development of the Antrim Shale as a gas resource, virtually all U.S. shale gas came from the Ohio Shale and other black shales of the Appalachian basin (de Witt et al., 1993).

The mid-Paleozoic black shales of the Appalachian basin (Fig. 11) were deposited in the distal, anoxic portions of a foredeep basin associated with the Devonian-age Acadian orogeny. For the most part, they are cyclic deposits linked to the transgressive-regressive cycles of the Catskill delta to the east. As such, the black shale units are time transgressive, progressively younger to the west and having depocenters that shift westward in front of the advancing delta complex (Fig. 12). The younger of these deposits (Fig. 11) in the westernmost part of the basin, the *Ohio Shale*, commonly gives its name to the entire group of Middle and Upper Devonian-Mississippian gas-bearing black shales.

During the latest Devonian and early Mississippian, black shales correlative with the Ohio Shale were deposited across much of the central part of North America. Now, these are preserved in intracontinental depressions such as the Michigan (Antrim Shale), Illinois (New Albany Shale) and Williston (Bakken Shale) basins, where they are established source rocks for oil and associated gas. In small portions of the Michigan and Illinois basins, non-associated gas is produced directly from the black shale reservoirs. The black shales extend at depth beneath much of the two basins, so the potential for deep thermogenic gas production remains to be tested. The current dry gas production is limited to the shallow edges of the basins and is related to special hydrogeologic conditions induced by Pleistocene glaciation (Martini et al., 1998; Walter et al., 2000; McIntosh et al., 2002). Repeated episodes of glacial loading induced both *hydrofracturing* in the freshly exhumed organic-rich shale and *fresh water recharge* that transported methanogens up to 2,000 ft deep within the source rock where they now are generating microbial methane.

The gas producing area of the Michigan basin is restricted to a crescent-shaped area on the northern margin of the basin where the Antrim Shale is subcropped beneath a thick glacial till (Fig. 13). Although the average well rate is low, just 116 mcfd with 30 barrels of water per day, here more than 5,000 shallow wells collectively produce about 425 mmcfd (Martini et al., 1986). Just a portion of the New Albany is organic-rich, the Lachine and Norwood Members (Fig. 14). These black shale units have a net thickness of about 150 ft and variable organic (immature Type II kerogen) content, 0.5-24% TOC.

The Antrim gas is a mixture of about 80% microbial and 20% thermogenic gas (Martini et al., 1998), but the portion of thermogenic gas increases with depth of the shale reservoir (Fig. 15). The isotope chemistry of the microbial gas indicates that it is the product of CO_2 reduction and is younger than 20,000 years. The thermogenic gas is derived from either the mid-basin Antrim Shale or the underlying Silurian Niagra Formation. The young age of the gas and the presence of an effective glacial till "topseal" are critical to the spectacular success of this gas play.

Gas from the New Albany Shale is produced almost entirely on the southern and eastern margin of the Illinois basin in Indiana and northwest Kentucky. The black shale facies of the New Albany does not extend to the western edge of the basin. The rather unpredictable gas rates and water cuts of the shallow producing wells is attributable, at least in part, to the greater complexity of the hydrogeology of the southeast Illinois basin (Walter et al., 2000; McIntosh et al., 2002) as compared to the northern Michigan basin described above. Otherwise, the gas composition and genesis of the gas is the same as for the Antrim Shale, i.e., young microbial gas with a variable mix of older thermogenic gas. The New Albany also subcrops beneath glacial till, which serves as a topseal. Here, however, the most reliable wells are situated in areas where fresh water recharge reaches deep into the New Albany Shale through either an underlying Silurian-Devonian carbonate aquifer system or by way of downward drainage through a relatively porous Mississippian carbonate aquifer. In the portion of the eastern basin margin where the New Albany is capped by Mississippian deltaic deposits of the Borden Group, a regional aquiclude, freshwater recharge is restricted and microbial methanogenesis inhibited. Here few successful New Albany gas wells have been completed.

The upper member of the Albany Shale (Clegg Creek Member) is the most organic-rich portion of the formation (>15% TOC and 0.6% Ro); it is the main gas producer. Reported initial production ranges from less than 10 to about 4,500 Mcfd; the basinwide average is only 187 Mcfd (Walter et al., 2000). Cluff et al. (1997) estimate that the total New Albany Shale gas in place is 323 Tcf, of which 65% is within the upper Grassy Creek Shale Member, the only unit likely to be exploited commercially.

Average reservoir characteristics of the principal shale gas deposits now in production in the United States is generalized in Table 2. It is clear from these data and from the spider plots extracted from the table (Fig. 16), that there is not a single set of properties that can lead to commercial exploitation of natural gas from organic-rich shales. Rather, there are a range of parameters that in combination can result in shale gas resources. Rapid advances in well completion techniques, principally in fracture stimulation, are expanding the scope of this now less-than-unconventional gas resource.

Table 2: Geological, geochemical and reservoir characteristics of the principal producing shale gas deposits in the United States (modified slightly from Hill and Nelson, 2000).

Property	Antrim	Ohio	New Albany	Barnett	Lewis
Depth (ft)	600–2400	2000–5000	600–4900	6500–8500	3000–6000
Gross thickness (ft)	160	300–1000	100–400	200–300	500–1900
Net thickness (ft)	70–120	30–100	50–100	50–200	200–300
Bottom-hole temperature (°F)	75	100	80–105	200	130–170
TOC (%)	0.3–24	0–4.7	1–25	4.50	0.45–2.5
Vitrinite reflectance (% R_o)	0.4–0.6	0.4–1.3	0.4–1.0	1.0–1.3	1.6–1.88
Total porosity (%)	9	4.7	10–14	4–5	3–5.5
Gas-filled porosity (%)	4	2.0	5	2.5	1–3.5
Water-filled porosity (%)	4	2.5–3.0	4–8	1.9	1–2
Permeability thickness [Kh (md-ft)]	1–5000	0.15–50	NA	0.01–2	6–400
Gas content (scf/ton)	40–100	60–100	40–80	300–350	15–45
Adsorbed gas (%)	70	50	40–60	20	60–85
Reservoir pressure (psi)	400	500–2000	300–600	3000–4000	1000–1500
Pressure gradient (psi/ft)	0.35	0.15–0.40	0.43	0.43–0.44	0.20–0.25
Well costs ($1000)	180–250	200–300	125–150	450–600	250–300
Completion costs ($1000)	25–50	25–50	25	100–150	100–300
Water production (b/day)	5–500	0	5–500	0	0
Gas production (mcf/day)	40–500	30–500	10–50	100–1000	100–200
Well spacing (ac)	40–160	40–160	80	80–160	80–320
Recovery factor (%)	20–60	10–20	10–20	8–15	5–15
Gas in place (bcf/section)	6–15	5–10	7–10	30–40	8–50
Reserves (mmcf/well)	200–1200	150–600	150–600	500–1500	600–2000
Historic production area basis for data	Otsego County, Michigan	Pike County, Kentucky	Harrison County, Indiana	Wise County, Texas	San Juan & Rio Arriba Counties, New Mexico

*Modified from Hill and Nelson (2000); data cited by those authors were compiled from Gas Technology Institute/Gas Research Institute research reports and operator surveys.

Shale Gas Reservoir Screening Criteria

In the Fort Worth basin where the level of source rock maturity is critical to the yield of thermogenic gas from the Barnett Shale, Jarvie and Claxton (2002) have proposed a prospect and well evaluation system basin on specific geochemical parameters:

- total organic carbon (TOC)
- the transformation ratio (TR) or extent of organic matter conversion into hydrocarbons
- thermal maturity as measured by vitrinite reflectance (Ro)
- gas composition, such as gas wetness
- volume of freely desorbed headspace gas
- volume of macerated cuttings headspace gas, a measure of gas yields upon fracturing of the Barnett Shale.

The prospects for development of a commercial gas well increase as the values of these parameters exceed threshold minimum values (Fig. 17). In addition to these geochemical criteria, Zhao (2004) draws attention to physical properties of the reservoir rock itself, specifically porosity and brittleness. Both of these properties are considered related to differential compaction over local structural relief on the unconformity surface separating the Barnett Shale from the underlying Ordovician Viola and Ellenburger Formations.

As with all hydrocarbon plays, many factors must come together to make a commercially successful shale gas reservoir. With our current level of knowledge, it appears that the six most critical factors are:

- *gas content*, which is a function of kerogen content/type, maturation history/level (or biogenesis) and gas retention;
- *high gas saturation*, or conversely very low water saturation;
- *net thickness* of high-gas shale interval;
- presence of a *natural fracture system* that is appropriate to the sealing characteristics of the shale reservoir;
- *conduits*, such as silt laminae and/or micro-fractures, for flow of gas from the shale matrix to the macro-fracture network; and
- ability to induce controlled *artificial fractures* deep within the shale reservoir without fracturing adjacent water-bearing rocks, i.e., the presence of fracture barriers.

It is clear that every shale gas reservoir is different with respect to these factors, and all are quite variable vertically and laterally. This is the challenge of discovering and developing new commercially viable shale gas resources.

Given the very limited amount and scope of information in the literature relevant to Utah's black shales, the 'screening criteria' that could be applied in this project in most instances was a very reduced subset of those cited above:

- organic richness and maturity of the black shale
- thickness of the kerogen-rich interval
- likelihood of natural and induced fracturing, determined subjectively
- potential barriers to hydraulic fracturing, or water-saturated zones, in adjacent strata.

The assessments are subjective and should be considered preliminary, pending further data gathering and analysis.

Geologic Setting for Utah's Organic-rich Shales

With the sole exception of the Park City-Phosphoria Formation, all of the organic-rich shales of Utah were deposited in structural basins that were tectonically active at the time of deposition. Excluding just two black shale units, the Hermosa Group and the Green River Formation, the organic-rich shales are located in regionally extensive foreland basins developed east of their respective active orogenic belts, the Mississippian Antler thrustbelt (Speed and Sleep, 1982; Fig. 18) and the Cretaceous Sevier thrustbelt.

The *Hermosa Group* was deposited in the Paradox basin which developed on the craton in response to transpressional uplift in late Early Pennsylvanian of a portion of the craton, the Uncompaghre uplift. These are elements of the regional Ancestrial Rockies (Fig. 19) structures that developed in front of the Marathon-Ouachita orogen during the collisional assembly of Pangea (Baars, 1988; Miller and others, 1992). Both uplift and subsidence of the Paradox basin to the southeast were very rapid.

The Oquirrh basin (*Manning Canyon Shale*), which formed on trend with the Uncompaghre uplift (Fig. 19) may also be an earlier Ancestrial Rockies depression, similar to the Paradox basin, or it might have formed by a similar process in response to late phase compression of the Antler orogen. Its position as a successor basin in the Antler foredeep favors this interpretation. During the Pennsyulvanian it accumulated an even thicker stratigraphic section than did the Paradox basin.

The very thick *Mancos Shale*, with its several kerogen-rich members, was deposited in the foredeep basin (Fig. 20) of the Sevier thrustbelt at a time of continental flooding in the mid- and early Late Cretaceous. The foredeep basin was thereby broader and deeper than it would have been at other times. These conditions lasted until global sea level fall in the early Campanian at which point sediments pouring eastward off the Sevier orogen quickly regressed across Utah (Fig. 21) ending kerogen-rich shale deposition. Laramide uplift of portions of the craton in front of the Sevier orogen, in a process similar to that of the Ancestrial Rockies, created an array of internally-drained basins superposed on the Sevier foredeep (Fig. 21). By early Paleogene time, these successor basins contained perennial lakes, one of which was early Eocene Lake Uinta in the Uinta Basin (*Green River oil shale*).

In most instances, the black shales accumulate early in the subsidence history of their respective basins. Whereas in many parts of the world black shales (source rocks) develop at times of especially high global sea level and flooding of the cratons (Ulmishek and Klemme, 1990), in Utah the black shales appear to relate to specific basin-forming tectonic events.

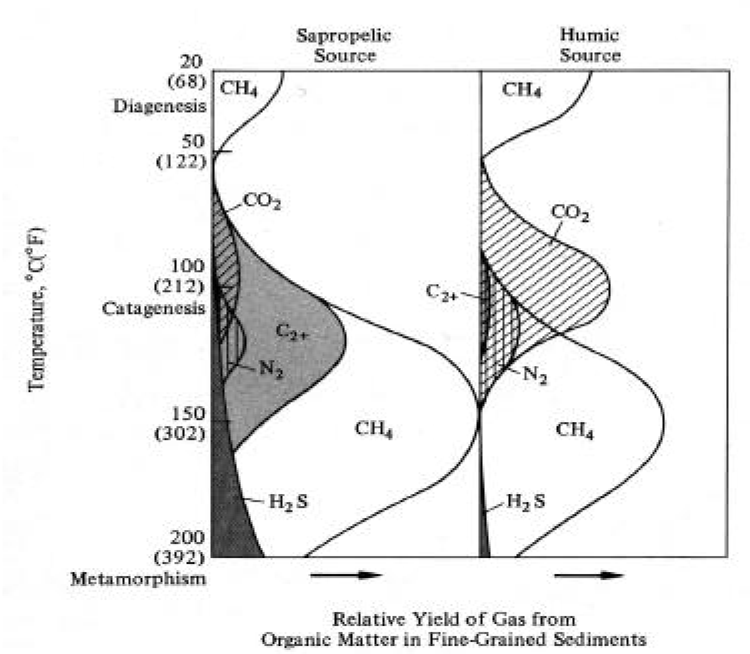

Figure 1: Relative yield of gas from sapropelic and humic organic matter in find-grained sediments (Hunt, 1979). The plots show gas generation as a function of increasing temperature (increase in depth of burial).

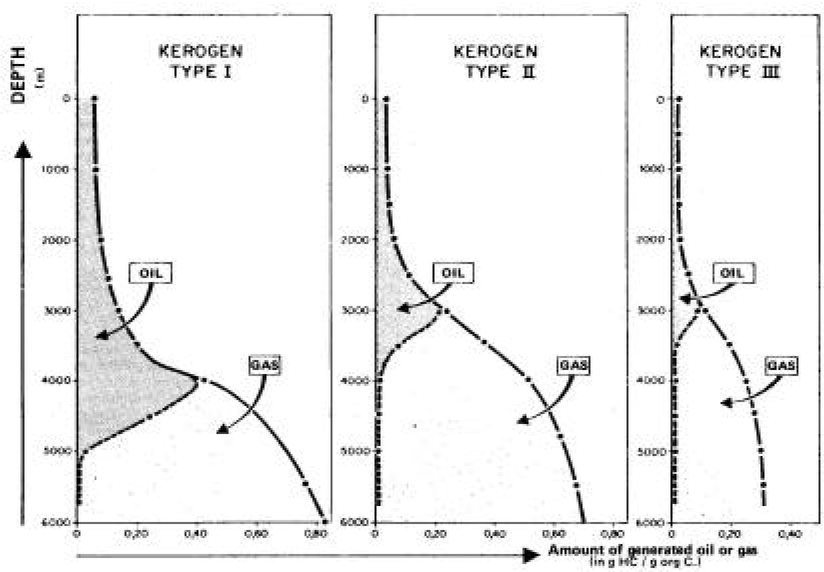

Figure 2: Evolution of oil and gas generation of different kerogen types compared (Robert, 1988). Note the larger total oil and gas yields from the sapropelic Type I and Type II kerogens compared to the humic Type III kerogen.

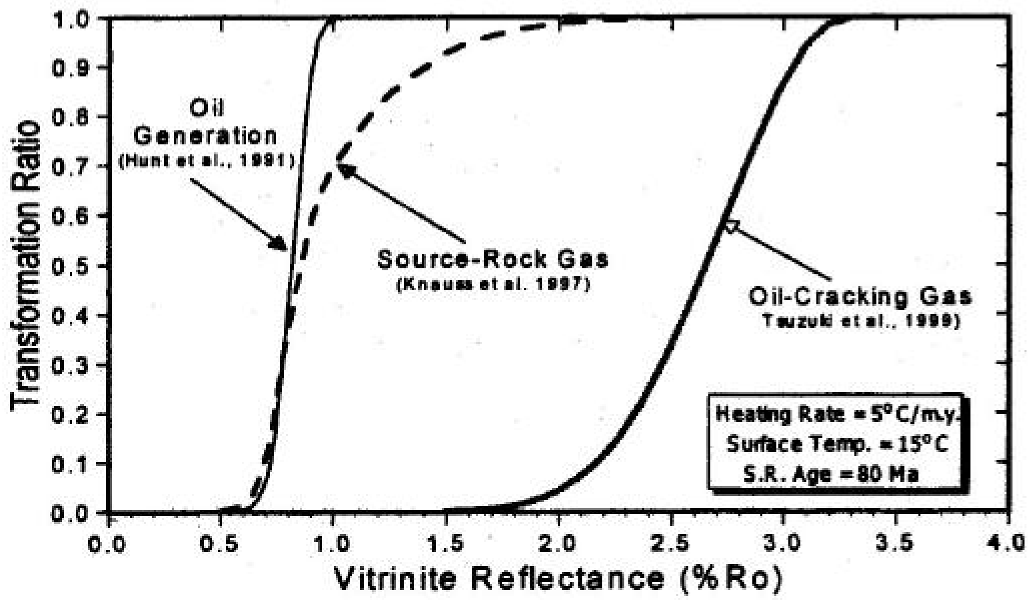

Figure 3: Calculated generation of oil and gas from an 80 Ma source rock with Type II kerogen and residual bitumen based on kenitic parameters derived from hydrous pyrolysis (Sweeney and Burnham, 1990).

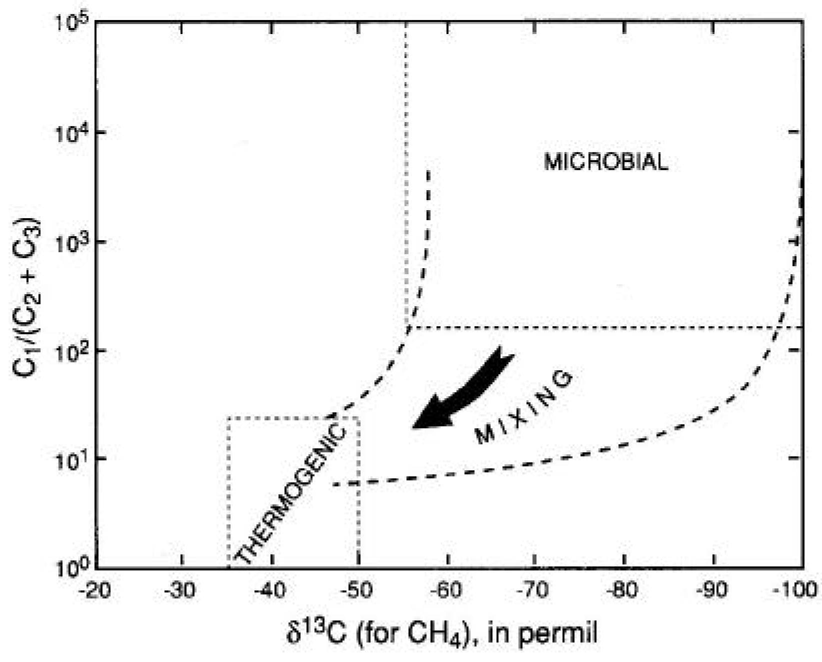

Figure 4: Carbon isotope ratio, ä^{13}C, vs. wetness ratio, $C_1/(C_2+C_3)$, for naturally occurring biogenic and thermogenic methane, C_1 (Wiese and Kvenvolden, 1993).

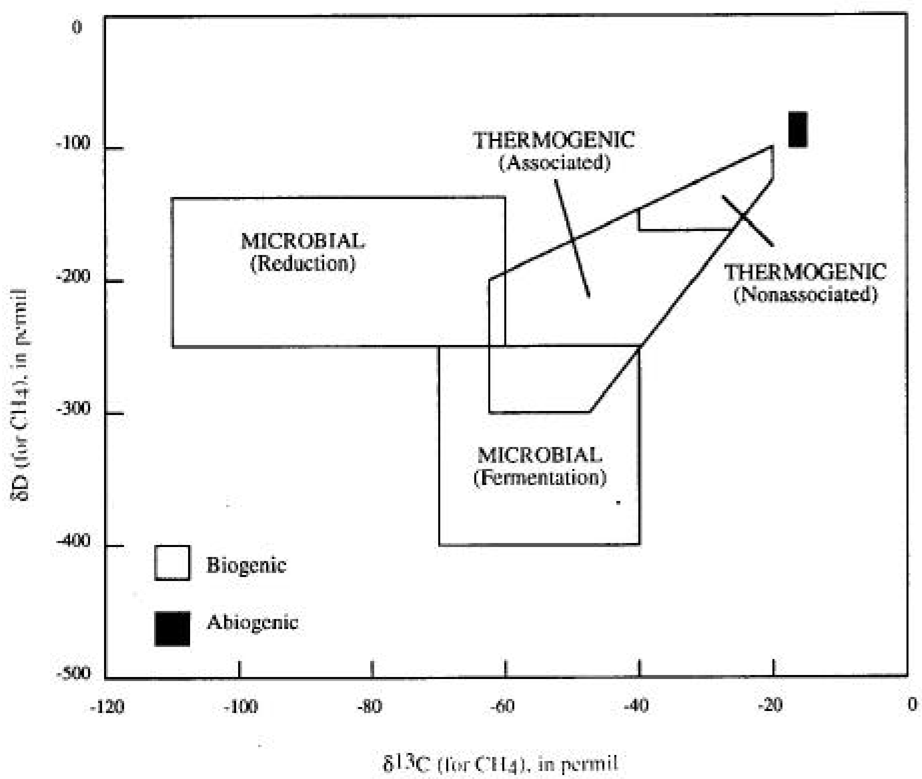

Figure 5: Source of methane determined by carbon isotopic ratio ($ä^{13}C$) vs. hydrogen isotopic ratio (äD). From Wiese and Kvenvolden (1993), modified after Whitticar and others (1986).

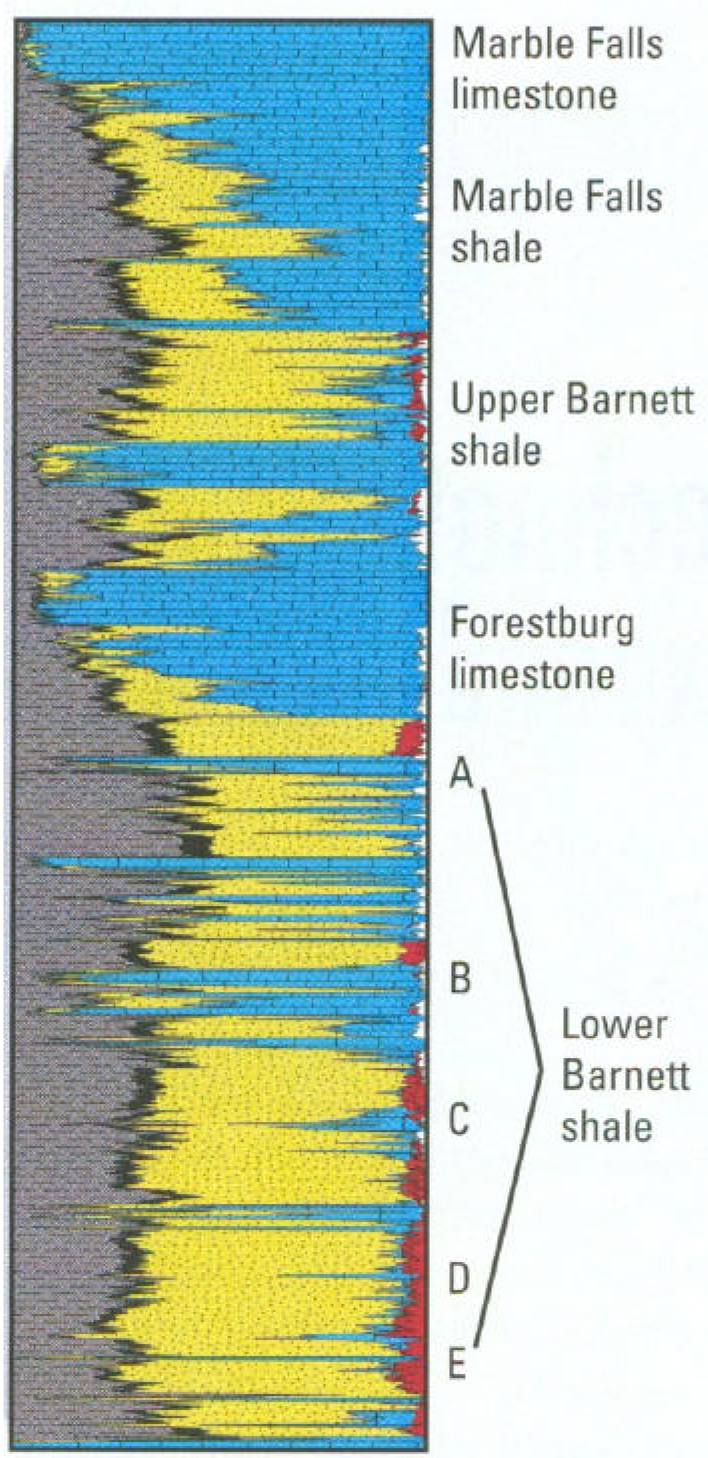

Figure 6: Representative lithology log for the Barnett Shale in the "core area" of the East Newark field, Forth Worth basin (Johnson, 2004a). Color code: white - water, red - gas, blue - calcite, yellow - quartz, black - bound water, gray - moved hydrocarbon. Note the common association of gas with the presumed more fracture-prone high-quartz zones, particularly in the lower Barnett Shale.

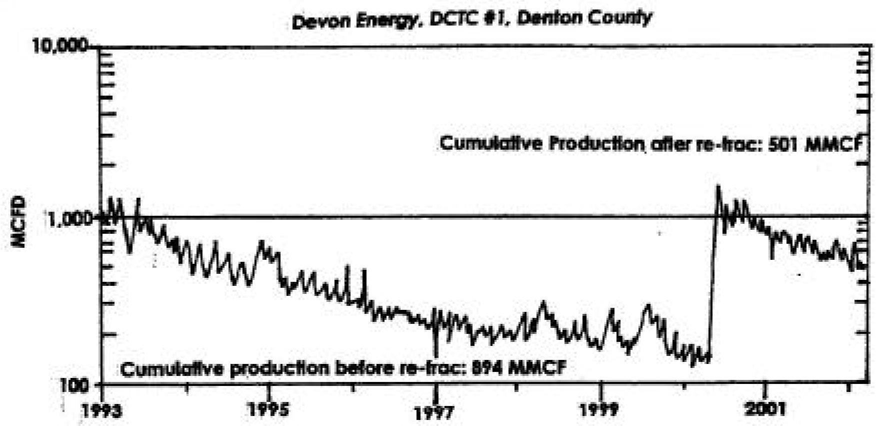

Figure 7: An example of production response to refracing an older well in the Barnett Shale.(Bowker, 2002).

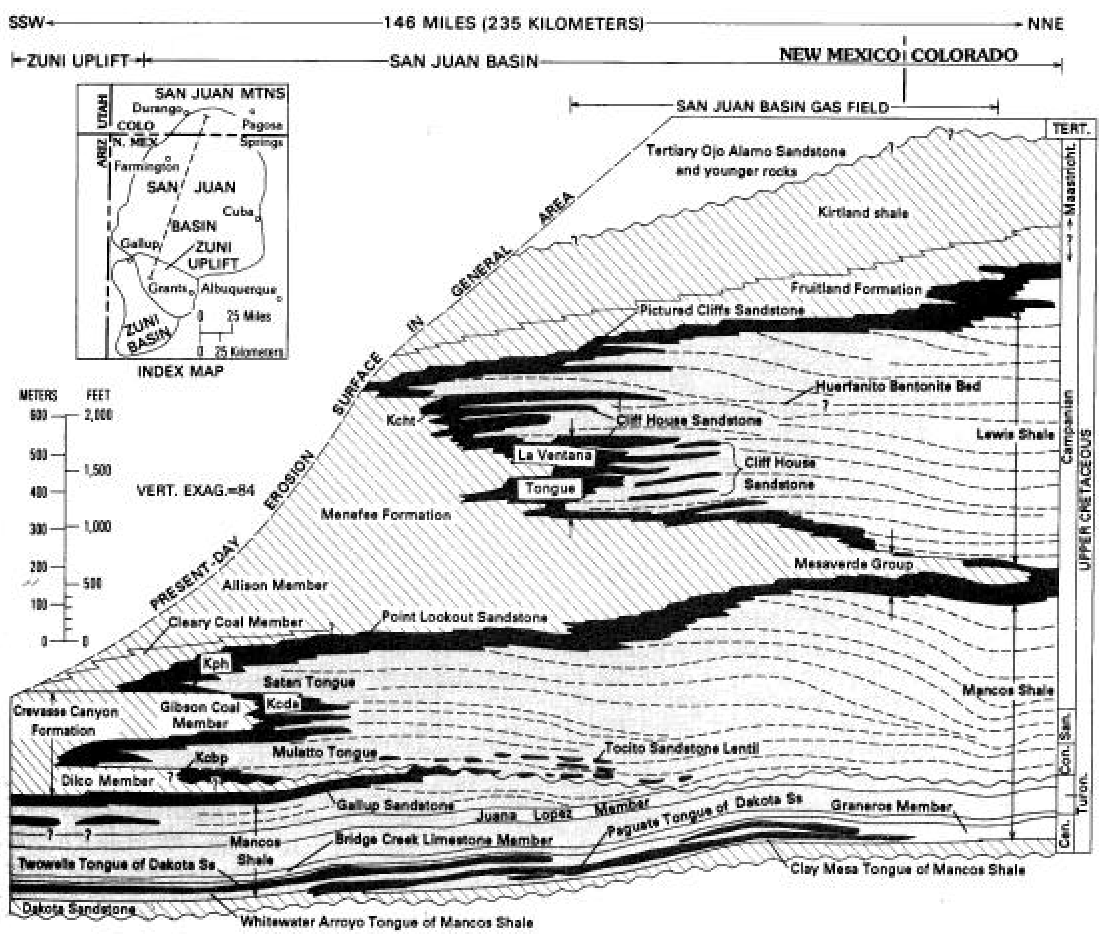

Figure 8: Stratigraphic profile across the San Juan basin showing the transgressive-regressive cycles during the Cretaceous (Nummendal and Molenaar, 1995). The Campanian Lewis Shale is the off-shore facies of the youngest of these cycles.

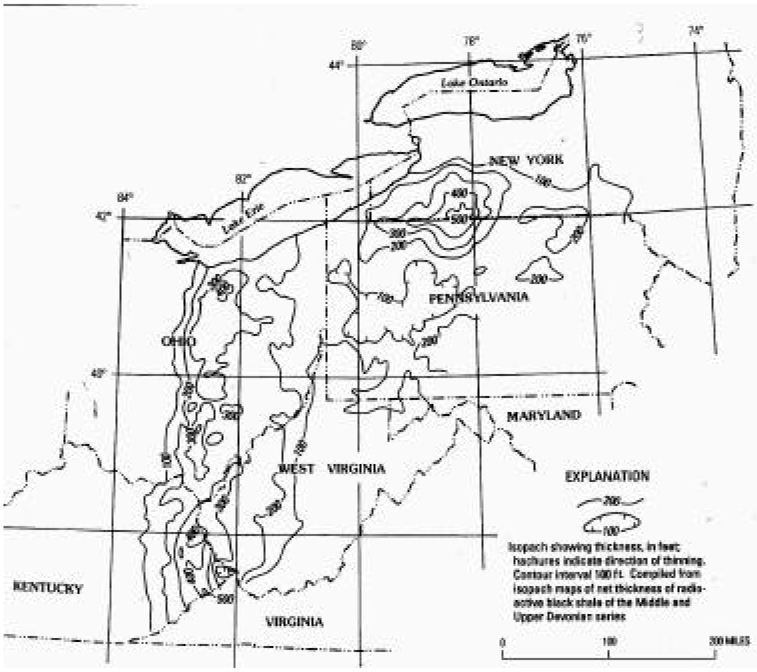

Figure 9: Total net thickness of Middle and Upper Devonian and Mississippian radioactive black shale in the Appalachian basin (Milici, 1993). The cutoff for 'radioactive' black shale is 20 API units above the gray shale baseline. Note the two centers of thick black shales in eastern Ohio and Kentucky and western New York-Pennsylvania.

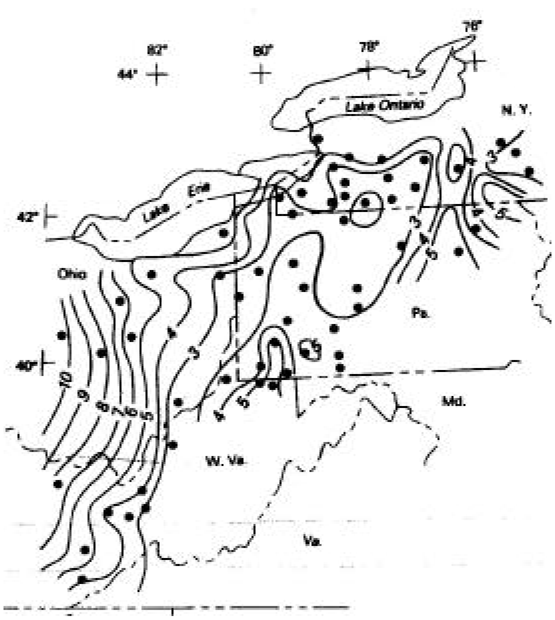

Figure 10: Average TOC (wt. %) of Middle and Upper Devonian black shales in the Applachian basin. The regions of principal shale gas production are eastern Ohio and Kentucky and southwest West Virginia, the part of the basin where TOC is relatively high and the kerogen less mature. From Roen (1984).

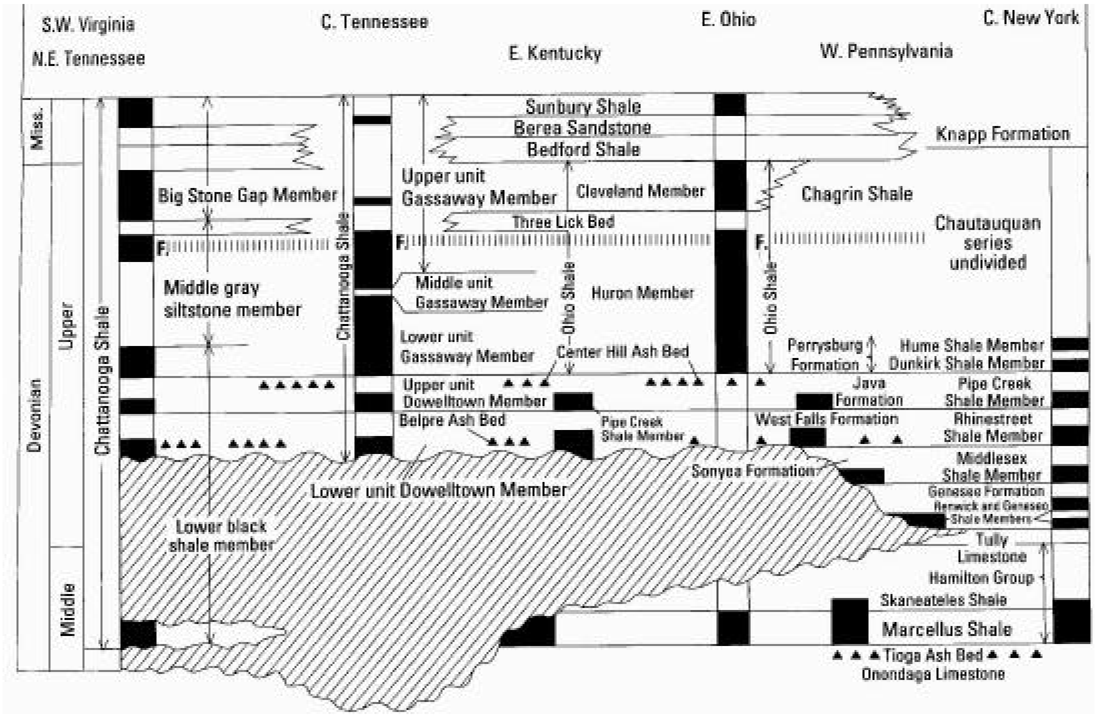

Figure 11: Correlation chart for Devonian-Mississippian black gas shales in the Appalachian basin. From de Witt et al. (1993), modified from Roen (1984).

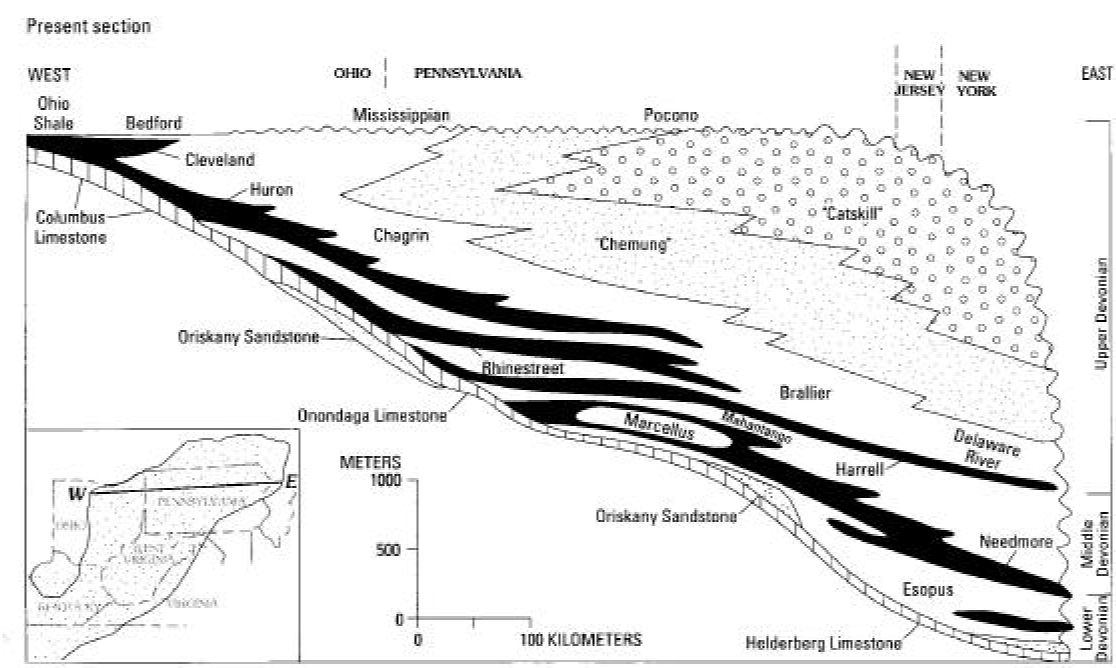

Figure 12: Lateral facies variations of the Devonian-Mississippian black shale units of the Appalachian basin. From Broadhead (1993).

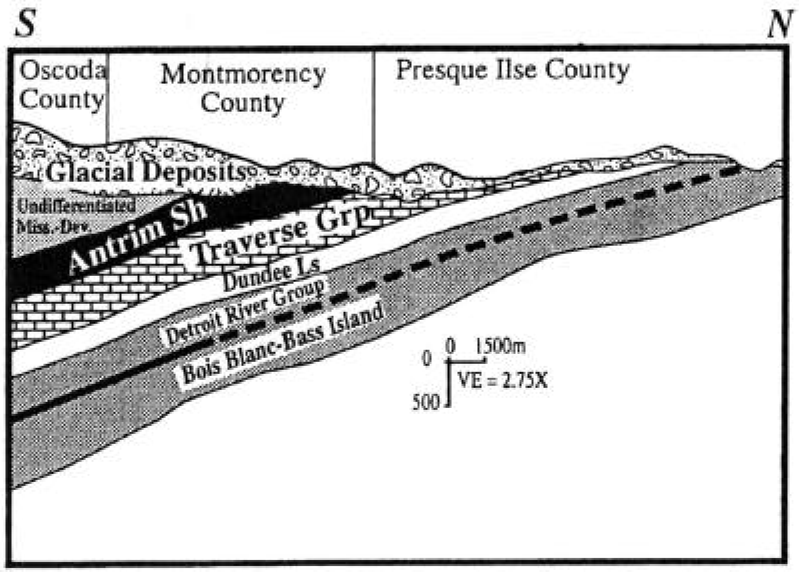

Figure 13: North-south cross section of the north rim of the Michigan basin showing the position of the Antrim Shale in the subcrop of thick glacial till (Martini and others, 1998).

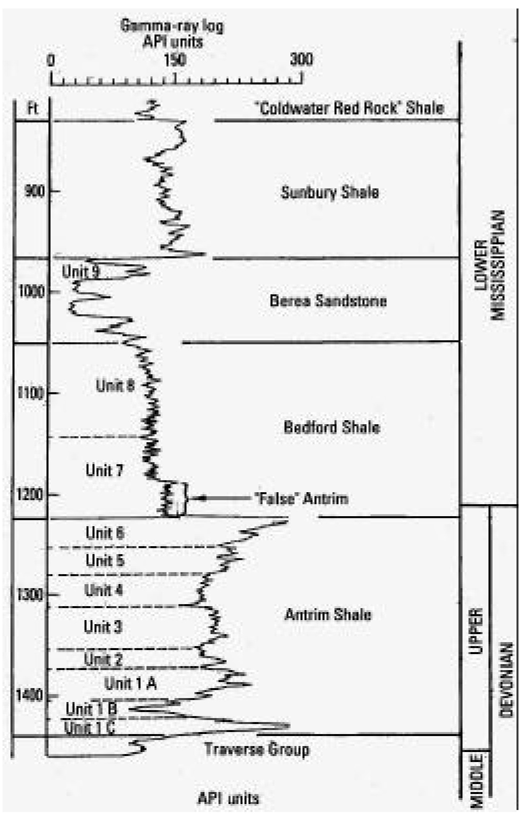

Figure 14: Gamma ray log of the Upper Devonian Antrim Shale and adjacent units in the northern Michigan basin. The main producing members are the Norwood Member (unit 1A) and Lachine Member (units 4-6). From Mathews (1993).

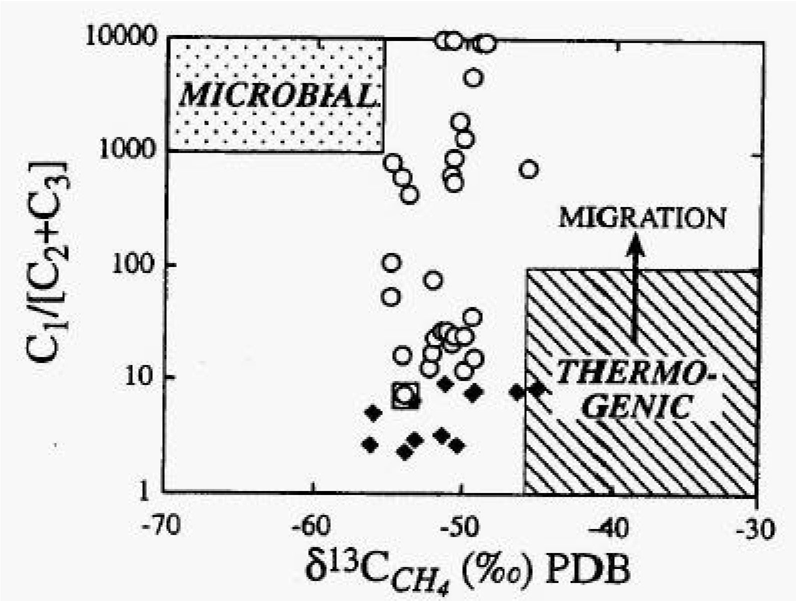

Figure 15: Isotopic composition of mixed microbial-thermogenic methane produced from the Antrim Shale in the northern Michigan basin, open circles (Martini and others, 1998).

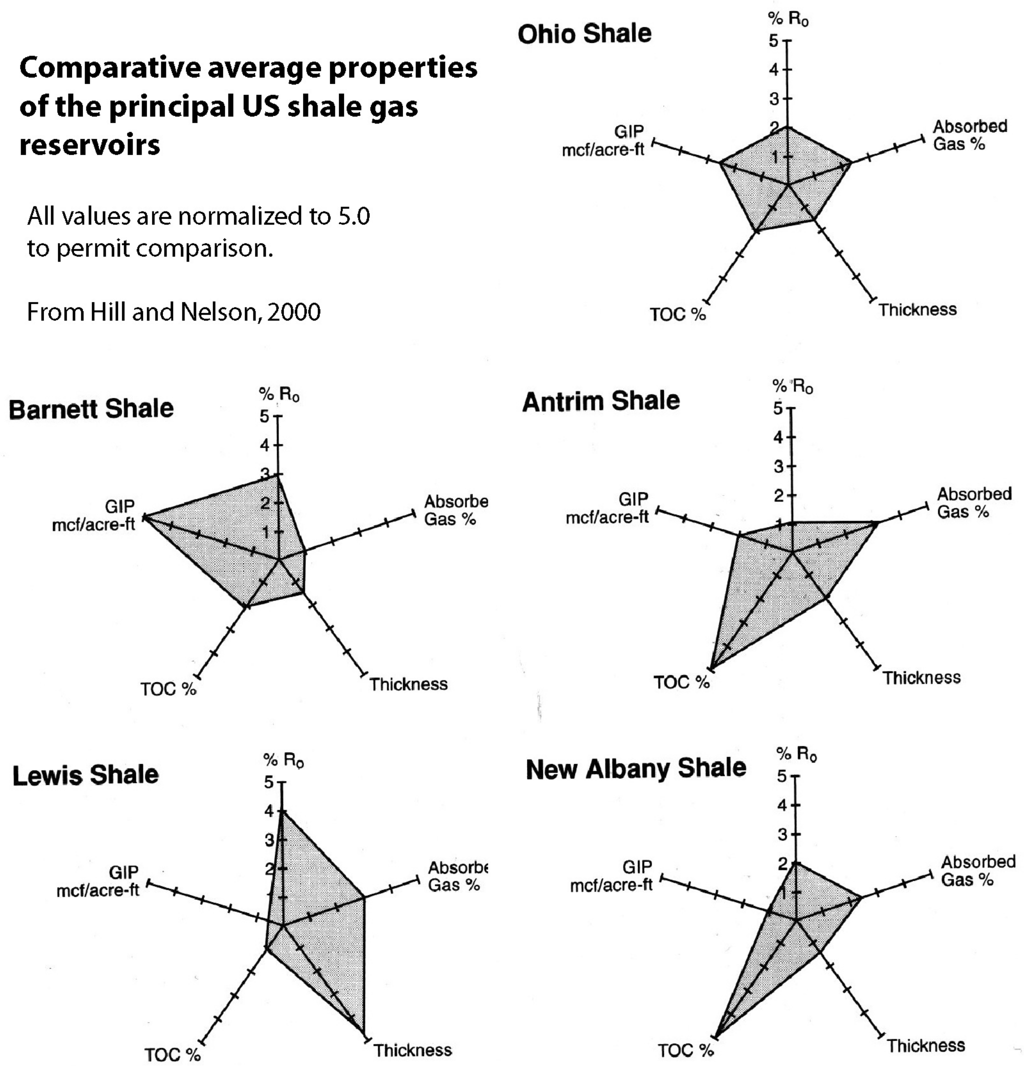

Figure 16: Spider plots permitting comparison of key characteristics of the five principal producing shale gas reservoirs in the United States (Curtis, 2002). Note the wide range in properties of the various reservoirs. The values are extracted from Table 2.

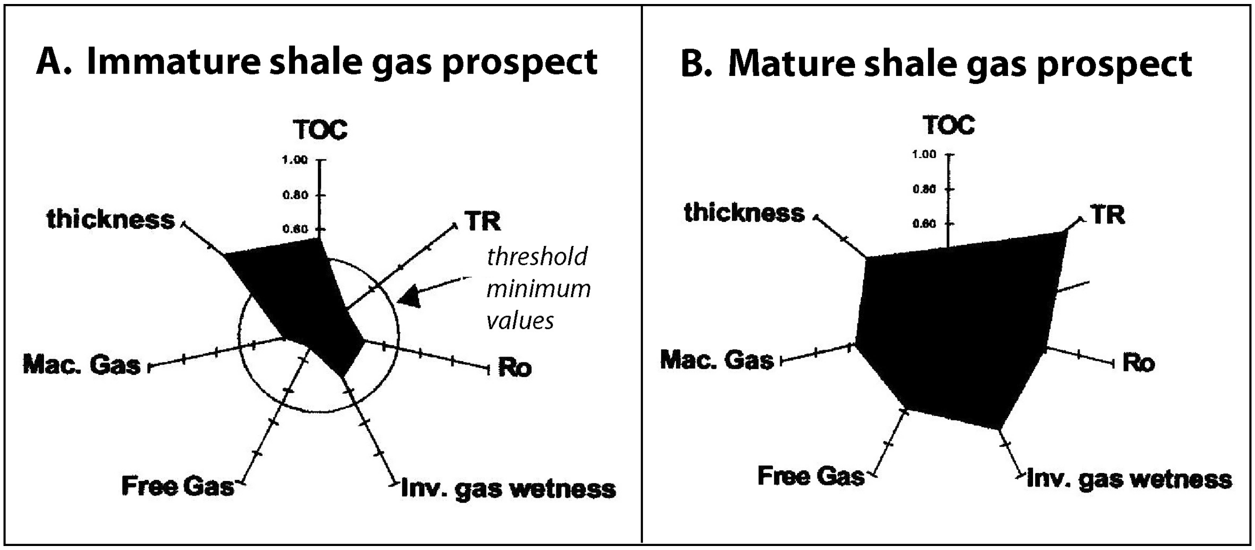

Figure 17: Prospect and well evaluation criteria based on geochemistry and source/reservoir thickness of the Barnett Shale (Jarvie and Claxton, 2002). Note that all values are normalized to 1.0 to aid in comparison.

A. Low maturity Barnett Shale has sufficient TOC and source thickness, but cannot generate and expel hydrocarbons.
B. Prospective areas in the wet and dry gas windows meet all screening requirements.

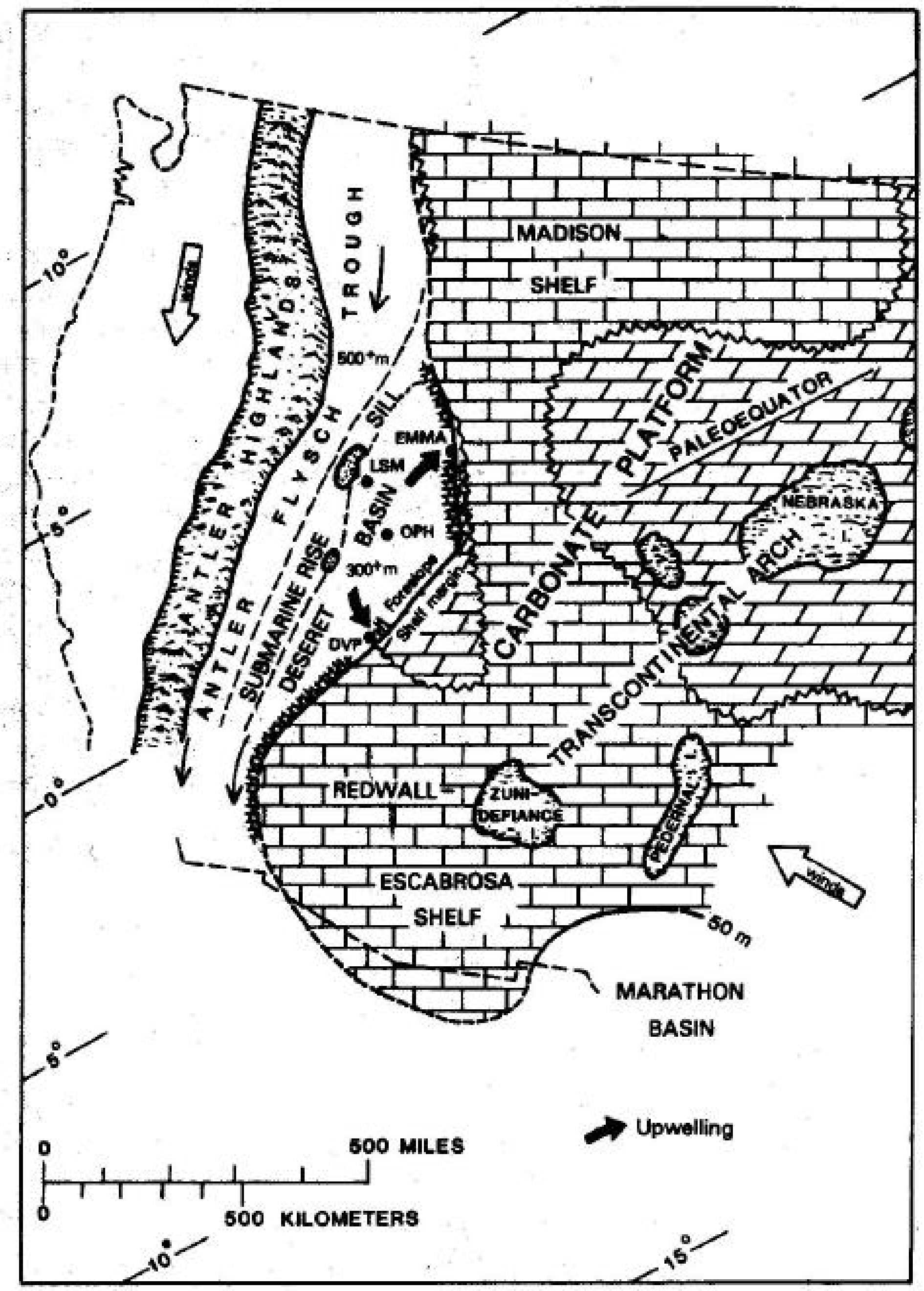

Figure 18: Mid-Mississippian paleogeographic map of western North America showing the position of the Deseret basin in relationship to the Antler orogen and foredeep and the cratonic carbonate platform (Sandberg and Gutschick, 1984).

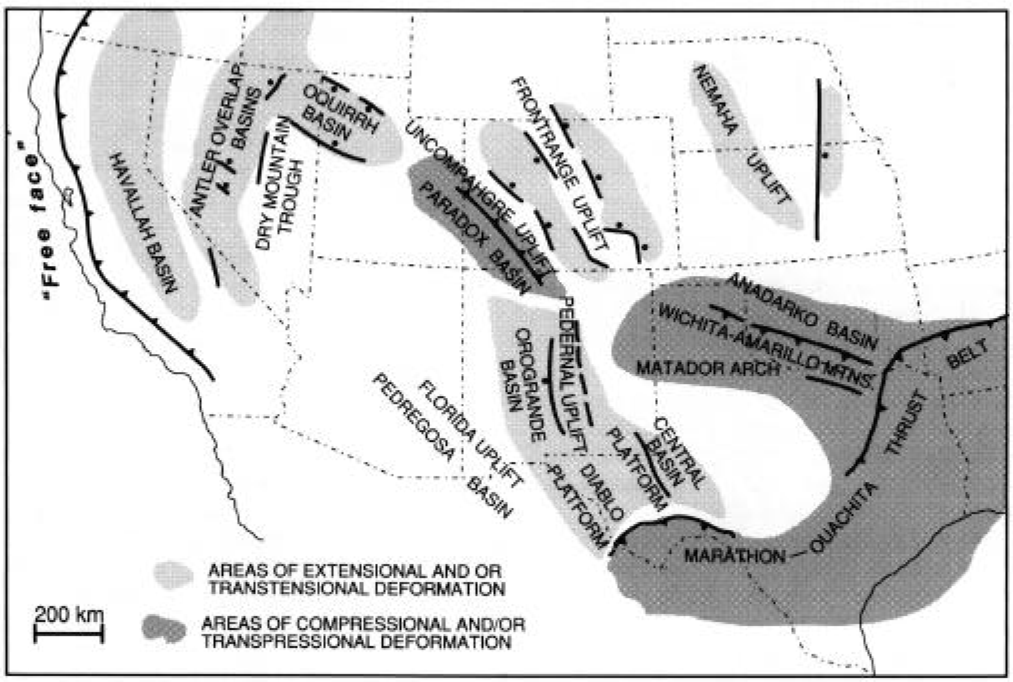

Figure 19: Continental interior basement uplifts and basins of the Ancestrial Rockies formed in response to emplacement of the Marathon-Ouachita orogen during collision of North America with Gondwana in Carboniferous-time (Smith and Miller, 1990). The two principal basins in Utah formed by this event are the Oquirrh and Paradox.

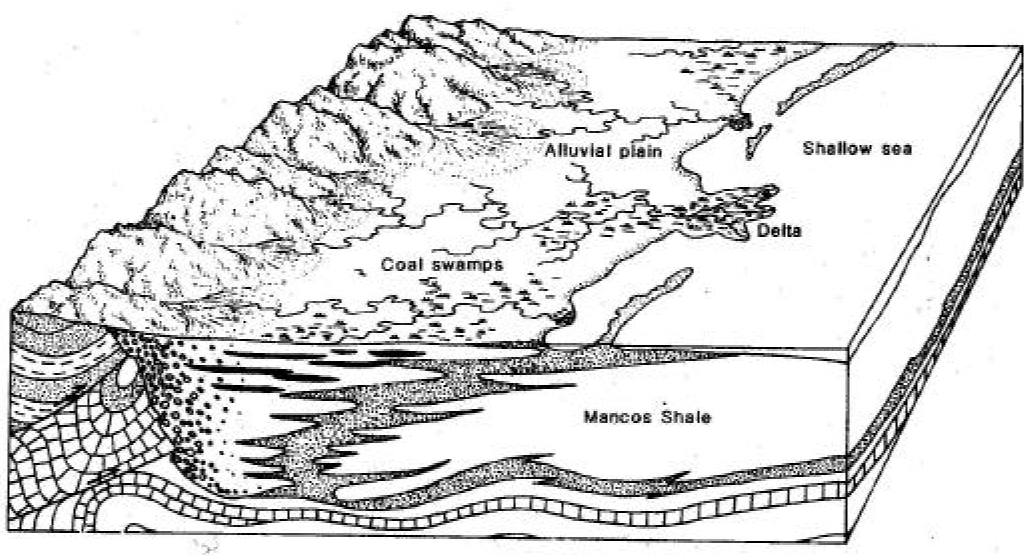

Figure 20: Late Cretaceous marine and non-marine depositional environments along the western margin of the Western Interior Seaway in Utah (Hinze, 1988).

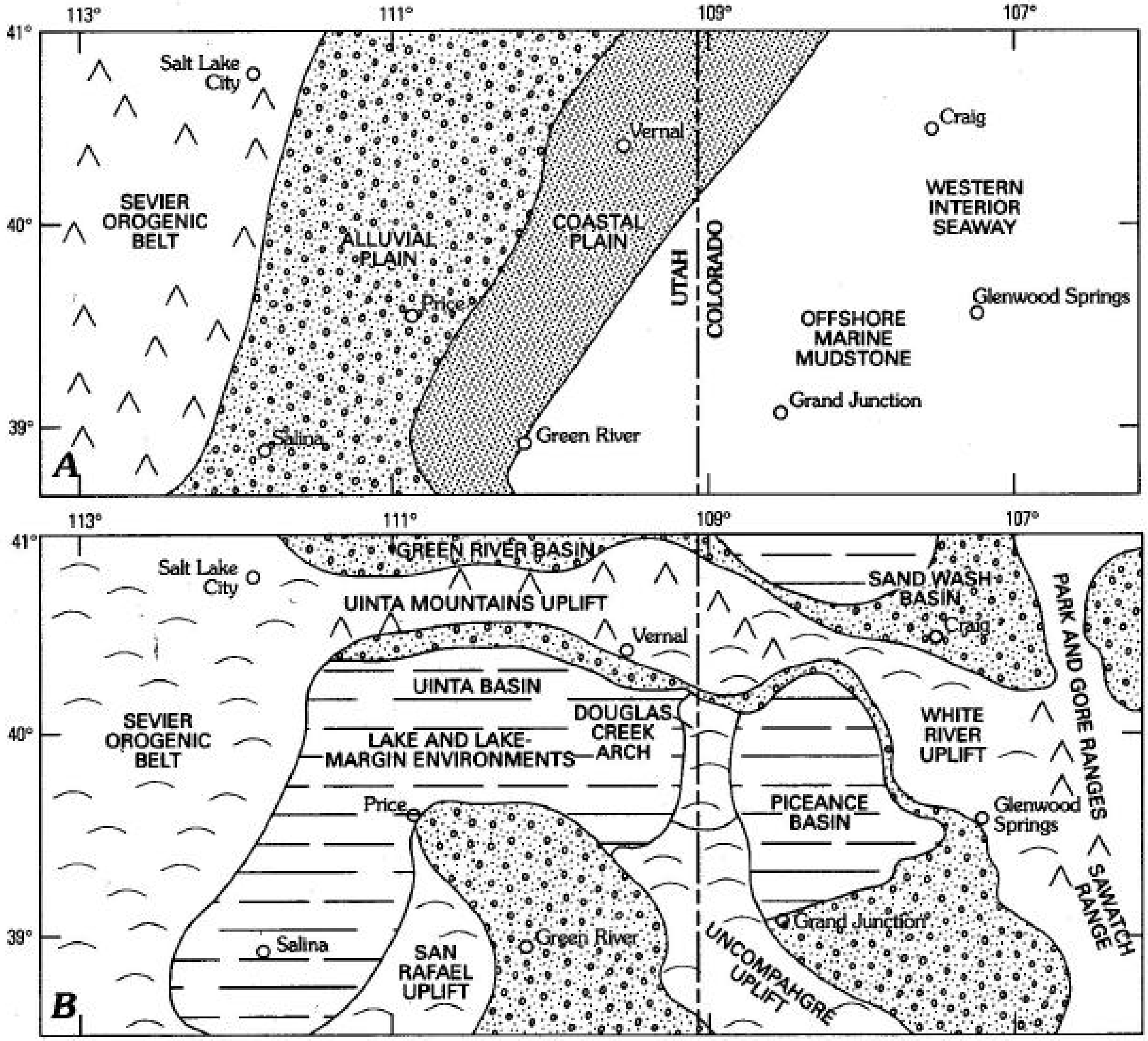

Figure 21: Paleogeographic maps showing the tectonic and depositional framework of the Uinta-Piceance basins during the (A) early Campanian and (B) early Eocene (Johnson, 1992).

Tertiary Black Shales: Green River Formation

The basal Green River Formation represents the initiation of Lake Uinta as a single, large lake. For much of the Eocene the lake occupied only a small part of the basin along the northern margin of the structural depression (Fig. 22, A). It was ringed by a 'marginal lacustrine' region that was periodically inundated by lake waters, the lake shoreline (Fig. 22, B). Beyond the shoreline were alluvial fans and delta complexes that sometimes encroached on the lake and at other times were flooded. The basin continued to receive sediments as long as the Uinta Mountains were rising, but latest Eocene or early Oligocene the lake had filled in with coarse fluvial sandstones and conglomerates of the Uinta and Duchesne River Formations.

The most important Tertiary source rocks in the Uinta basin are the kerogen-rich calcareous claystones and marlstones deposited as the open-lacustrine facies of the Green River Formation (Katz, 1995; Ruble and Philp, 1998). A distinction is drawn between those open-lacustrine facies assembledges that are *offshore* and continuously subaqueous and those that are *nearshore* and subjected to shoreline influences, including periodic subaerial exposure. The offshore open-lacustirine facies is characterized by black to beige, laminated or very thin bedded calcareous claystone and shaly carbonate. The kerogen in these high-grade *oil shales* is type I. They formed in relatively deep, quiet anoxic lake waters as alternating laminae of bacterial/algal ooze (Ruble and others, 1994) and algae-derived low-Mg calcite. The clay content is minor. The nearshore open-lacustrine facies is lithogically diverse and includes weakly laminated organic-rich mud-supported carbonate containing large Unionid pelecypods (Fig. 23, A) with black laminated mudstone and coal beds (Fig. 23, B) and scattered thin sandstone-siltstone beds (Fig. 23, C). Present also are beds of wachestone/packstone rich in ostracods and gastropod fragments (Wiggins and Harris, 1994). The siliciclastics accumulated mainly in offshore bars related spatially to deltas (Castle, 1990; Remy, 1992) entering the lake. In the interdeltaic portions of the shoreline (marginal lacustrine facies) were carbonate mudflats, ephemeral ponds and small peat mires that may or may not have preserved organic-matter (Ryder and others, 1976).

Subvertical fractures of several inches to several foot lengths are common in the Marsing 16 core (Fig. 23, A and B). Some fractures are lined with or bridged by sparry calcite; other fractures contain residual asphalt. Fracture orientations could not be determined in this unoriented core.

The open-lacustrine (black shale) facies rocks are distributed in two principal zones (Figs. 24 and 25) representing extended periods of lake flooding. The lower black shale interval is near the base of the Green River Formation. The upper black shale is the Parachute Creek Member, which contains the Mahogany oil shale bed. Near the paleo-axis of the lake, the two black shale intervals merge (Fig. 25, Duchesne section).

The total organic carbon in the open lacustrine (black shale) facies averages 3.1%, with a range of 0.5% to 8.1% (Wiggins and Harris, 1994). The kerogen in this facies, which constitutes the main Green River source rock, is exclusively type I (Fig. 26). The less organic-rich marginal lacustrine facies has kerogen ranging from type I to type III. The coaly matter in associated fluvial-alluvial sediments is exclusively type III kerogen.

Rice and others (1992) recognize two groups of natural gas in the Uinta basin based on carbon isotopic composition of methane and ethane (Fig. 27, A). Natural gas generated from type I kerogen and produced from the Green River Formation in the Altamont-Bluebell and Red Wash fields have methane ä^{13}C values of -58.1 to -46.9 $^{o}/_{oo}$, ethane ä^{13}C values of -39.4 to -34.1 $^{o}/_{oo}$, and methane äD values of -286 to -228 $^{o}/_{oo}$. C_{2+} values vary from 0 to 23.3%. The Green River natural gas is observed in the Altamont-Bluebell field to be progressively lighter with decreasing reservoir depth (Fig. 27, B) implying mixing of shallow microbial with deeper thermogenic gas. Natural gas produced from Tertiary reservoirs in the Natural Buttes field and generated from Cretaceous type III kerogens in the Mesaverde coals or Mancos Shale have a distinctly heavier isotopic carbon composition (Fig. 27, A). The methane ä^{13}C values are -35.7 to -35.2 $^{o}/_{oo}$, ethane ä^{13}C values are -26.2 to -26.0 $^{o}/_{oo}$, and methane äD values are -167 to -166 $^{o}/_{oo}$. The C_{2+} component of the gas is small, just 4.9 to 9.1%.

Even in the deeper part of the Uinta basin at the Altamont-Bluebell field (Fig. 28) the Mahogany oil shale bed is situated above the normal oil generative window for a type II kerogen and the pre-Eocene portions of the basal Green River black shale have thermal maturities of about 1.1-1.2% Ro (Nuccio and others, 1992), sufficient for generation of oil and associated gas. Closer to the basin margins the level of thermal maturity in the Green River Formation decreases such that in the western Natural Butts area it is merely 0.75% Ro at the Eocene-Paleocene boundary beneath the black shale. All but the lower black shales of the Green River Formation in the deeper parts of the Uinta basin are undermature with respect to hydrocarbon generation.

Thermal maturity is even more constrained if closed system, hydrous pyrolysis experiments on the Green River black shale (Ruble and others, 2001) provide the best description of the reaction kinetics of this source rock. The very large activation energy determined from the experiments of 68.7 kcal/mole and relatively small frequency factor (Ao) of 1.65 x 10^{32} my^{-1} suggest that the onset of oil generation from the Green River black shales will be delayed to about 0.75% Ro. The peak of oil generation would be at the equivalent of about 1.0 Ro and oil and gas generation would occur together over a relatively narrow generative window. A separate gas generative window, if even relevant in the Green River black shales, would have been reached only in the very deepest parts of the Uinta basin, if at all.

At normal depths of production, overpressuring occurs throughout the Uinta basin (Nelson, 2002). The highest overpressures are encountered in the Altamont-Bluebell field at depths greater than 10,000 ft (Bredehoeft and others, 1994). As this also is the basin center, the top of the overpressured region is within the lower Green River/Wasatch Formation. In this part of the basin the interval of maximum pressure gradient (0.60-0.80 psi/ft) is about 4,000 ft thick and extends to near the top of the Upper Cretaceous. This overpressured zone is considered to be associated with the active generation of oil and associated gas from the lower black shale of the Green River Formation (Bredehoeft and others, 1992).

The hydrogen-rich type I kerogen and waxy (high saturate) residual bitumen in the black shale facies of the Green River Formation can be expected to yield through thermal cracking very large volumes of natural gas (Lewen and Henry, 2001). Under high pressures, much of this gas is dissolved within the bitumen and resevoired crude, or adsorbed in kerogen. The principal drive mechanism throughout the Uinta basin is gas dissolution and gas expansion. Although oil generation is considered to be the reason for the overpressures locally reaching 80% of lithostatic in the Green River Formation beneath the Altamont-Bluebell district (Bredehoeft and others, 1994; Ruble and others, 2001), early generation of gas also must be a contributing factor. Fluid pressures approaching lithostatic pressure, in turn, can lead to permeability-enhancing microfractures that are required for obtaining commercial gas rates from the very low matrix-permeability Green River carbonates and mudstones. These oil shales could be considered a potential natural gas reservoir only in the deeper, abnormally-pressured portions of the Altamont-Bluebell field. But even here, occluded oil might seriously retard release of gas from the shale matrix. It is demonstrated in the Barnett Shale (Montgomery and others, 2005) that gas production is inhibited from oil saturated shale due to relative permeabilities issues.

Given the very large volume of kerogen-rich shales in the Uinta basin, much of which is close to the erosion surface, it is reasonable to speculate on the potential for commercial exploitation of microbial gas. It is known that some component of microbial gas is co-produced with oil in the Altamont field (Rice and others, 1992), but it is not known if this is merely associated gas, or co-mingled non-associated microbial gas. To develop a microbial gas play in the basin it is necessary to identify an effective shallow seal that would retard gas leakage, but that could be bypassed by meteoric waters bringing nutrients to the methanogenic microbes. Very shallow congealed oil mats that are known in some scattered parts of the Uinta basin might play this role. These oil mats are formed where ambient reservoir temperature is less than the pour point of the waxy crude. In the Bluebell field, non-associated natural gas is produced only from shallow wells penetrating the uppermost section of the Green River Formation (Morgan, 2003). It would be worthwhile to investigate the isotopic composition and mechanism of entrapment of this shallow gas resource.

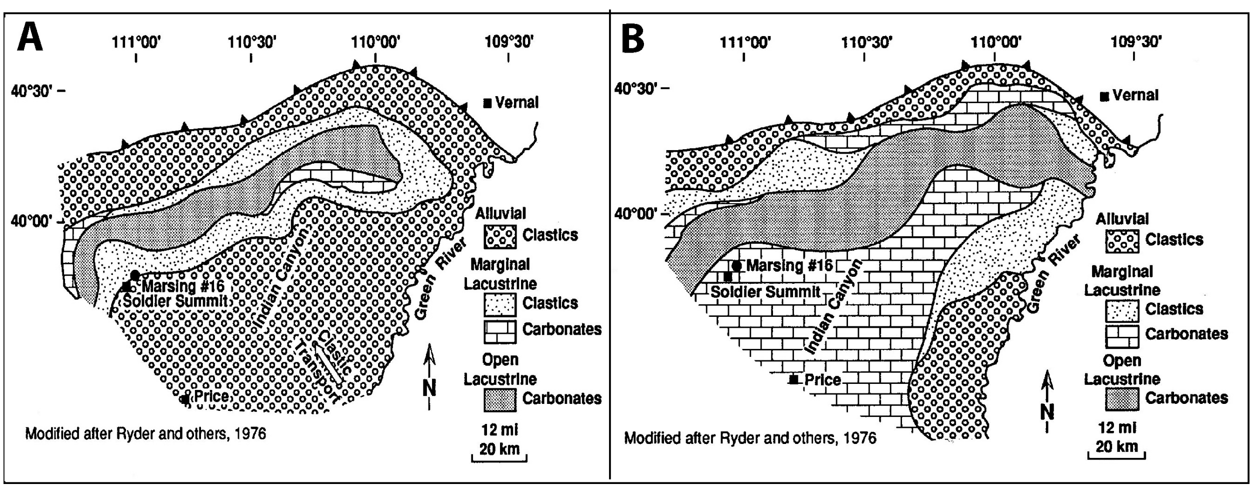

Figure 22: Green River Formation facies distributions in western Lake Uinta, that part of the Uinta basin west of the Green River (Wiggins and Harris, 1994). A. Late Paleocene - at this time the lacustrine facies had relatively limited extent in the foredeep immediately to the South Uinta thrust. B. Early Eocene - time of expanded open and marginal lacustrine deposition.

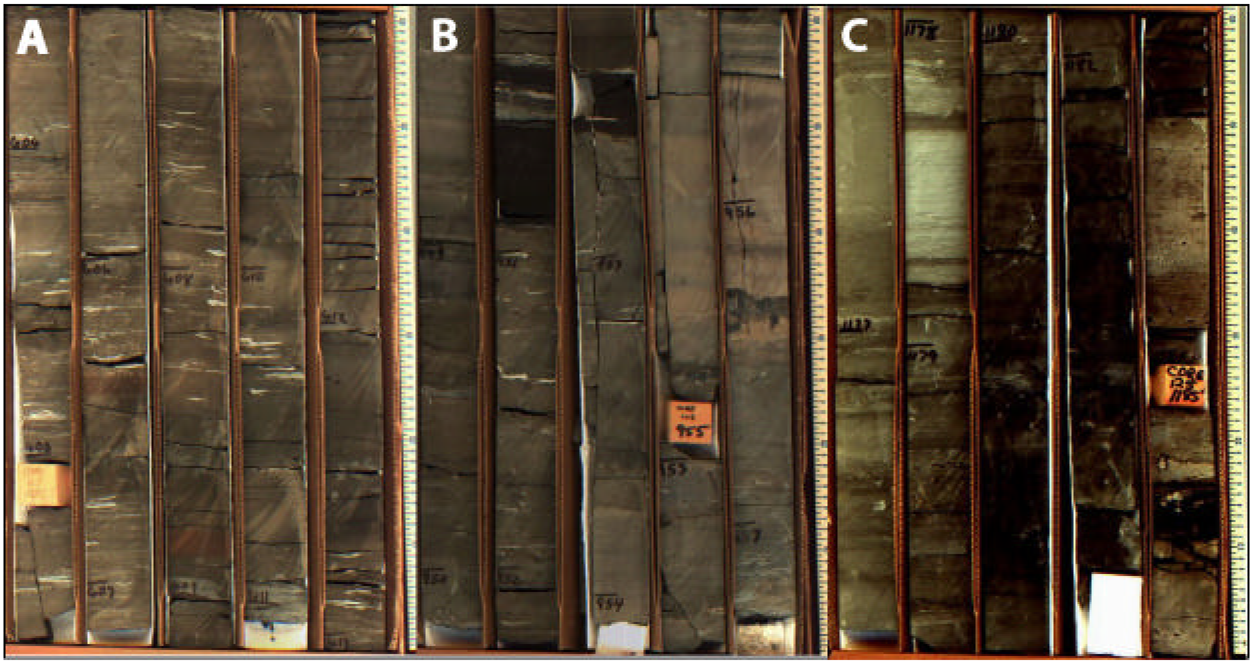

Figure 23: Representative nearshore open lacustrine to marginal lacustrine lithologies in the lower Green River Formation, Marsing 16 core. (Source: UGS files) A. Shelly organic-rich mud-supported carbonate at 604-613 ft depth; B. Organic-rich mud-supported carbonate with a 0.5 ft black sapropellic coal at 949-957 ft depth; C. Sandstone, shaly carbonate and carbonaceous mudstone at 1176-1185 ft depth. Note the subvertical fractures of 1-2 ft length in panels A and B.

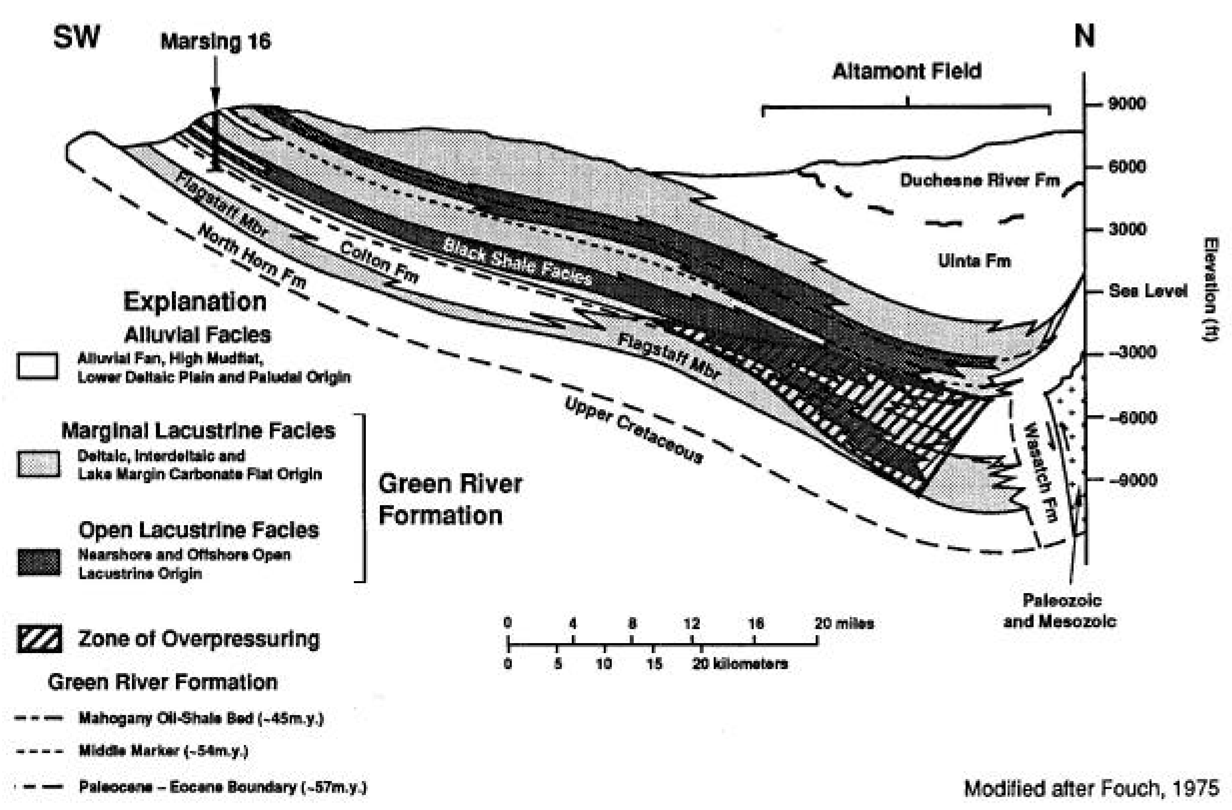

Figure 24: Structural cross section from Soldier Summit (Marsing 16 well) northeast to the Altamont field and South Uinta thrust fault near the structural and depositional axis of the Uinta basin (Wiggins and Harris, 1994). The open lacustrine facies, dark gray in the cross section, constitute the main body of 'black shales' in the Green River Formation.

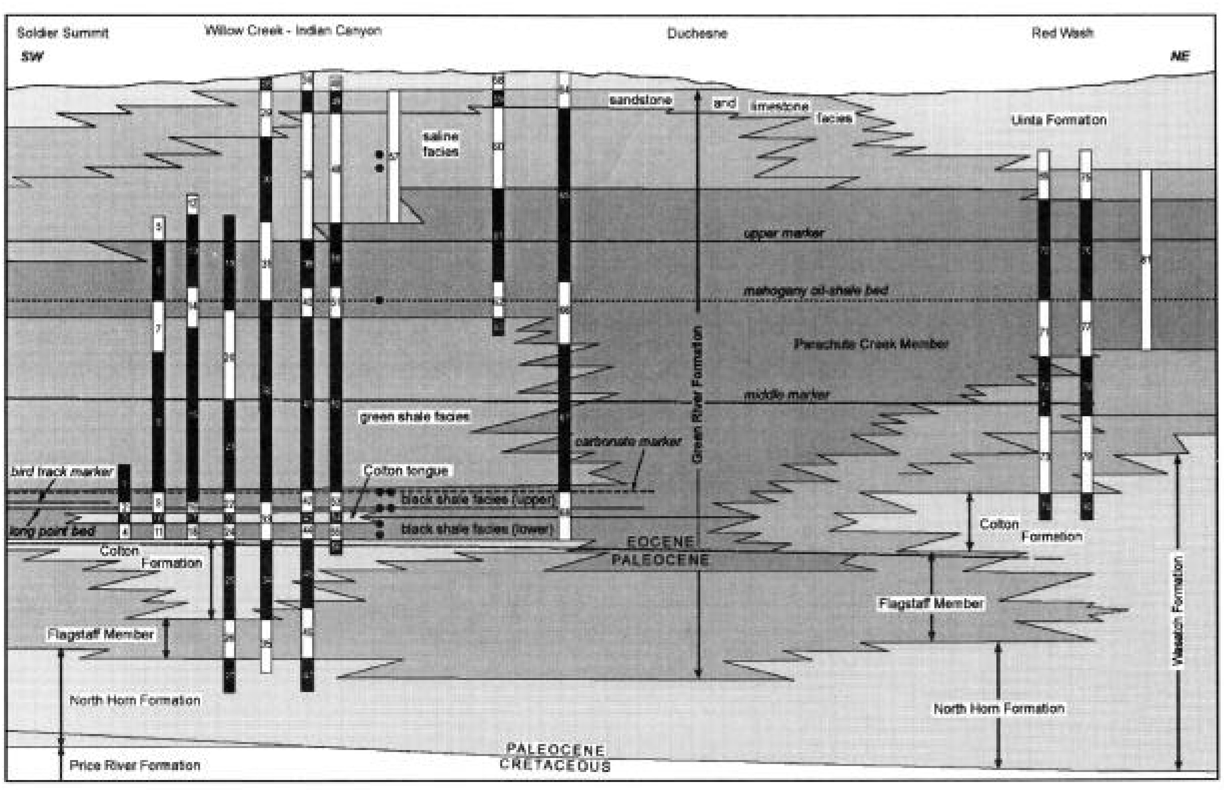

Figure 25: Stratigraphic cross section from Soldier Summit northeast across the Uinta basin to the Red Wash field, just east of the Green River south of Vernal (Ruble and Philp, 1998). The section illustrates temporal expansions and contractions of the open lacustrine (dark gray) and marginal lacustrine (medium gray) facies associations.

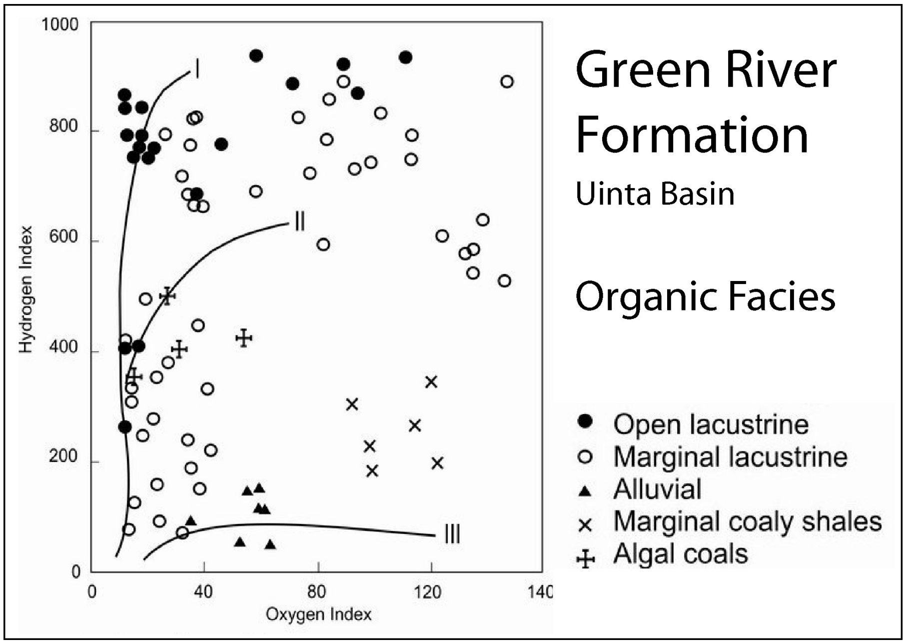

Figure 26: Highly variable kerogen types within the Green River Formation are dependent on the depositional setting. Based on RockEval pyrolysis data from Anders and Gerrild (1984) and Fouch and others (1994).

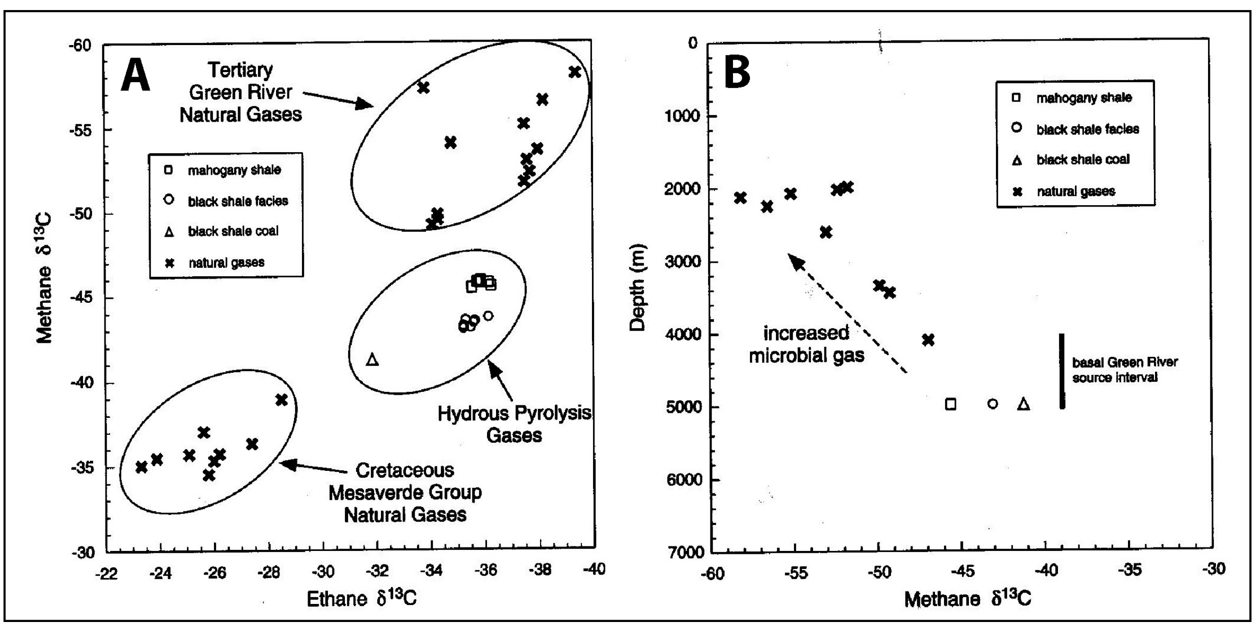

Figure 27: Isotopic composition of Green River natural gas (Ruble and others, 2001, adapted from Rice and others, 1992). A. Two groups of Uinta basin natural gases based on carbon isotopic composition of methane and ethane. B. Variation in methane ä^{13}C with depth of producing reservoir in the Altamont field, Uinta basin showing contribution of biogenic methane.

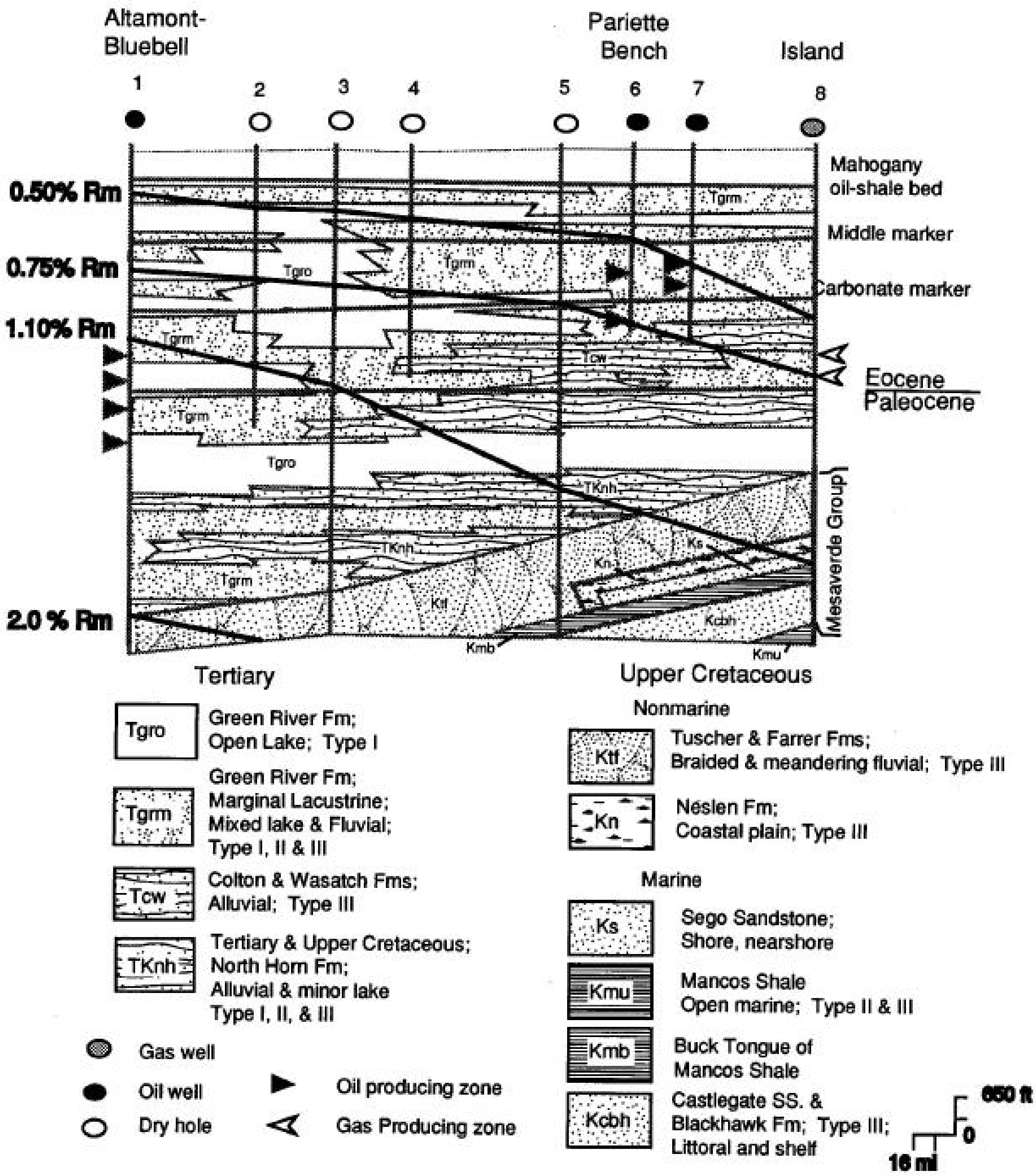

Figure 28: Thermal maturity levels superposed on a generalized northwest-to-southeast stratigraphic cross section of the Uinta basin from the Altamont field near the basin center to Island (Greater Natural Buttes gas field) near the eastern margin (Nuccio and others, 1992).

Potential Cretaceous Shale Gas Reservoirs

General Statement

All of the potential shale gas reservoirs of Cretaceous age are portions of the extremely thick Mancos Shale (or Mancos Group) deposited in a basinward position within the Western Interoir Seaway, the foredeep basin to the Sevier thrustbelt (Fig. 20). Most of the units represent transgressive episodes within the depositional history of the basin, but several of the higher units appear to have been deposited during times of overall regression. In every case, the organic-rich shale was deposited several tens of miles eastward of the coeval wave-dominated, sand-rich, fluvial-deltaic shoreline deposits and widespread peat mires. Deposition in proximity to these heavily vegetated high-stand shorelines resulted in a substantial humic (terrigenous) component of organic matter in the basinal shales.

The five units identified as having shale gas potential are:

1. the *Mowry Shale* of Cenomanian age, the lateral equivalent of the Dakota Sandstone in east-central and southern Utah,
2. the *Tropic-Tununk Shale* (Fig. 29) of lower and middle Turonian age and widely distributed across the eastern half of Utah,
3. the *Juana Lopez Member* of upper Turonian-Santonian age, a probable 'detached' siltstone-santstone body enclosed within the Mancos Shale and in part coeval with the Ferron Sandstone,
4. the *Lower Blue Gate Member* (Fig. 30), a thick uniform dark gray shale succession of Santonian age, and
5. the *Prairie Canyon (Mancos B) Member* (Fig. 30), a second 'detached' siltstone-sandstone body coeval with the Emery-Star Point-Blackhawk (Campanian) highstand shoreline successions.

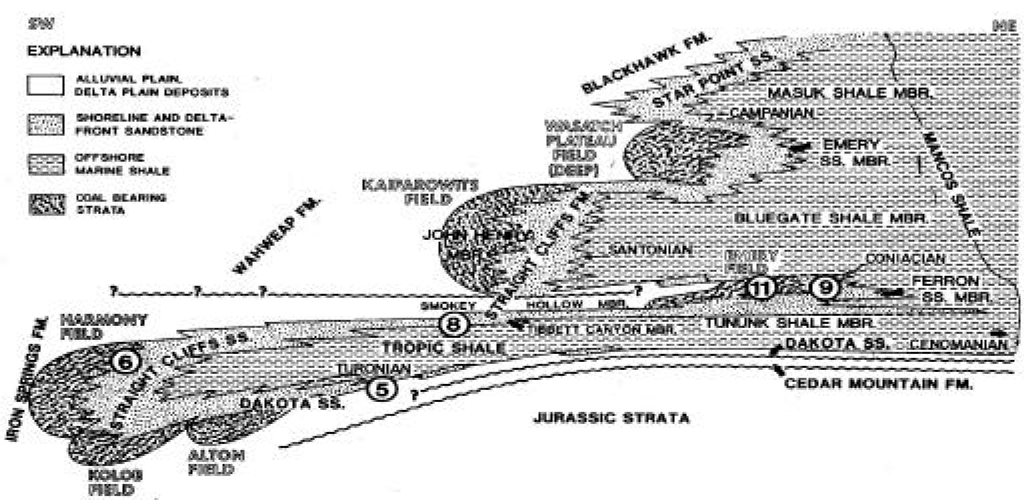

Figure 29: Generalized stratigraphy of the Cretaceous foreland basin in southern and east-central Utah (Ryer, 1984).

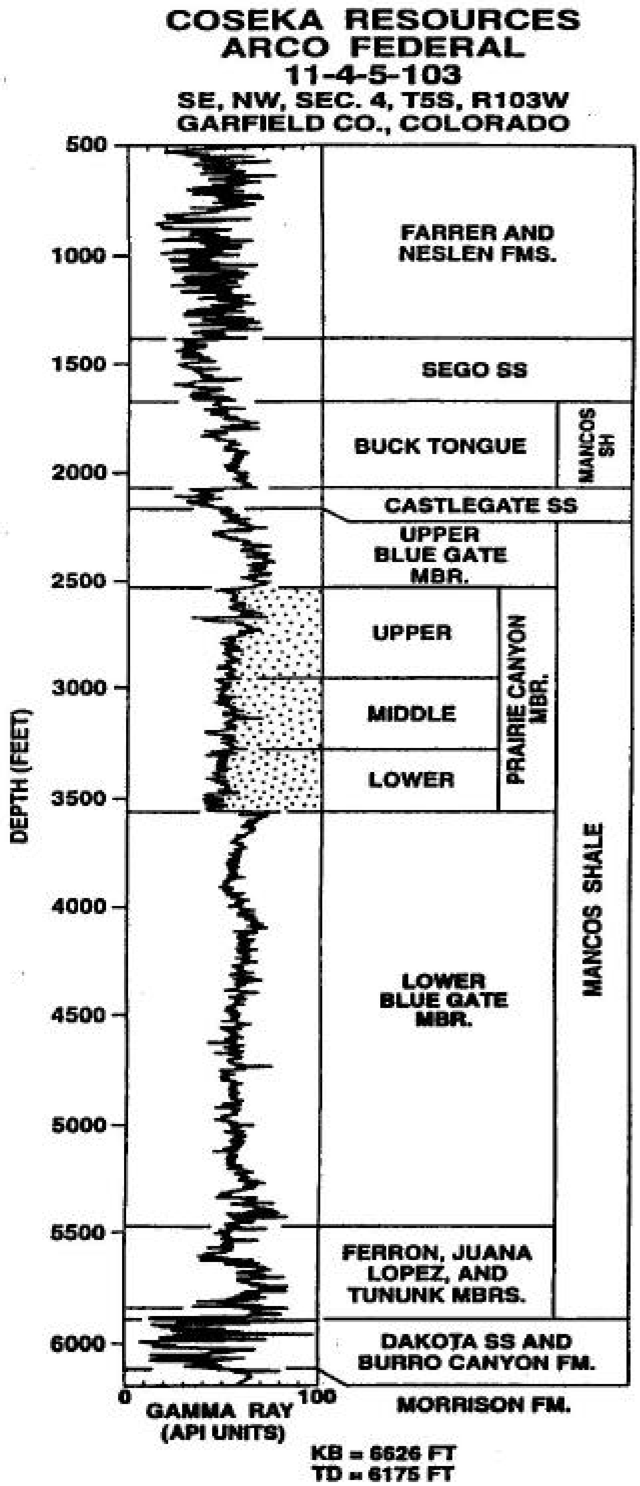

Figure 30: Stratigraphy of the Mancos Shale over the Douglas Creek arch (from Cole and others, 1997).

Mowry Shale

The Mowry Shale is an important source of commercial gas and oil accumulations in the Southwestern Wyoming Province (Kirschbaum and Roberts, 2005). In Utah, the Mowry Shale is platy to dark gray, fissile, hard siliceous shale with beds of porcelanite, a hard siliceous nonfissile radiolarian chert-like rock having conchoidal fracture, and scattered bentonite layers (Reeside and Cobban, 1960; Molenaar and Wilson, 1990). The unit is characterized by an abundance of fish remains, scales up to 20 mm in diameter, ribs and vertebrae, but only rare ammonites. In northeasternmost Utah, thin gray limestone beds occur near the base of the unit (Hansen, 1965). In electric logs, the Mowry Shale is distinguished from shales of the overlying Frontier Formation by higher resistivity of the Mowry Shale due to higher silica content.

It is the equivalent of the thick Aspen Shale in western Wyoming, but which thins dramatically southward towards the Dakota shoreline (Fig. 31) and westward towards the Sevier orogenic front (Ryer, 1976; Ryer, 1977).

The Mowry Shale is lower Cenomanian in age and rests conformably on the underlying Dakota Sandstone, but it is separated from the overlying Frontier Formation by a hiatus representing the middle and upper Cenomanian and lower Turonian (Molenaar and Cobban, 1991).

In northeast Utah, the Mowry Shale varies in thickness from 285 ft in the northwest Uinta Mountains at the Bridger Lake field to just 80-90 ft southeast of Vernal. Along the north flank of the Uinta Mountains (Hansen, 1965; Molenaar and Cobban, 1991) the unit is nearly everywhere greater than 200 ft thick (Fig. 32). Beneath the Uinta basin, at approximately 40°N, the Mowry Shale dies out southward by facies change and interfingering into the Dakota Sandstone and/or by erosional beveling. The facies change from Mowry Shale to Dakota Sandstone is reported to be observed in outcrops 4 to 18 miles southwest of Rangely, Colorado (Molenaar and Cobban, 1991). The unit is totally absent beneath the southern Uinta basin and Book Cliffs area.

In northeast Utah organic richness (Fig. 31) ranges from 1.2 to 2.4% TOC, and the kerogen type (Fig. 33) is mixed type III and type II, gas-prone humic-sapropelic (Burtner and Warner, 1984). Nevertheless, the Mowry Shale is a known oil source rock in the Wyoming overthrust belt (Warner, 1982) and throughout Wyoming, Colorado and the northern Rocky Mountain basins (Kirschbaum, 2003).

Kirschbaum and Roberts (2005) assert that the Mowry source rocks are mature across much of the Southwestern Wyoming Province, but in Utah there are no published data for the organic maturity of the Mowry Shale. The only constraint on maturity are Ro values of 0.6% in the younger Adaville Formation coals in a well penetrating the hanging wall sheet of the Hogsback thrust (Tabet and Quick, 1999). Given that the kerogen has a large humic component, the Mowry Shale could be gas-generative east of the Absakora thrust. Also, as a siliceous shale it might respond favorably to fracture stimulation. However, the parts of Utah north of the Uinta Mountains where a play might be possible has problems. The Mowry Shale is likely too deep in the hanging wall plate of the Hogsback thrust in eastern Summit County (Lammerson, 1982;

Section G). The strip north of the Uinta Mountains in Daggett County where the Mowry Shale is nearer the surface is only a few miles wide.

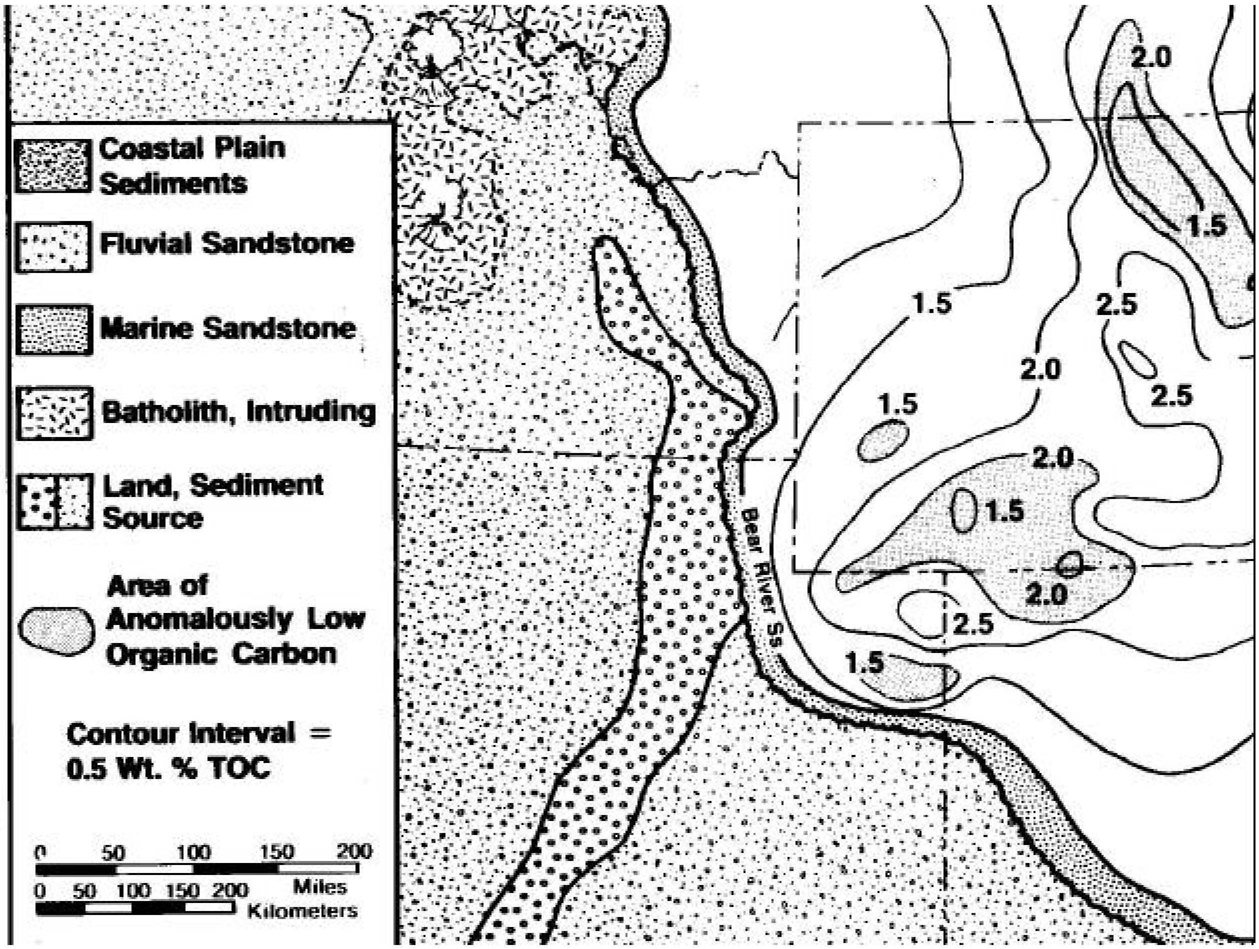

Figure 31: Approximate location of the Dakota (Bear River) shoreline in the early Cenomanian and the distribution of average organic richness (TOC) in the Mowry Shale in northeast Utah and adjacent parts of Wyoming and Colorado (modified from Butner and Warner, 1984).

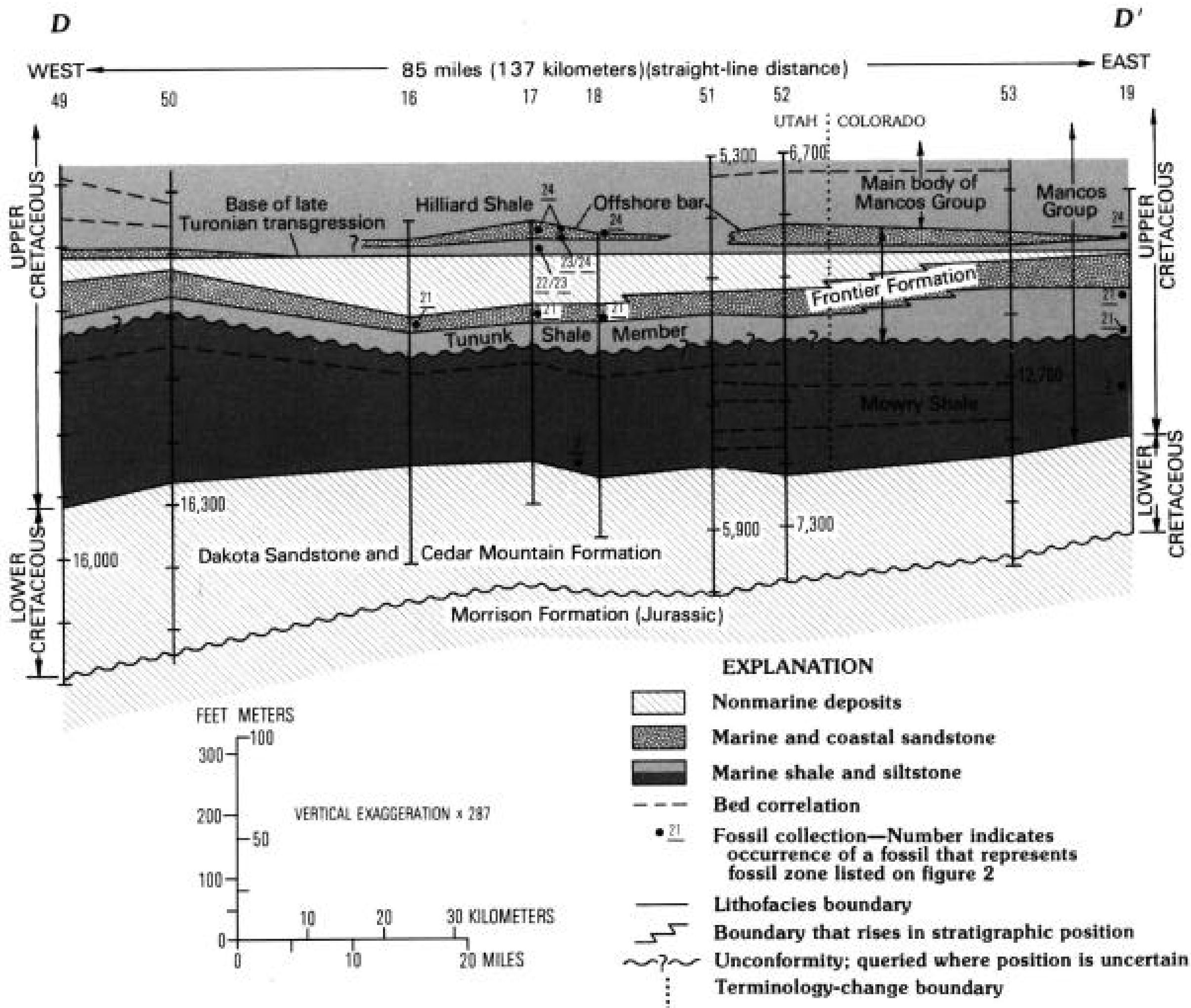

Figure 32: Stratigraphic section for the Mowry Shale (dark gray pattern) and adjacent units along the north flank of the Uinta Mountains from the Bridger Lake field on the west to Vermillion Creek, Colorado on the east (Molenaar and Wilson, 1990). Along this traverse, the Mowry Shale is unconformably overlain by the Tununk Shale.

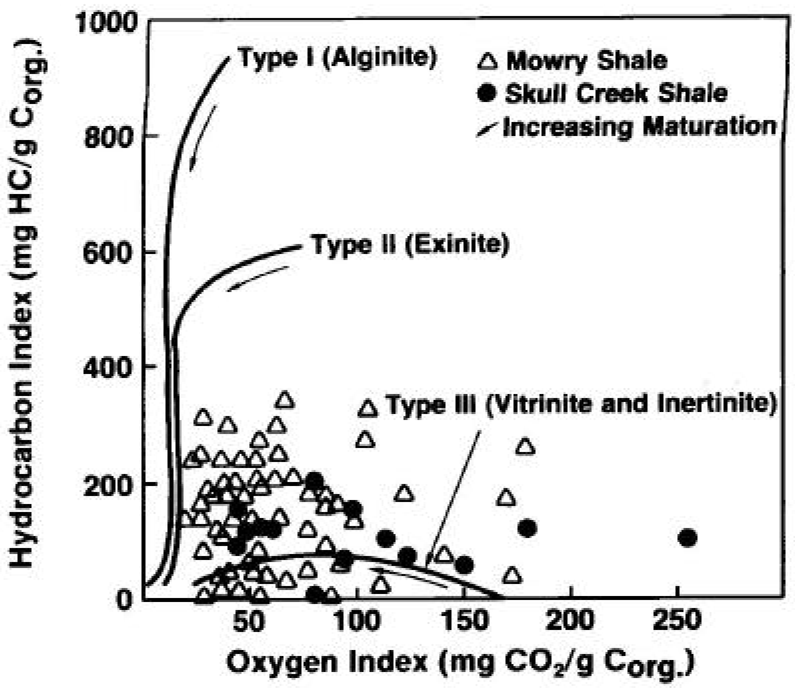

Figure 33: The Mowry Shale (open triangles) is dominantly Type III and Type II-III kerogen of low to intermediate maturities, based on open-system pyrolysis analyses reported in Burtner and Warner (1984).

Tropic-Tununk Shale

The Tropic Shale of the Kaiparowitz Plateau region of southern Utah (Lawrence, 1965) is correlative with the Tununk Shale of east-central and northeast Utah (Molenaar and Cobban, 1991). The Tropic-Tununk shales are composed primarily of dark gray calcareous claystone and mudstone with 17 bentonite beds that can serve as regional markers (Zelt, 1985). Except in east-central and northeast Utah where a regional hiatus is present, both shales are of latest Cenomanian to upper middle Turonian age, form the base of the Mancos Formation, and rest conformably on the Dakota Sandstone of Cenomanian age.

In southern Utah, the Tropic Shale (Fig. 34) is 500-825 feet of dark gray claystone containing thin lenses of siltstone and very fine-grained sandstone, bentionite beds and limestone concretions (Lawrence, 1965). Fossils include dwarfed ammonites, shark teeth, fish scales and bones, and thin calarenite beds with Ostrea fragments and shark teeth. The unit passes gradually downward into coal-bearing sandstone, conglomerate and bentonite of the uppermost Dakota Sandstone, with no unconformity present. Upward the Tropic Shale is overlain by 100-300 ft interval of interbedded shale and thin sandstone beds of the Tibbet Canyon Member of the Straight Cliff Formation, which is transitional into the main coal-bearing sandstones of the Smokey Hollow and John Henry Members (Ryer, 1984). Beneath the Kaiparowits Plateau and Henry Mountains, the Tropic Shale is underlain and overlain by commercial coal beds (Doelling, 1972). At maximum flooding the Straight Cliff shoreline coeval with the Tropic Shale was stabilized near Zion National Park (Fig. 34).

In east-central Utah (Castle Valley and Book Cliffs areas) the Tununk Shale is about 300-650 ft of dark gray calcareous claystone with bentonite beds passing upward into interbedded dark gray silty mudstone and bioturbated siltstone (Molenaar and Cobban, 1991). The Tununk Shale thins eastward towards the Utah-Colorado border, possibly on to a reactivated Uncompahre uplift. The unit is reported to be 400-650 ft thick in the Castle Valley (Witkind, 1988; Weiss and others, 1990), 400 ft thick immediately east of Price, and about 300 ft thick east of the Green River (Gualtieri, 1988; Molenaar and Cobban, 1991). The base of the Tununk Shale is a regional unconformity on the Cedar Mountain Formation.

In the vicinity of the Uinta Mountains, the base of the Tununk Shale is of lower or middle Turonian age (Molenaar and Cobban, 1991). The Tununk Shale passes upward into upper shoreface or delta front sandstones (Ryer and McPhillips, 1983) of the Ferron Sandstone of late middle Turonian age. The Ferron Sandstone is the facies and approximate age equivalent of the Straight Cliff Formation (Fig. 29) in southern Utah (Ryer, 1984).

With a single notable exception, detailed core-based stratigraphic descriptions and quality geochemical analyses of the Tropic-Tununk Shale are absent in the public domain. The 901 ft Escalante #1 well (36-35S-2E, Garfield County) was drilled (Fig. 35) and cored in June 1992 by the U.S. Geological Survey as a stratigraphic well under the auspices of the U.S. Continental Scientific Drilling Program (Dean and Arthur, 1998). The core has been described by several groups and no fewer than three independent geochemical studies of the core material exist (refer to material in Appendix A). At present, this core is the best window available into the character of this lower portion of the Mancos Shale in Utah.

In describing the lithology of the Tropic Shale in the Escalante #1 core, Leithold and Dean (1998) distinguish a calcareous, organic-lean lower unit from a less calcareous, organic-rich upper unit. The upper unit (341-459 ft depth) is thinly interlaminated siltstone and silty claystone grading upward into silt-free claystone (Fig. 36). This unit is dominated by 1-2 cm thick, graded, ripple-cross-laminated siltstone beds with sharp bases against scoured dary gray claystone. The lower unit (459-689 ft) is dominantly finely laminated marlstone and calcareous claystone with scattered fecal pellets, foraminiferal tests and fine shell debris. Laminae commonly are concentrations of fecal pellets, and they may be disrupted by burrows.

The majority of the the graded siltstone and claystone beds with sharp bases are interpreted as turbidites (Leithold and Dean, 1997). But the presence of wave-rippled siltstone in the upper unit and the pellet-rich laminated claystone in the lower unit indicate sediment reworking by bottom currents, perhaps during extreme storms or due to large-scale basinal gyres.

The organic richness of the Tropic Shale (Fig. 37) in the Escalante #1 well is variable ranging up to 3.86% and averaging 1.40±0.52% (White, 1999). Bojesen-Koefoed and Nytoft (2003) cite a slightly higher average of 1.56% and a range of 0.89% to 2.64%. The values are lowest in the lower carbonate-rich portion of the section, but then increase upward as the carbonate-content diminishes in the upper section. The profile of hydrogen index (HI) with depth mirrors the TOC profile (Fig. 38) with the highest values of 200-250 occurring near the top of the Tropic Shale. The general low values of HI, however, are indicative of a type II and mixed type II-III kerogen (Fig. 39). There can be little doubt of the significant humic component in the organic matter given the low HI and proximity to coastal peat mires, yet Bojesen-Koefoed and Nytoft (2003) interpret gas chromatography data showing poly-modal, strongly light-end skewed n-alkane distributions as indicating that the kerogen is dominantly of marine algal origin with very limited terrestrial input.

In the upper 75 feet of the Tununk Shale penetrated by the River Gas of Utah #1 well in Carbon County (see next section for details), Dumitrescu (2002) reports three TOC values in the range 1.62-1.71%. Here the rock is a dark gray calcareous mudstone with silt to very fine sand laminae and interbeds, and silt-filled burrows (Fig. 40).

The Tropic-Tununk shales appear to have relatively low thermal maturities throughout southern and east-central Utah. In the Escalante #1 core, Tmax values average 424.2 ±3.7°C, increasing slightly with depth in the well (Bojesen-Koefoed and Nytoft, 2003). These values are approximately equivalent to a vitrinite reflectance (Ro) of 0.5-0.6% and in line with the maturity of coal in the region. The rank of Straight Cliffs coal in the Carcass Canyon coal area (Doelling, 1968) on the Kaiparowits Plateau about 10 miles southeast of the Escalante #1 well is high volatile C bituminous, equivalent to 0.6% Ro. To the north in the Emery coalfield (Emery County) the coals in the Ferron Sandstone also are high volatile C bituminous rank (Gloyn and others, 2003), but further north in the Drunkards Wash CBM field (Carbon County) the rank of the Ferron coals (Montgomery and others, 2001) is high volatile B bituminous (0.7-0.8% Ro). Across southern Utah the Tropic Shale may be generating little natural gas, but in east-central Utah the Tununk Shale is likely a significant gas generator. This is especially true beneath the Wasatch plateau and Uinta basin.

Vitrinite reflectance values beneath the central and southern Uinta basin (Fig. 41) are well within the gas generative window at the level of the Tununk Shale, especially for type II-III kerogens. This shale unit must be seen as a possible shale gas reservoir in this region.

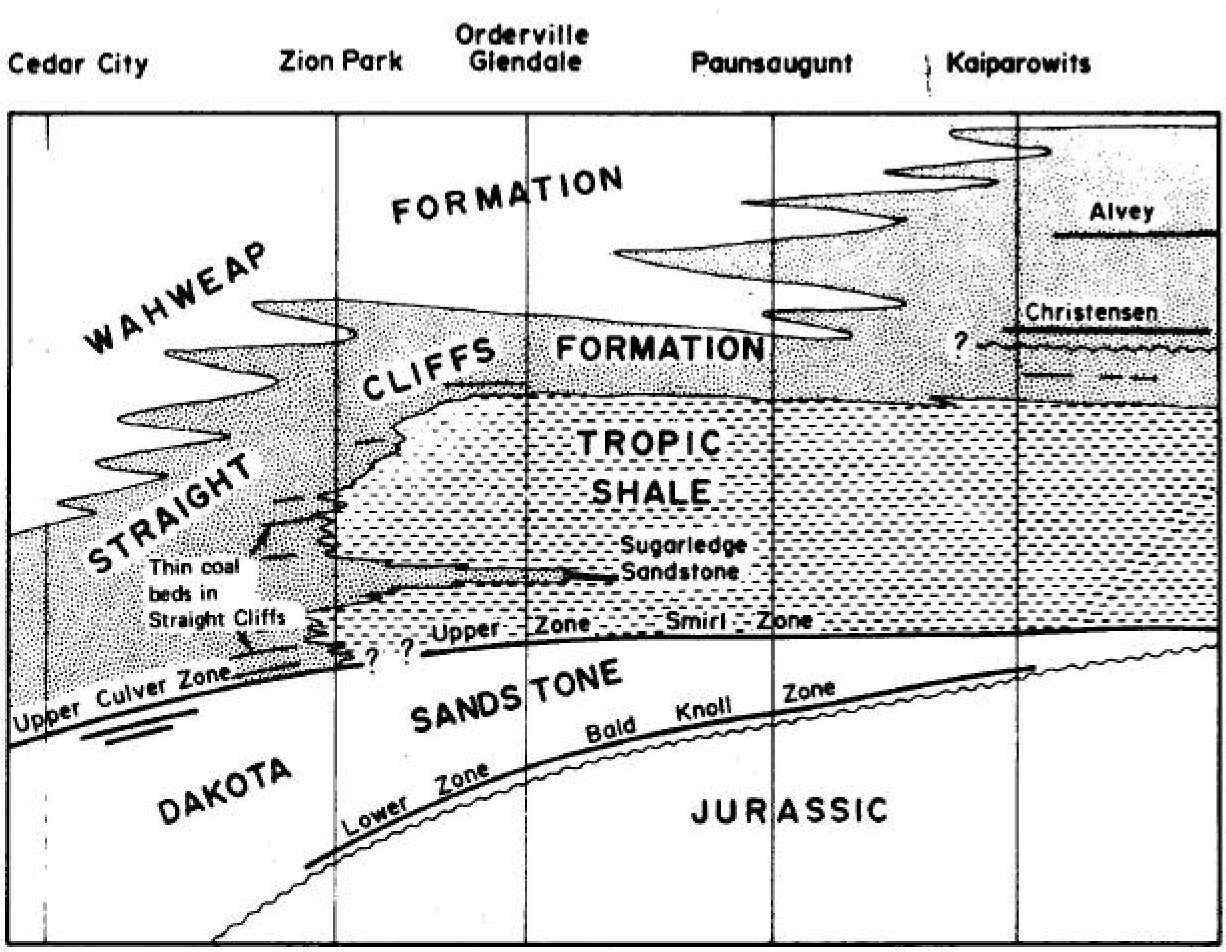

Figure 34: Stratigraphic position of the Tropic Shale in southern Utah in relation to the Dakota Sandstone and Straight Cliffs Formation (Doelling, 1972, modified from Lawrence, 1962). Note the presence of commercial coal zones both below and above the Tropic Shale.

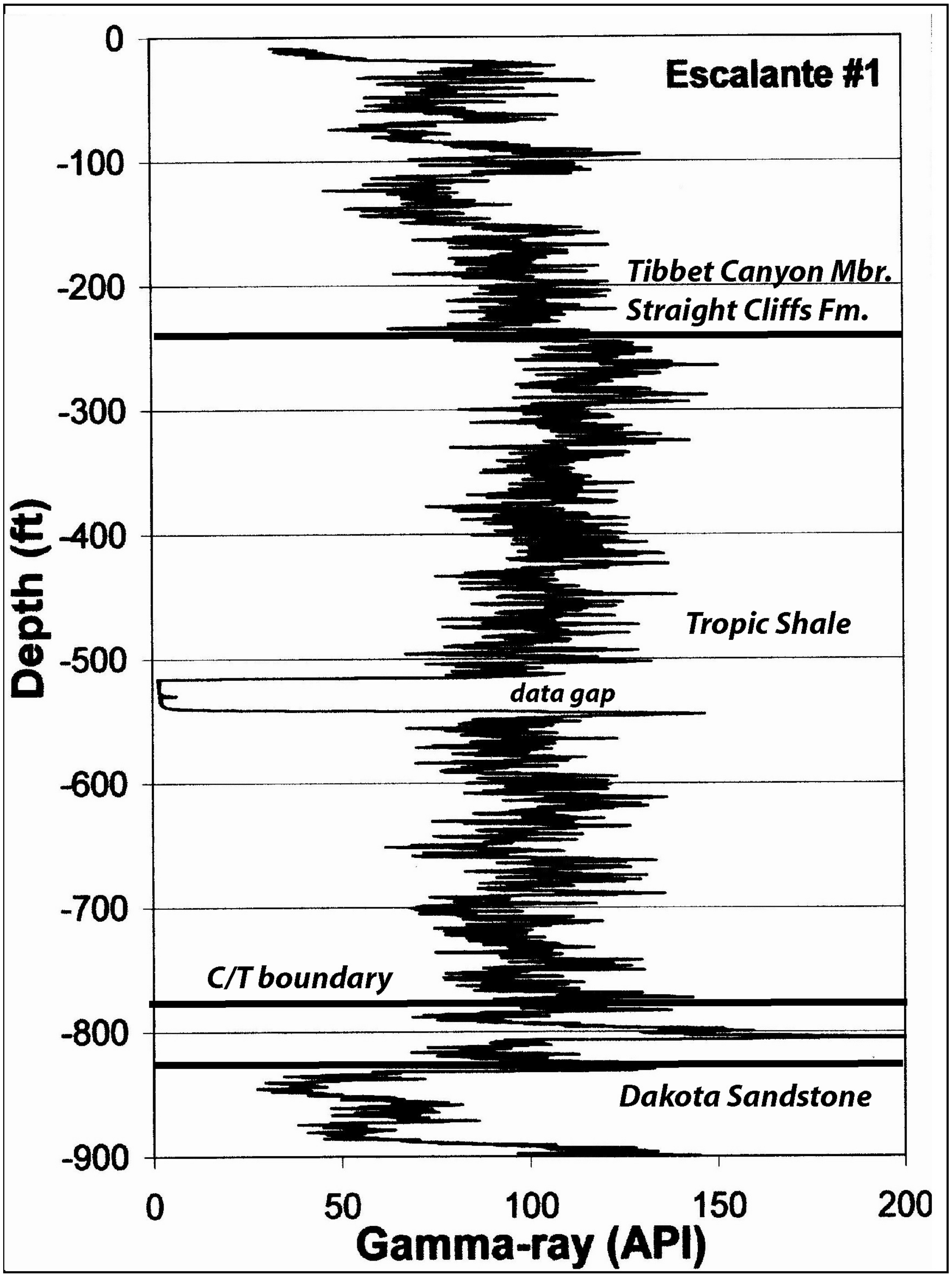

Figure 35: Gamma-ray log through the Tropic Shale at the Escalante # 1 well in the northern Kaiparowits Plateau, Garfield County. The Tropic Shale stands apart from the overlying Tibbet Canyon Member of the Straight Cliffs Formation and the underlying Dakota Sandstone in having uniformly higher GR values that generally increase upward. The Cenomanian-Turonian boundary is near the base of the Tropic Shale. Gamma-ray log data and boundaries courtesy of Walter E. Dean, U.S. Geological Survey.

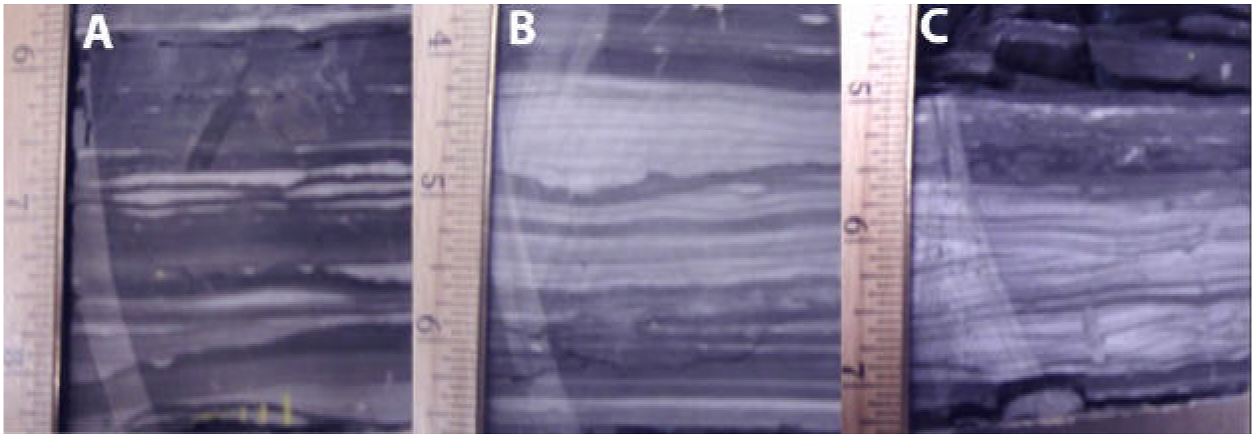

Figure 36: Photos of representative sedimentologic features in the Escalante #1 core.
A. Graded laminated siltstone lenses within very dark gray laminated calcareous claystone at 340.9 ft depth in well; B. Interbedded thinly laminated, graded siltstone with loadcasts and dark gray claystone at 434 ft depth; C. Cross-bedded and burrowed thinly laminated siltstone overlain by very dark gray calcareous claystone at 444 ft depth.

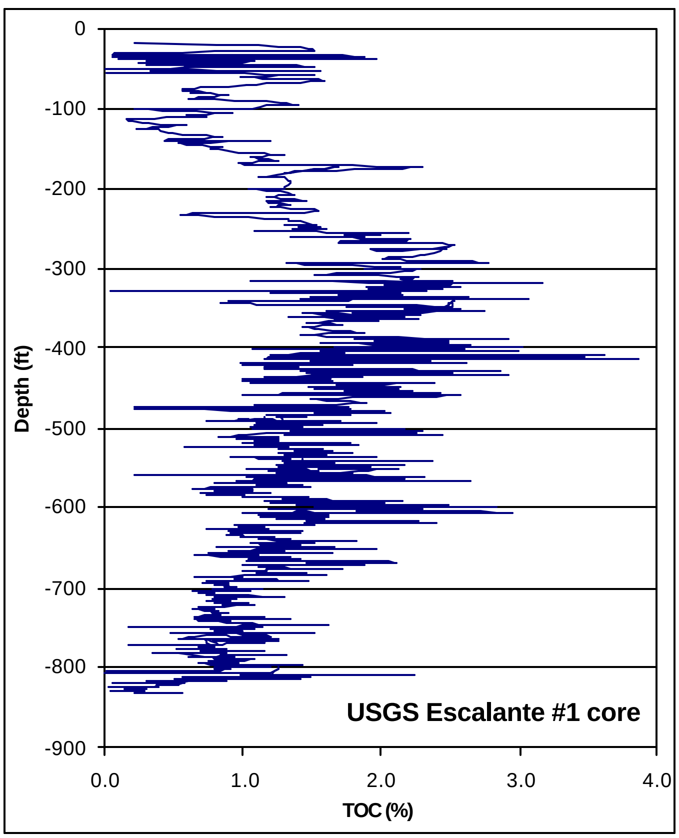

Figure 37: Vertical variation in organic richness in the Escalante #1 core. Data from White (1999).

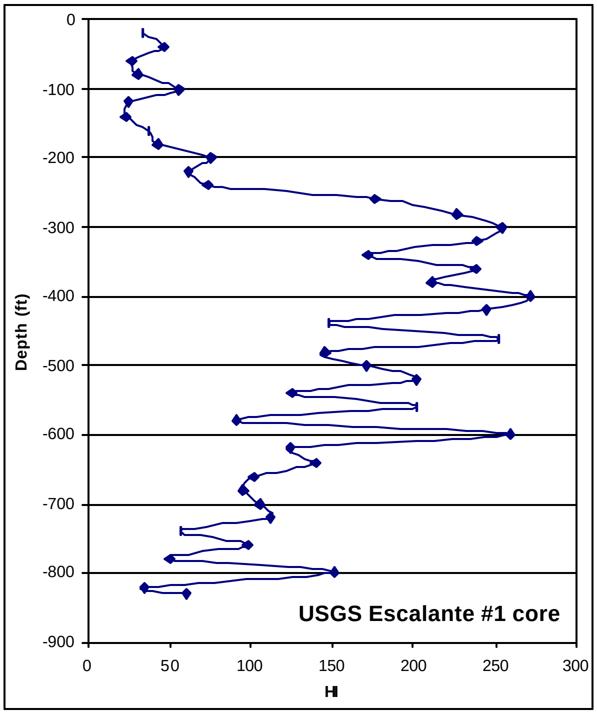

Figure 38: Variation of RockEval-derived Hydrogen Index (HI) in the Escalante #1 core. Data from White (1999).

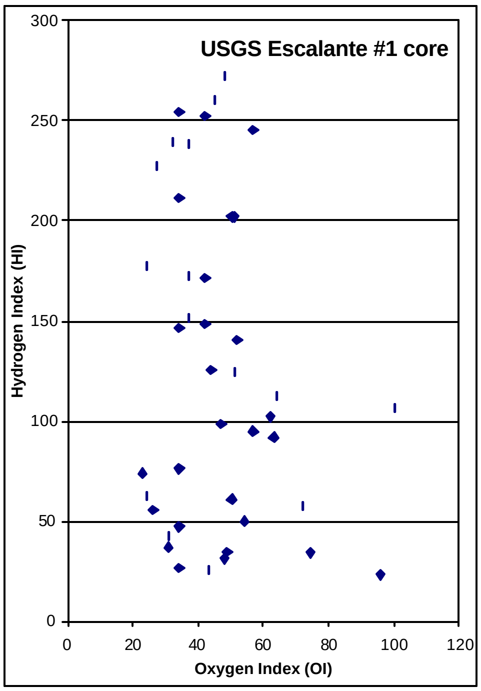

Figure 39: HI versus OI plot based on Rock-Eval pyrolysis of whole rock indicates the presence of Type III and mixed Type II-III gas-prone kerogen in the Tropic Shale and immediately adjacent units. Data from White (1999).

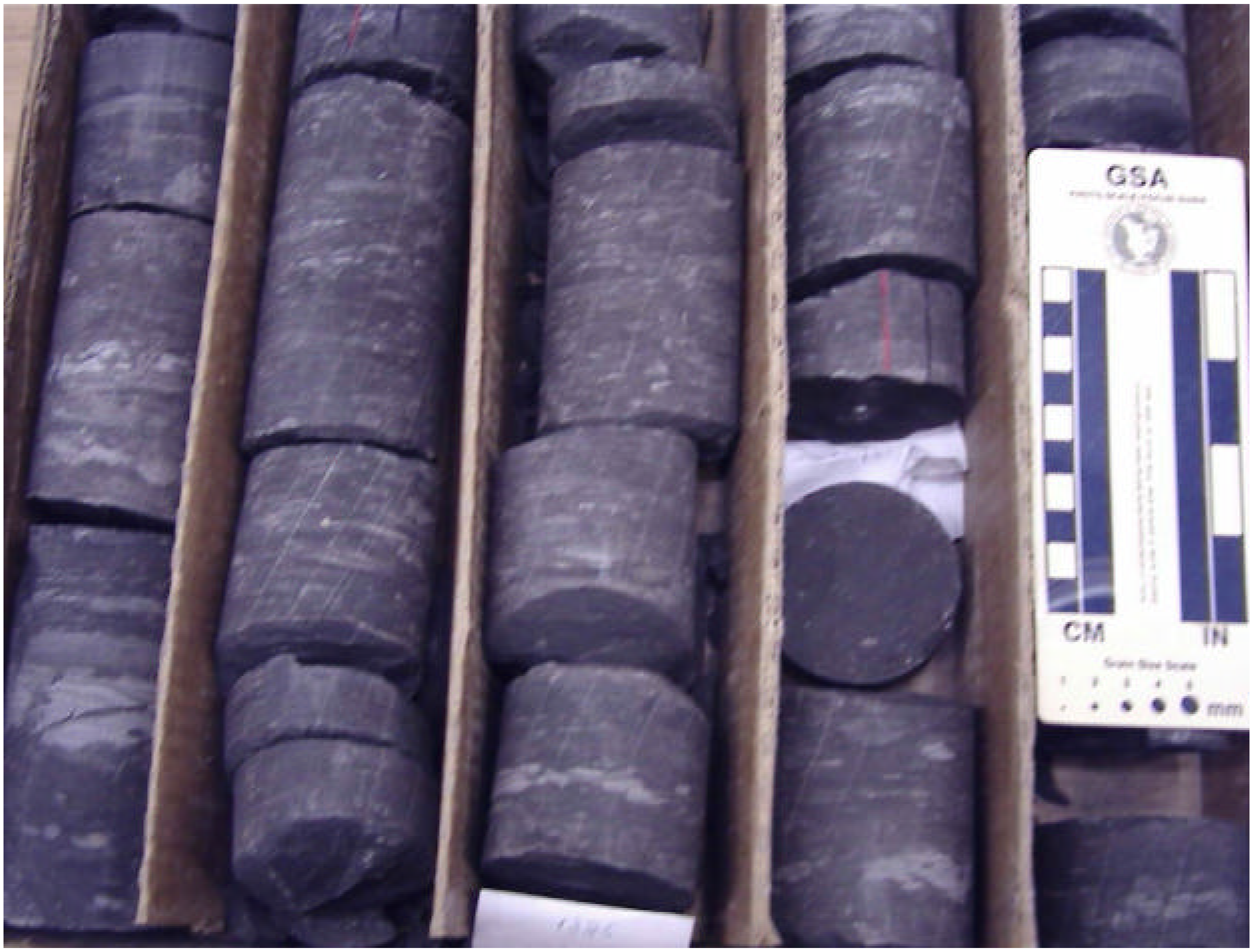

Figure 40: Core from the upper part of the Tununk Shale Member at approximately 1,885 ft in the River Gas of Utah #1 well (36-14S-9E, Carbon County). The rock is burrowed dark gray (N3) calcareous mudstone with silt to very fine grained sand laminae.

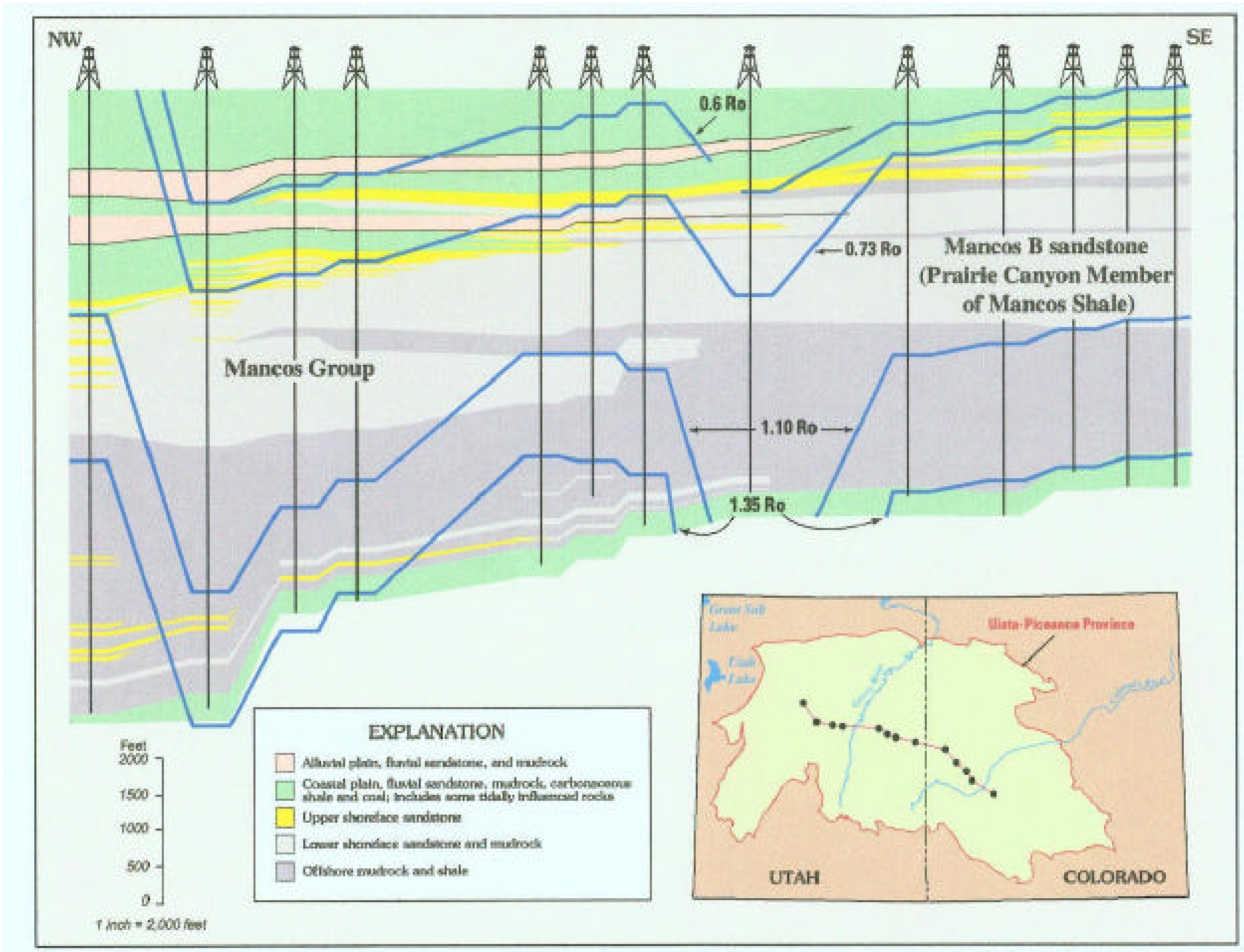

Figure 41: Generalized stratigraphic cross section of the Mancos Shale in the Uinta-Piceance basin showing organic maturity levels (Ro) relative to depth within the section (Kirschbaum, 2003). Dark gray is equivalent to the Tununk and Blue Gate Shale Members; light gray is equivalent to the Ferron Sandstone and Prairie Canyon Members.

Lower Blue Gate Member

In the Castle Valley and south of the Book Cliffs up to 2,000 ft of dark shales, the Lower Blue Gate Member, separate the Ferron and Emery Sandstone Members of the Mancos Shale (Witkind, 1988; Weiss and others, 1990). The poorly exposed succession is uniform dark gray, thin- to medium-bedded shale and shaly siltstone with a few thin beds of fine-grained sandstone and rare bentonites. Along the Utah-Colorado state line, the Lower Blue Gate Member is about 1,900 ft thick (Fig. 30; Cole and others, 1997).

The River Gas of Utah #1 well (36-14S-9E) is located in the Drunkards Wash CBM field near the northern end of Castle Valley. The well is spudded into the upper part of the Lower Blue Gate Member 50-100 ft below ledges supported by the Garley Canyon Beds of the Emery Sandstone Member, which directly overlies the Lower Blue Gate Member (Weiss and others, 1990). The well penetrates 1,621 ft of dark gray shales overlying coal-bearing Ferron Sandstone. The well was continuously cored from 212 ft to 1,889 ft; the TD is at 1,931 ft depth. The cores through the Blue Gate Member (Fig. 42) reveal a very uniform succession of dark gray (N3) to very dark gray (N2) dense and nonfissile calcareous claystone with scattered light to medium gray laminae of siltstone (see Appendix A for detailed core description). Fragments of heavy shelled bivalves (Fig. 42, A) are common. Some intervals are mottled and exhibit birdseye structures, but on the whole these shales are largely unstructured and lack obvious burrowing. A single 0.5 ft thick very fine-grained sandstone bed is penetrated at 799 ft depth. Also, there is a scattering of shaly bentonite beds each less than 1.0 ft thick. A scattering of subvertical fractures is observed throughout the core, but in general the shales are unfractured.

The organic richness and elemental chemistry of the rocks penetrated by the River Gas of Utah #1 well was investigated by Dumitrescu (2002). A plot of TOC with depth (Fig. 43) indicates that, on the whole, the Lower Blue Gate Member is organic-rich, with over 1,000 ft of the 1,409 ft cored interval having TOC greater than 1.0% and 680 ft net section having TOC greater than 1.5%. Two intervals of about 100 to 200 ft thickness have TOC values greater than 2.0 % (Fig. 43). The kerogen in these two high-organic carbon intervals is type II to mixed type II-III based on their atomic hydrogen and oxygen compositions (Fig. 44). The upper of the two intervals has dominantly type II kerogen.

Organic maturity of this succession can be estimated by the coal rank and/or vitrinite reflectance observed in the underlying Ferron Sandstone and overlying Star Point-Blackhawk Formation. As noted above, the rank of Ferron coals in the northern Castle Valley is high-volitile B bituminous (0.6-0.7% Ro); these coals are currently generating thermogenic gas (Montgomery and others, 2001). The vitrinite reflectance observed in the Blackhawk Formation, at the base of the Mesaverde Group, in the Book Cliffs is 0.65% (Fig. 45) and these coals also are generating small quantities of thermogenic gas. It can be expected that beneath the southern Uinta basin and possibly also beneath parts of the Wasatch Plateau the Lower Blue Gate shale has a residual gas content.

The Lower Blue Gate Member is a prospective reservoir for shale gas development in northeast Utah due to its substantial thickness of kerogen-rich shale and level of organic maturity.

However, the overall uniformity of the shale might present problems for effective fracture stimulation. This is a question requiring investigation using the RGU #1 core.

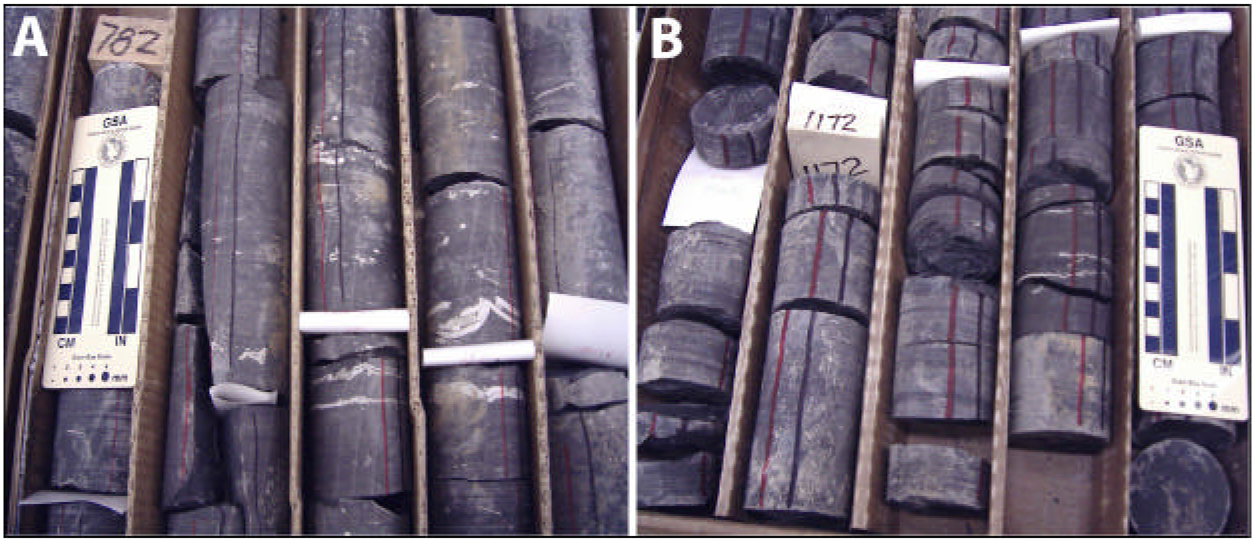

Figure 42: Lower Blue Gate Member core samples from the River Gas of Utah #1 well in Carbon County. Dense, non-fissile dark gray (N3) to very dark gray (N2) claystone with scattered light gray silt laminae and fragments of large bivalves. Note that the rock is uniformly dark gray, but mud cake on some core segments results in an apparent medium brown color.

A. Upper high-TOC interval at approximately 782 ft depth; B. Lower high-TOC interval at approximately 1172 ft depth.

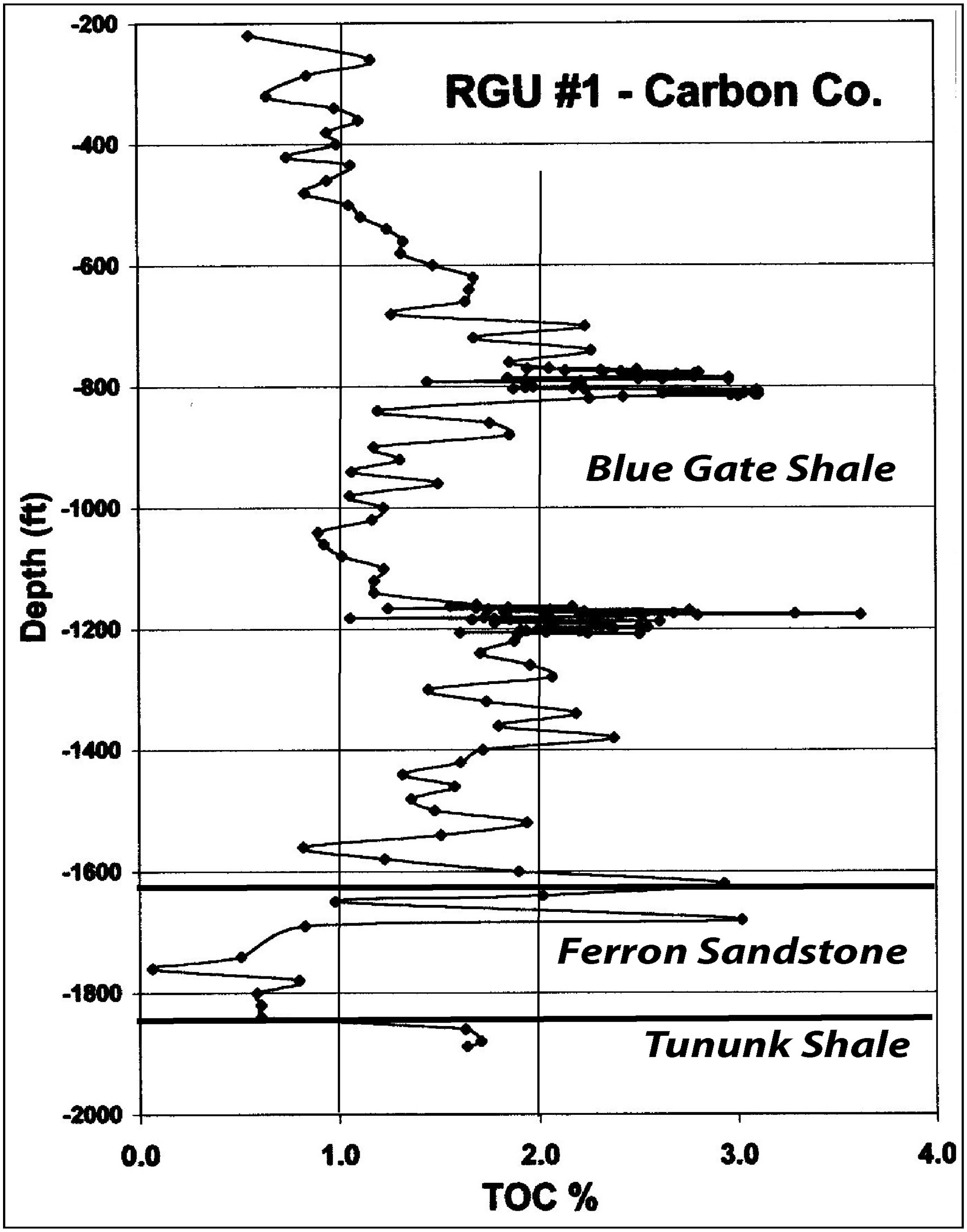

Figure 43: Organic richness of the Lower Blue Gate Shale in the River Gas of Utah #1 core. Data are from Dumitrescu (2002). Note the presence of two intervals in which the TOC is greater than 2.0%. The elevated TOC values observed in the Ferron Sandstone are in carbonaceous shales.

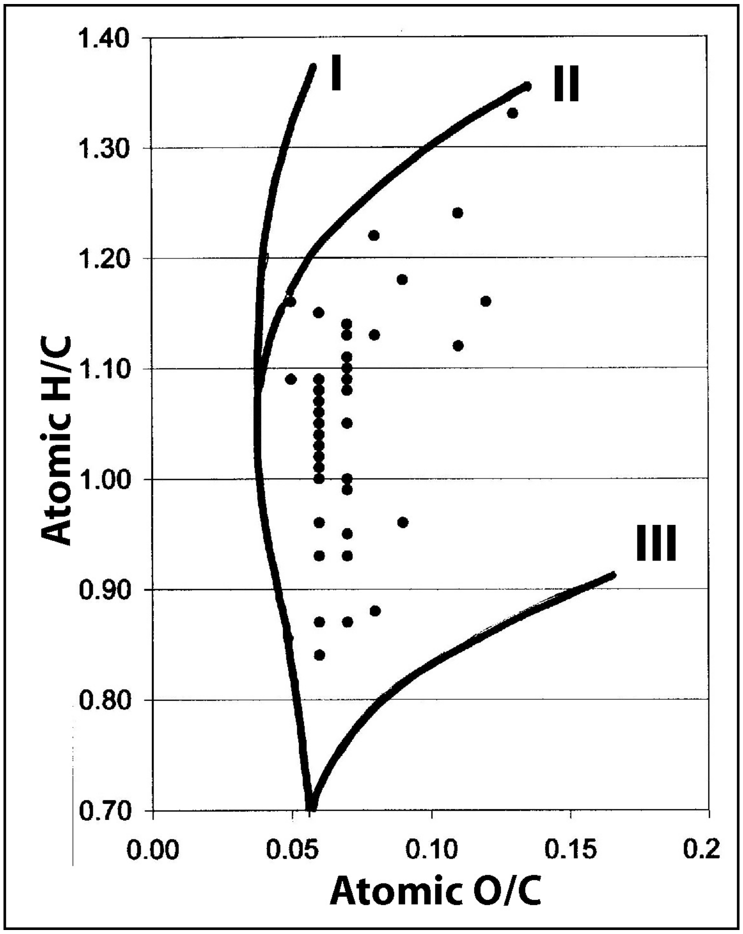

Figure 44: Van Krevelen plot showing the atomic composition of kerogen extracts from the Blue Gate Shale in the RGU #1 core. The kerogen is type II and mixed type II-III, sapropelic to humic. Data from Dumitrescu (2002).

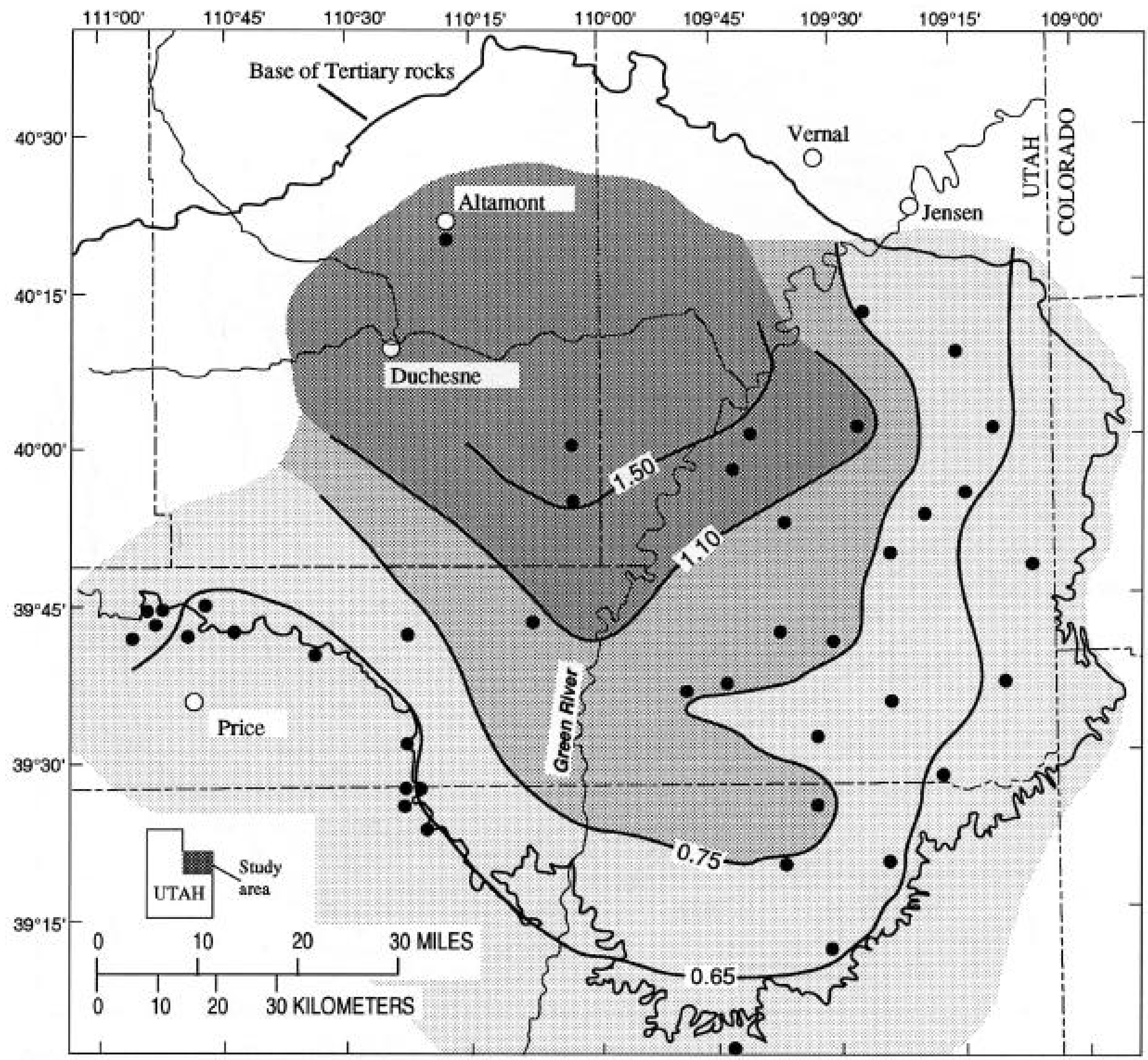

Figure 45: Thermal maturities at the base of the Mesaverde Group or top of the Mancos Shale beneath the Uinta basin (Nuccio and others, 1992).

Juana Lopez Member

The Juana Lopez Member of the Mancos Shale is widespread across the central and southern Colorado Plateau. In the eastern San Juan basin, the type locality (Dane and others, 1966; Hook and Cobban, 1980), the unit is a distal, deep-basin deposit composed of interbedded dark gray claystone and thin beds of calcarenite. However, in central Utah the Juana Lopez Member is represented by a more proximal, terrigeneous facies deposited closer to the western margin of the Western Interior Seaway.

The variety and abundance of fossils in the Juana Lopez Member dates the unit as upper Turonian, which makes it coeval with the upper half of the Ferron Sandstone (Fig. 46). Yet, nowhere on the north plunge of the San Rafael swell do rocks of the Juana Lopez Member interfinger with the delta front or shoreface strata of the Ferron Sandstone (Molenaar and Cobban, 1991). The Juana Lopez Member appears to be a 'detached' siltstone-sandstone body enclosed within the Mancos Shale (Fig. 46). The unit underlies the southeast Uinta basin, the Douglas Creek arch, and at least portions of the Piceance basin (Fig. 47).

The Juana Lopez Member, where it is exposed south of the Book Cliffs, is 80-100 ft thick (Molenaar and Cobban, 1991). The unit consists of thinly interbedded dark gray claystone, coarse siltstone and very fine- to fine-grained sandstone, with a few thin beds of bentonite. The lower 10-20 ft interval is dominated by dark gray to black fissil shale, possibly deposited during the transgression at the middle-to-upper Turonian boundary. The thicker upper interval is principally thinly interbedded dark gray noncalcareous claystone and coarse siltstone to fine-grained sandstone in beds less than a few inches thick (Fig. 48). The siltstone-sandstone beds have sharp bases against the underlying claystone, and they exhibit current- and wave-ripple bedding. In general, grain-size decreases towards the east. Calcarenite beds are relatively rare, but they increase in abundance eastward.

Along the Grand Valley south of the eastern Book Cliffs, Gualtieri (1988) maps an 80-foot thick ledge-forming unit within the Mancos Shale characterized by interbedded very fine- to fine-grained sandstone and silty shale, but he incorrectly identifies the unit as the Ferron Sandstone.

Although relatively thin, this silt-sandstone look-alike to the gas-producing Lewis Shale in the San Juan basin might be a gas reservoir where naturally fractured beneath the Tavaputs plateau. It would unlikely be a target in itself, but could provide add-on gas to wells completed at multiple objectives. Fracture completions should be successful in this hertrogeneous, quartz-rich 'shale'.

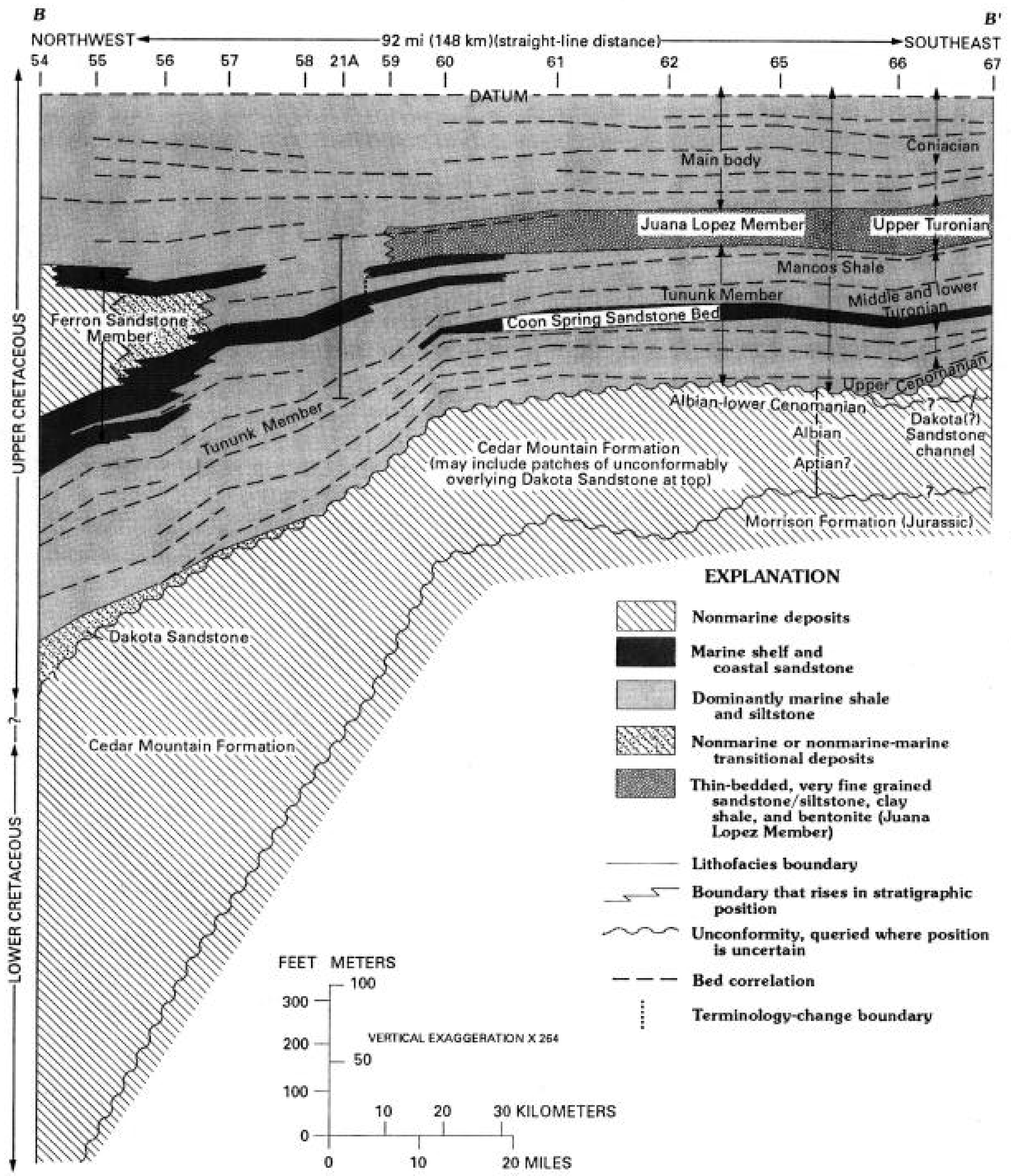

Figure 46: Stratigraphic correlations along the south side of the Uinta basin showing the Juana Lopez Member and Coon Spring Sandstone Bed as 'detached' siltstone-sandstone bodies within the main body of the Mancos Shale (Molenaar and Cobban, 1991).

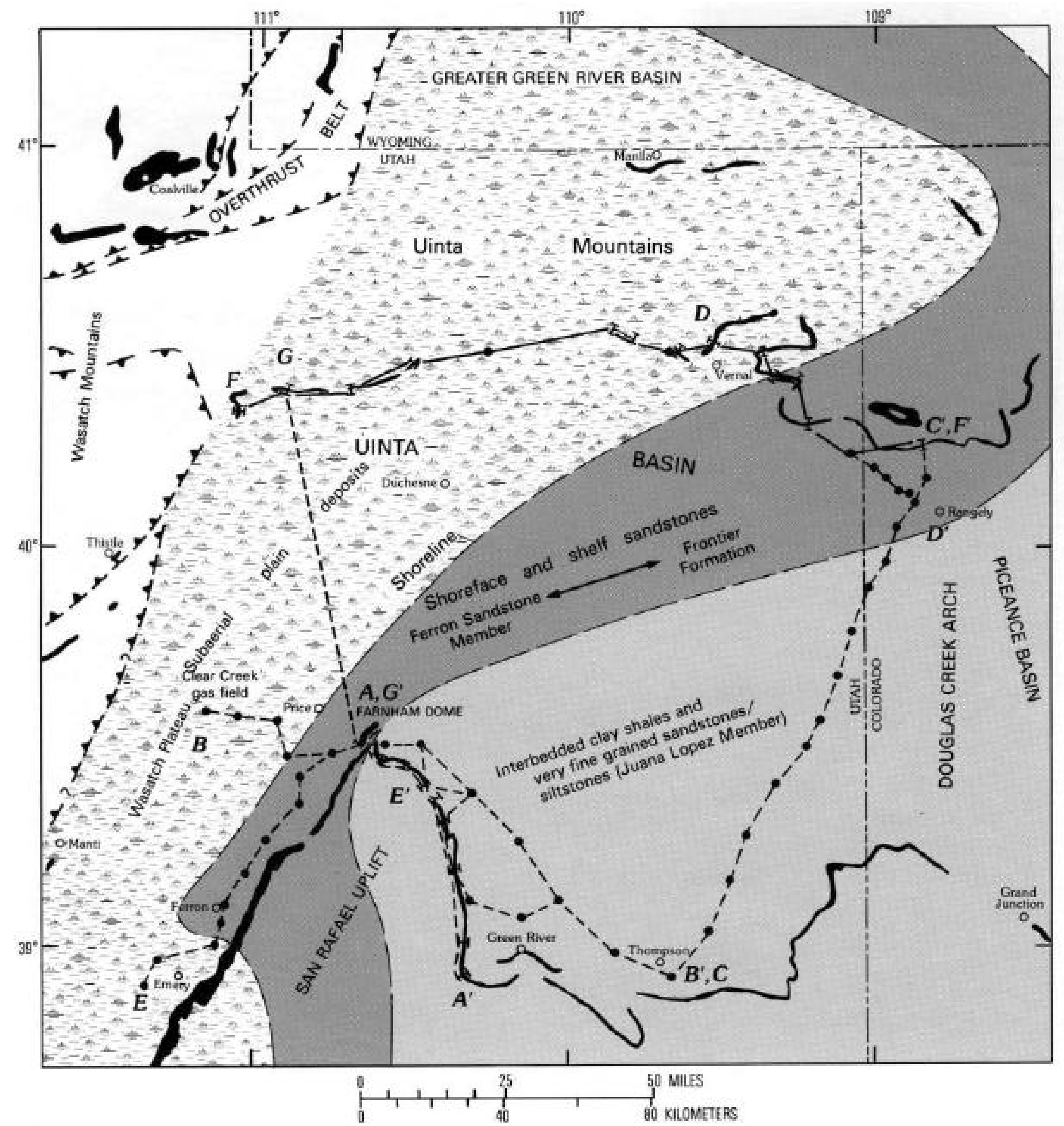

Figure 47: Distribution and lithofacies of rocks deposited at the time of maximum regression of the Vernal delta in the late Turonian (Molenaar and Cobban, 1991). The Ferron-Frontier delta plain and shoreface deposits pass offshore into interbedded shales, siltstones and very fine-grained sandstones of the Juana Lopez Member, which underlies the southeast Uinta basin and Douglas Creek arch areas.

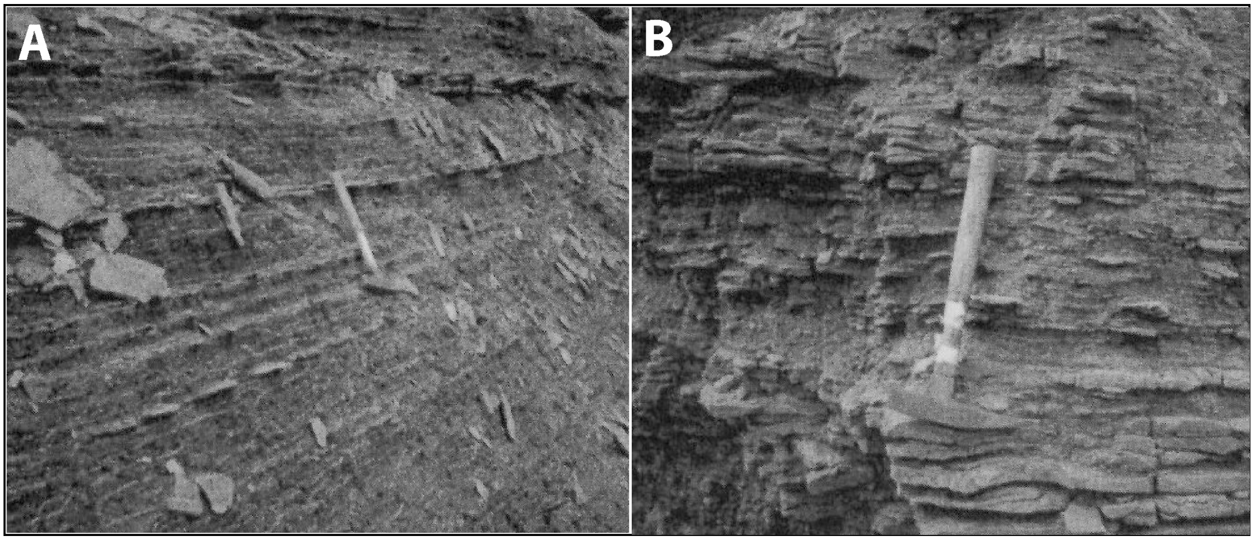

Figure 48: Outcrop photographs of the Juana Lopez interbedded siltstone and shale (Molenaar and Cobban, 1992).

Prairie Canyon Member

The Prairie Canyon Member of the Mancos Shale (Cole and others, 1997) is the principal gas reservoir on the crest and western flank of the Douglas Creek arch (Fig. 49) along the Utah-Colorado state line (Noe, 1993). The unit consists of claystone, siltstone, and very fine- to fine-grained sandstone interbedded on a scale of inches or less. Sandstone beds are rarely thicker than one foot. The average petrophysical properties on the crest of the arch are comparable to those of the Lewis Shale with porosity and permeability of 2-8% and less than 0.01 md, respectively. Like the Lewis Shale, the Prairie Canyon Member is very sensitive to formation damage by introduced water. The unit has become a significant gas producer only through the introduction of air drilling techniques (Kellogg, 1977). Due to the extensive network of fractures and faults on the crest and tested flanks of the Douglas Creek arch and the general gas-saturated nature of the siltstone-sandstone reservoir, the nearly 40 separate gas fields through time have converged into essentially a single field. This strongly suggests the presence of a subtle-trapped or continuous-type gas resource in the Prairie Canyon Member.

Historic per well gas recovery from the Prairie Canyon reservoir has ranged from 1.5 Bcf in naturally fractured areas on the crest of the arch to 0.25 Bcf on the apparently less-fractured flanks (Noe, 1993). After initial production is stabilized, 6% annual decline rates are usual, similar to those of the Lewis Shale (Dube and others, 2000). The natural gas produced has a high heating value of 1,100-1,200 BTU/ft^3, but oil production is both rare and very minor (Noe, 1993).

The Prairie Canyon Member was deposited more than 30 miles seaward of coeval Emery-Star Point-Blackhawk highstand shorelines (Fig. 50). The silt and fine-grained sand successions were laid down either below the storm-wave base (Cole and others, 1997) or as low-stand shoreline deposits resulting from a forced regression on a shallow ramp basin margin (Hampsen and others, 1999).

The Prairie Canyon Member is about 1.000 ft thick at the type locality near the Utah-Colorado state line, but it thins westward towards Green River and presumably also eastward. As a more resistant unit, it tends to form low cuestas (Fig. 51).

Cole and Young (1991) recognize five distinct lithofacies within the Prairie Canyon Member. Chan and others (1991) and Hampson and others (1999) describe a sixth lithofacies, *channelized sandstone and shale*, which is acknowledged by Cole and others (1997) as being most prevalent in the Pinto Wash and Hatch Mesa (Woodside) areas to the west of Prairie Canyon (see Fig. 49 for locations). The six lithofacies are:

- Silty claystone: dominantly dark gray, laminated and slightly carbonaceous claystone with variable proportions of coarse siltstone and very fine- to fine-grained sandstone forming discontinuous thin laminae (Fig. 52, A and B).
- Sandstone-claystone: interlaminated very fine- to fine-grained silty sandstone and silty claystone exhibiting a wide range of sedimentary structures (Figure 53), including wave-ripple, current-ripple, bi-directional ripple and wavy lamination, lenticular lamination, flaser bedding, and small-scale sole marks. Borrowing (*Chondrites* and *Planolites*) is common, but graded bedding is virtually absent.
- Sandy siltstone: poorly stratified siltstone with variable amounts of very fine- to fine-grained sandstone (Fig.52, C), generally increasing upward. The poor stratification is due to intense burrowing.
- Bioturbated muddy sandstone: distinguished from the sandy siltstone lithofacies by having a sand component greater than 50%. This lithofacies (Fig. 52, D) commonly overlies the sandy siltstone lithofacies in coarsening-upward sequences.
- Sandy dolomite: dark brown weathering, sandy ankeritic dolomite in discrete beds and concretions up to 3.5 ft thick and 20 ft long (Cole and others, 1997). Commonly located at the top of upward-coarsening sequences associated with bioturbated muddy sandstone.
- Channelized sandstone and shale: thinly interbedded very fine- to fine-grained sandstone (10-50%), fissile silty to sandy claystone, and fissile sandy siltstone (Cole and others, 1997). The channels (Fig. 54) typically are 30-70 ft across and up to 15 ft deep, and paleocurrent indicators indicate flow to the east-southeast (Chan and others, 1991).

The Prairie Canyon Member is organized into several coarsening-upward sequences (Fig. 55), some capped by sandy dolomite lithofacies. These mark distinct transgressive-regressive cycles, some perhaps ending in brief subaerial exposure before the next flood event. Just a few lithofacies are present in some cycles. The average sediment transport direction is to the southeast, as determined from flute casts and cross-bed sets (Cole and Young, 1991).

Hampson and others (1999) interpret the rocks of the Prairie Canyon Member as belonging to one of three nearshore facies:

- Tidally-influenced fluvial channel fill
- Fluvial-dominated delta fronts

- Weakly storm-influenced shorefaces

In contrast to the high-energy, wave-dominated, sand-rich shorelines of the Emery-Star Point-Blackhawk highstand system tracts, the correlative Prairie Canyon forced-regressive, lowstand and transgressive shorefaces are sand-poor and weakly wave-storm influenced.

Organic matter is present in the sandstone-siltstone facies of the Prairie Canyon Member as dark microlaminae or as descrete plant fragments (Gautier, 1983). Organic richness has not been reported for the shales or shaly siltstone-sandstone lithofacies, but it can be presumed to be similar to those of the underlying Blue Gate Shale Member, in the range 1.0-2.0% TOC. The presence of plant debris suggests that the kerogen is Type II-III. The vitrinite reflectance in the upper Mancos Shale across the crest of the Douglas Creek arch is reported as 0.6-0.7% Ro (Gautier, 1983; Kirschbaum, 2003; refer to Fig. 41).

The sandstones of the Prairie Canyon Member are tight, water-sensitive gas reservoirs with permeabilities in the microdarcy range. Natural fracturing is considered essential to sustain commercial production (Kellogg, 1977; Noe, 1993). Recent petrophysical measurements (see Appendix A for tables) from core in four wells on the Douglas Creek arch and southeast Uinta basin (Fig. 56) have a median porosity of 5.4 % (range of 2.8-11.6%; N = 60) and median Klingenberg permeability of .008 md (range of 0.001 - 0.427 md; N = 36). These data do not support the assertion (Gautier, 1983) that the matrix porosity and permeability of the sandstone-siltstone reservoir decreases off the flank of the arch. The Coseka Resources 8-2-15-22 State of Utah well (2-15S-22E) is located more than 20 miles west of the arch and the sampled interval (5,246-5,496 ft) is about 2,000 ft deeper than the wells near the crest of the arch. Yet the median porosity and Klinkenberg permeabilities are nearly identical to the other three wells, 5.4% and 0.006 md (N = 19), respectively. The ranges are 3.9-7.7% and 0.001-0.280, respectively. It should be noted that natural fractures were not observed in any of the four cores examined for this study at the U.S. Geological Survey Core Research Center.

The Prairie Canyon Member is ideally suited as a shale gas reservoir similar to the Lewis Shale in the San Juan basin. It is a succession of thinly intercalated kerogen-rich shale and siltstone-sandstone up to 1,000 ft or more thick. Being quartz-rich and herterogeneous, it should fracture easily, both naturally and hydraulically induced. It is likely that the earliest shale gas production in Utah will occur in wells soon to be drilled on the East Tavaputs plateau that penetrate the Prairie Canyon Member on the way down to deeper targets (Eckels, 2005). This interval should be tested.

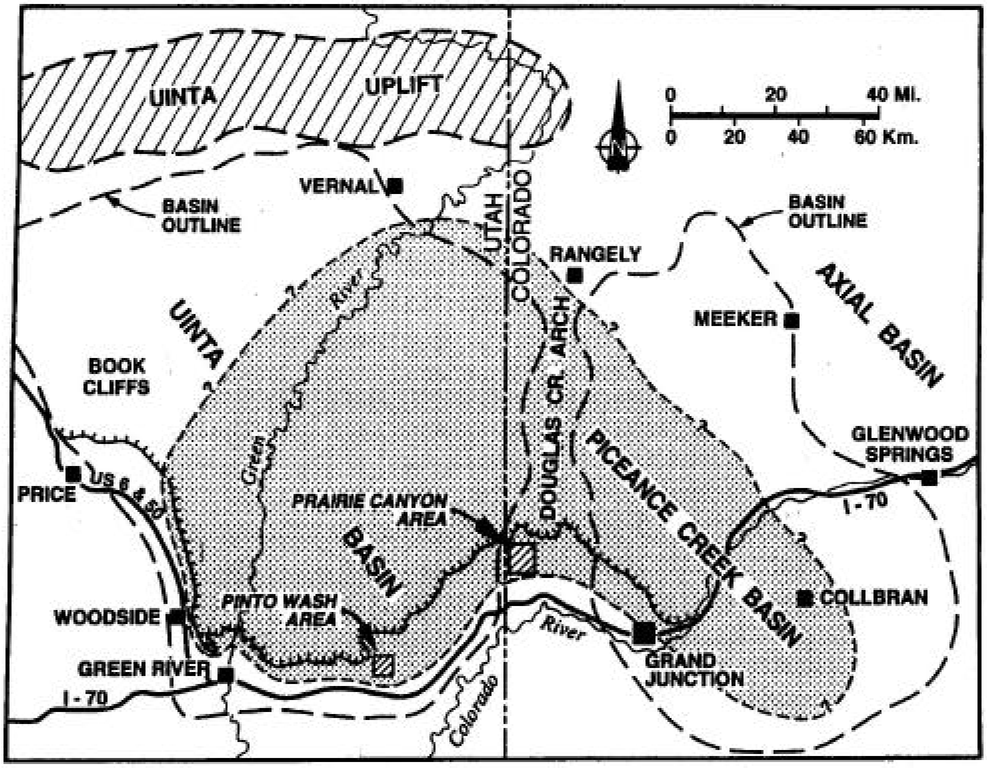

Figure 49: Approximate distribution of the Prairie Canyon Member beneath the southeast Uinta basin, across the Douglas Creek arch, and beneath the Piceance basin (Cole and others, 1997).

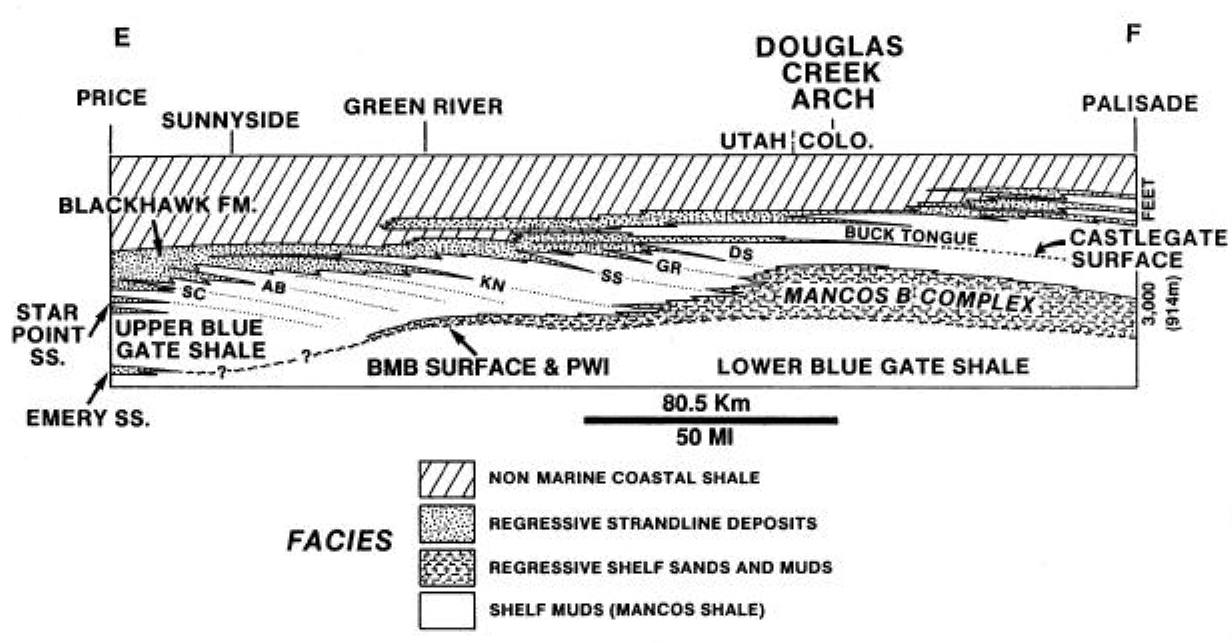

Figure 50: Generalized regional stratigraphic cross section from Price, Utah to Palisade, Colorado showing the relationship between the prograding Emery-Star Point-Blackhawk highstand shoreline stages and the 'detached' siltstone-sandstone deposits of the Prairie Canyon (Mancos B) Member (Cole and Young, 1991).

Figure 51: Light brown cuesta (foreground) supported by sandstones of the Prairie Canyon Member at Vista, east of Thompson Springs, Grand County. The high cuesta on the horizon is Castlegate Sandstone at the base of the Book Cliffs.

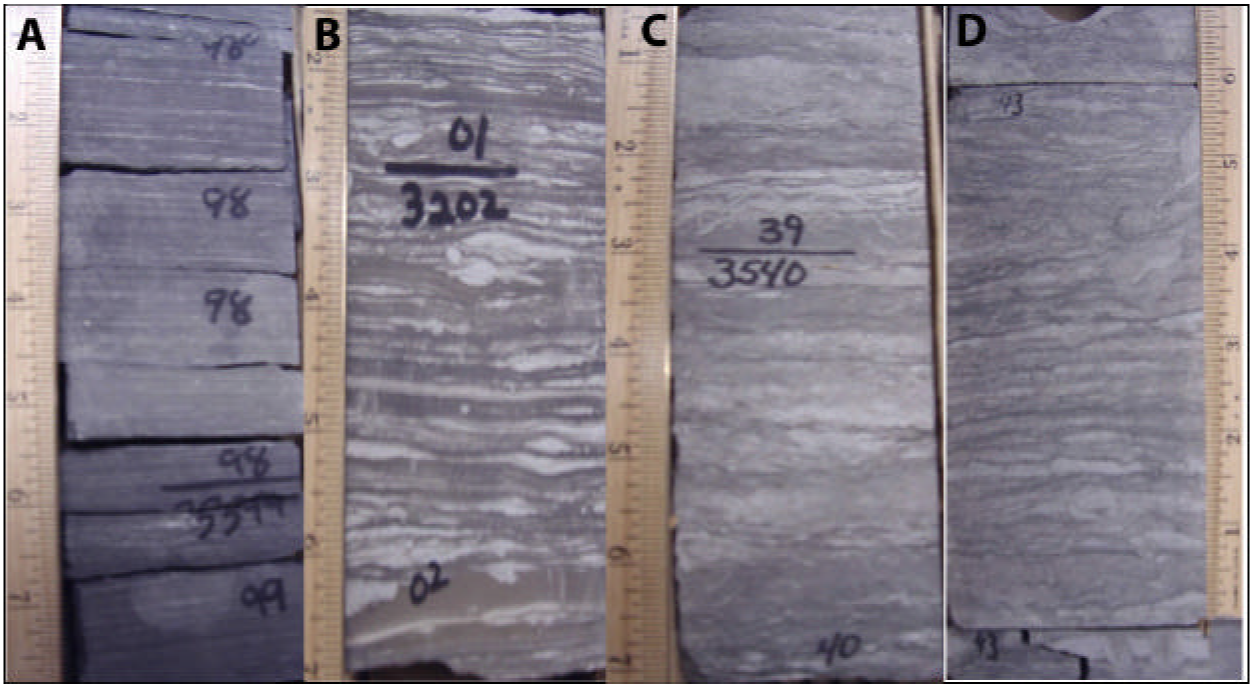

Figure 52: Representative cores of various Prairie Canyon Member lithofacies in northeast Utah and northwest Colorado. Scale in inches.

A. *Silty claystone lithofacies* in Coseka Resources 6-15-1S-103 Federal well, Rio Blanco County, 3399 ft depth; B. *Silty claystone lithofacies* in Tenneco Brunel E 28-10 well, Rio Blanco County, 3203 ft depth; C. *Sandy siltstone lithofacies* in Coseka Resources 15-29-4-103 Gentry well, Rio Blanco County, 3540 ft depth; D. *Bioturbated muddy sandstone lithofacies* in Coseka Resources 8-2-15-22 State of Utah well, Uintah County, 5242 ft depth.

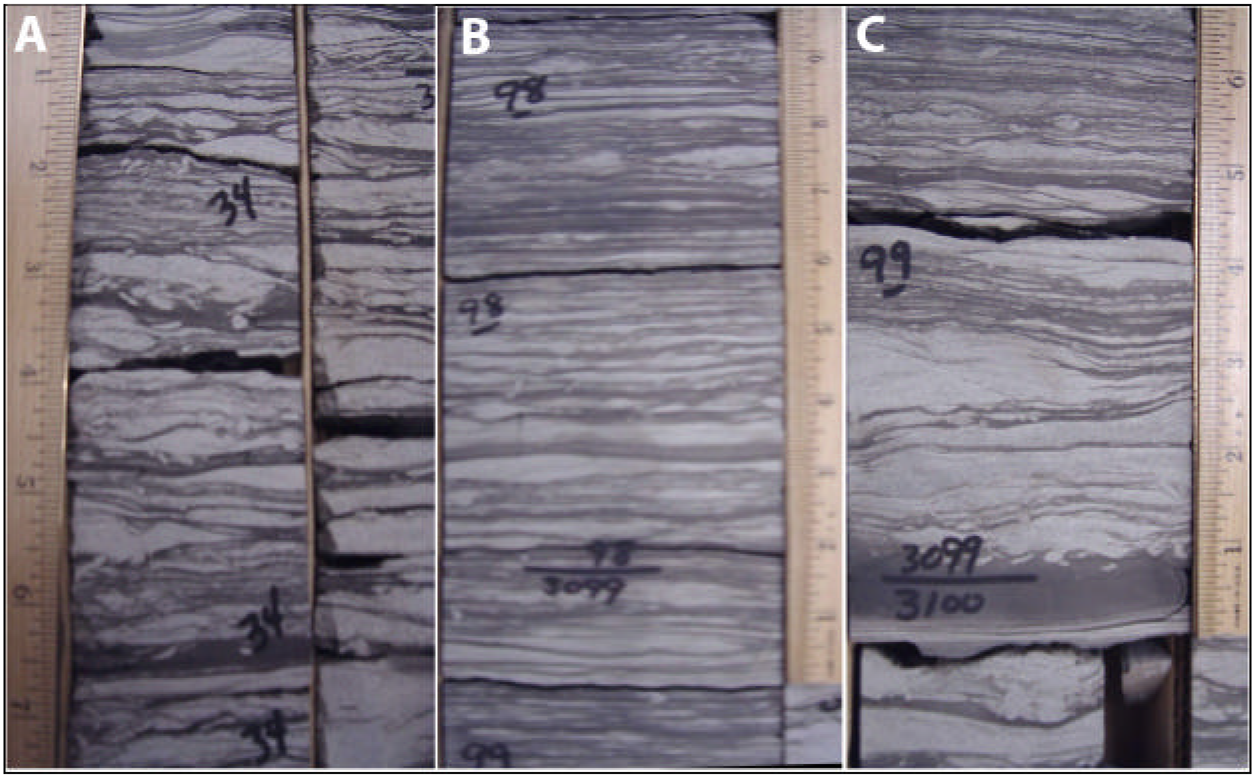

Figure 53: Representative cores of the *sandstone-claystone lithofacies*, Prairie Canyon Member, in northwest Colorado. Scale in inches. Note examples of lenticular lamination, wave-ripple and current-ripple lamination, and small-scale sole marks.

A. Coseka Resources 6-15-1S-103 Federal well, Rio Blanco County, 3334 ft depth; B and C. Tenneco Brunel E 28-10 well, Rio Blanco County, 3099 ft and 3100 ft, respectively.

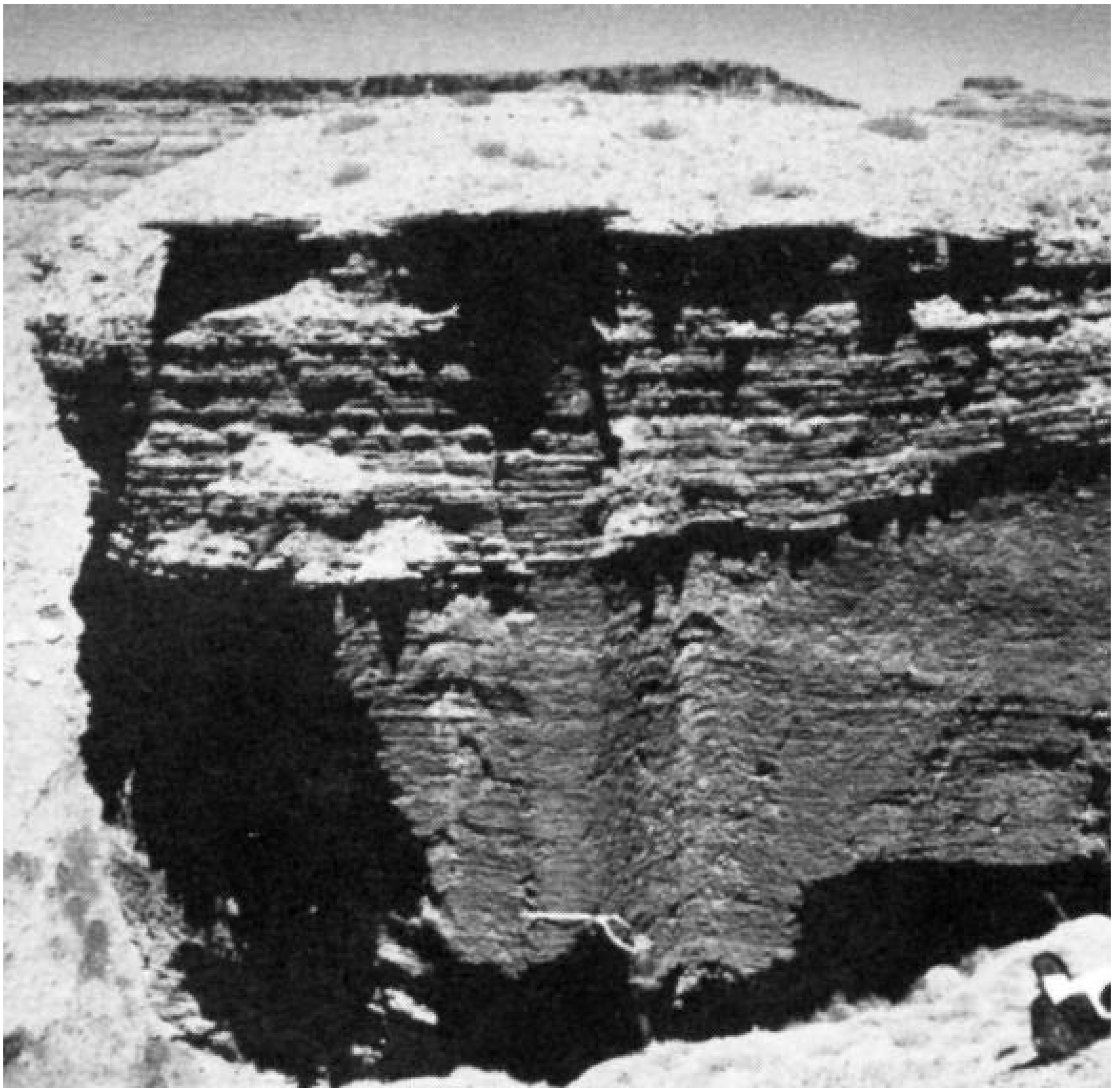

Figure 54: Channelized sandstone and shale lithofacies (Chan and others, 1991) of the Prairie Canyon Member at Tusher Canyon (18-20S-17E, Grand County). The channel is approximately 15 ft thick.

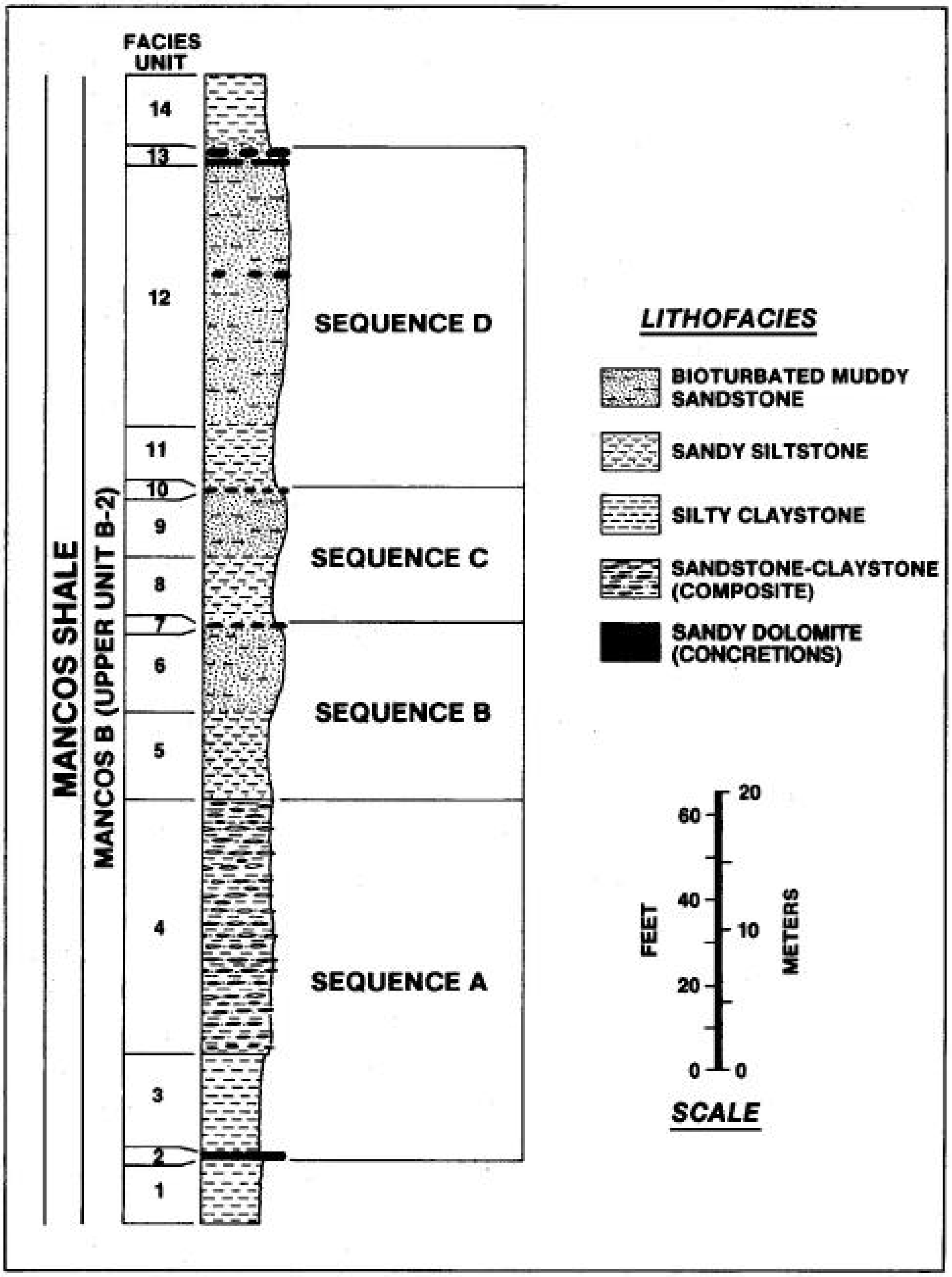

Figure 55: Arrangement of Prairie Canyon lithofacies into a succession of upward-coarsening sequences (Cole and Young, 1991).

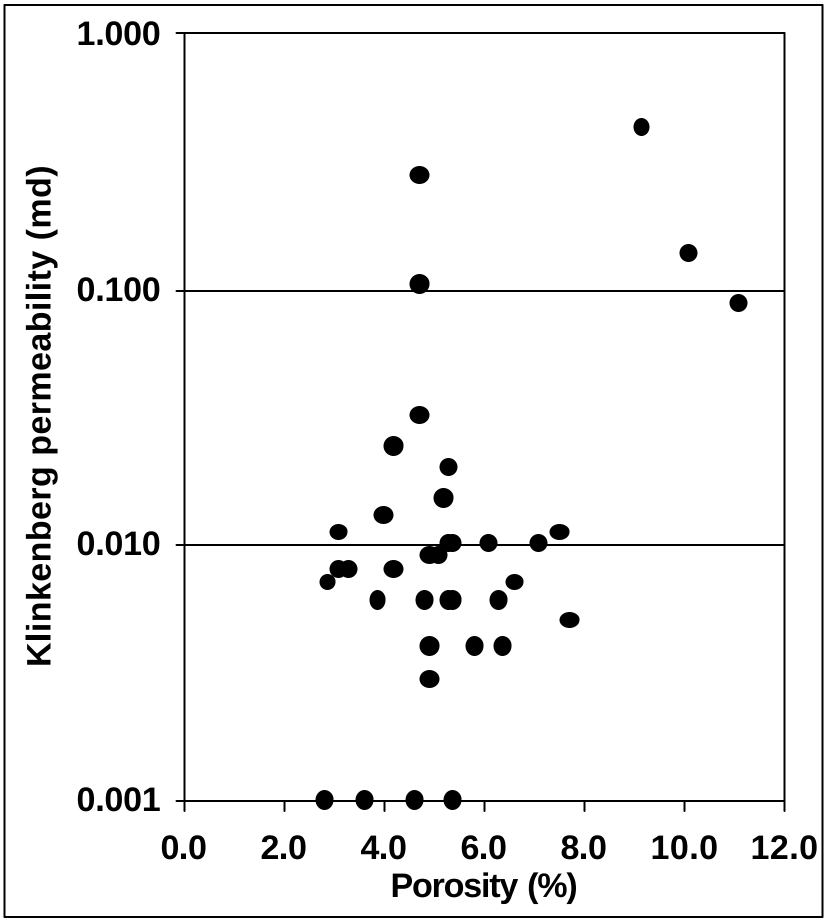

Figure 56: Porosity and Klinkenberg permeability (md) for 36 core samples from four wells in northwest Colorado and northeast Utah. Analyses were carried out in June 2004 for EnCana Oil and Gas (USA) Inc. Data from the U.S.Geological Survey Core Research Center public records.

Paleozoic Black Shales

General Statement

The thicker Paleozoic sediment accumulations were deposited west of western edge of an extensive carbonate shelf and cratonic platform in the center of North America. This break in isopach thicknesses served as a major tectonic province boundary through the Phanerozoic (Sloss, 1988). In Utah, the boundary is the commonly referred to as the 'Hingeline'. During the Sevier orogeny in the Cretaceous, the Paleozoic thickness and facies changes along the 'Hingeline' were exploited as structural ramps delineating the frontal thrusts. As a consequence, the thicker and commonly organically-richer Paleozoic black shale units are allochthonous, carried in the structurally complex Sevier thrust sheets. Cenozoic crustal extension in the Basin and Range province has only added to the degree of structural complexity west of the 'Hinge' zone.

The Pennsylvanian and Permian was a time of continental glaciation on Pangea resulting in frequent rise and fall of sea level (Ross and Ross, 1985). The resulting eustatically-driven sedimentation cycles are well displayed in the Late Paleozoic strata of Utah (Johnson and others, 1992). For the most part, the black shale units of the Late Paleozoic are deposited as a consequence of eustatic cycling in young structural depressions, such as the Oquirrh and Paradox basins.

Delle Phosphatic Shale Member

The Delle Phosphatic Shale Member (Sandberg and Gutschick, 1984) was deposited in the Deseret 'starved' basin (Fig. 57) during the mid-Mississippian time (early Osagean-early Meramecian stages; late Tournaisian-early Visean). The Deseret basin lay at the foot of a carbonate ramp extending off of an extensive carbonate platform to the east. It was thought to have been bounded on the west by a submarine rise that partially blocked terrigeneous sediments deposited in the Antler flysch trough (Sandberg and others, 1982). In time the Delle was buried by syn-orogenic sands and muds spilling across the submarine rise (Fig. 57) to eventually fill much of the Antler foredeep.

Expressing a contrarian view of the depositional setting of the Delle Phosphatic Shale Member, Nichols and Silberling (1991) propose an upwelling event on the mid-Mississippian shelf that resulted in the incursion of nutrient-rich waters leading to deposition and preservation of the phosphatic, organic-rich claystones and micrites.

The Delle Phosphatic Shale Member is present near the base of a variety of formations in western Utah, eastern Nevada and southern Idaho, including the Deseret Limestone (Rigby and Clark, 1962), the Woodman Formation (Sandberg and Gutschick, 1984), and Chainman Shale (Poole and Claypool, 1984). The Delle Member is everywhere less than 200 ft thick (Fig. 58, A), and in most areas less than 100 ft thick. The 'thicks' on the isopach map define the depositional axis of the Deseret basin. Nearly all of the Delle Member is situated west of the frontal thrusts of the Sevier thrustbelt. At the 'type' locality (Fig. 58, B) in the South Lakeside Mountains (Tooele County), the total thickness is 194 ft, of which a net 82 ft is organic-rich phosphatic shale and siltstone. Immediately to the south in the Oquirrh Mountains, the unit is less than half as thick and is relatively poor in the phosphatic shale lithotype.

The Delle Phosphatic Shale Member is composed mainly of interbedded dark organic-rich phosphatic claystone, mudstone and siltstone containing large micritic limestone concretions, bedded black radiolarian chert, thin beds of peloidal phosphorite, thick beds and lenses of dark cherty micrite, coarse debris-flow encrinite derived from the carbonate shelf and rare lenses of varicolored siltstone spilling out of the flysch trough to the west. The thickness and general character of the unit is quite variable depending on its location within the Deseret basin.

Organic richness varies with lithofacies (Sandberg and others, 1979; Sandberg and Gutschink, 1984). The phosphatic shale averages 4.3% TOC (1.5-7.9% range), the bedded phosphorites average 2.6% (0.7-5.1% range), but the micritic limestones average just 1.3% (0.3-3.2% range). The overall hydrocarbon generative capacity of this unit will depend on the particular mix of these lithotypes at any given location. In general, the average TOC (Fig. 59, A) follows the depositional axis of the Deseret basin. The kerogen type is not reported, but from the depositional setting it might be presumed to be type II.

Conodont alteration index (CAI) is an older, qualitative measure of thermal maturity that uses the color of conodonts (Epstein and others, 1977) in a passage from translucent (immature) to black (ulta-mature). The spatial variations in CAI in the Delle Phosphatic Shale Member are shown in Figure 59 B together with approximate Ro equivalent values. The most striking feature of this map is the extremely high maturity (> 3.0 CAI = 1.8% Ro) in the area of northwest Utah that in Pennsylvanian time is buried beneath more than 10,000 ft of Oquirrh Formation limestones and sandstones. In general, the lower TOC values coincide with very high levels of maturity suggesting that the mature source rocks had become 'burned out'. Initially organic richness was higher, perhaps considerably higher, than what is now observed in surface samples of variable maturity levels.

The area of Utah with both high average TOC and maturities within the gas window (Fig. 59) includes Millard and Beaver Counties. Other areas are likely unfavorable for development of gas from this unit due to extreme organic maturities, but its high degree of heterogeneity and generally low net shale thickness possibly disqualify it throughout Utah.

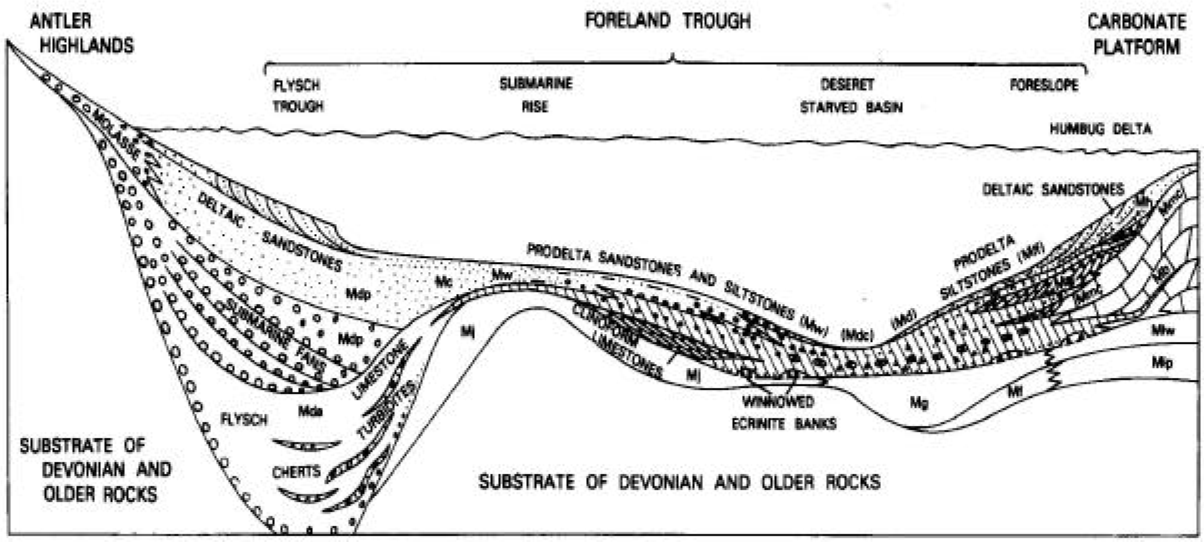

Figure 57: Stratigraphic relationships of terrigeneous and carbonate rocks in the Antler trough in middle Meramacian (mid-Mississippian) time (Sandberg and Gutschick, 1984). The Delle Phosphatic Shale Member is deposited in the Deseret 'starved' basin, at the foot of the carbonate ramp extending from the broad carbonate platform to the east. In time the Delle is buried by syn-orogenic sands and muds spilling across the submarine rise that had isolated the Deseret basin during Delle time.

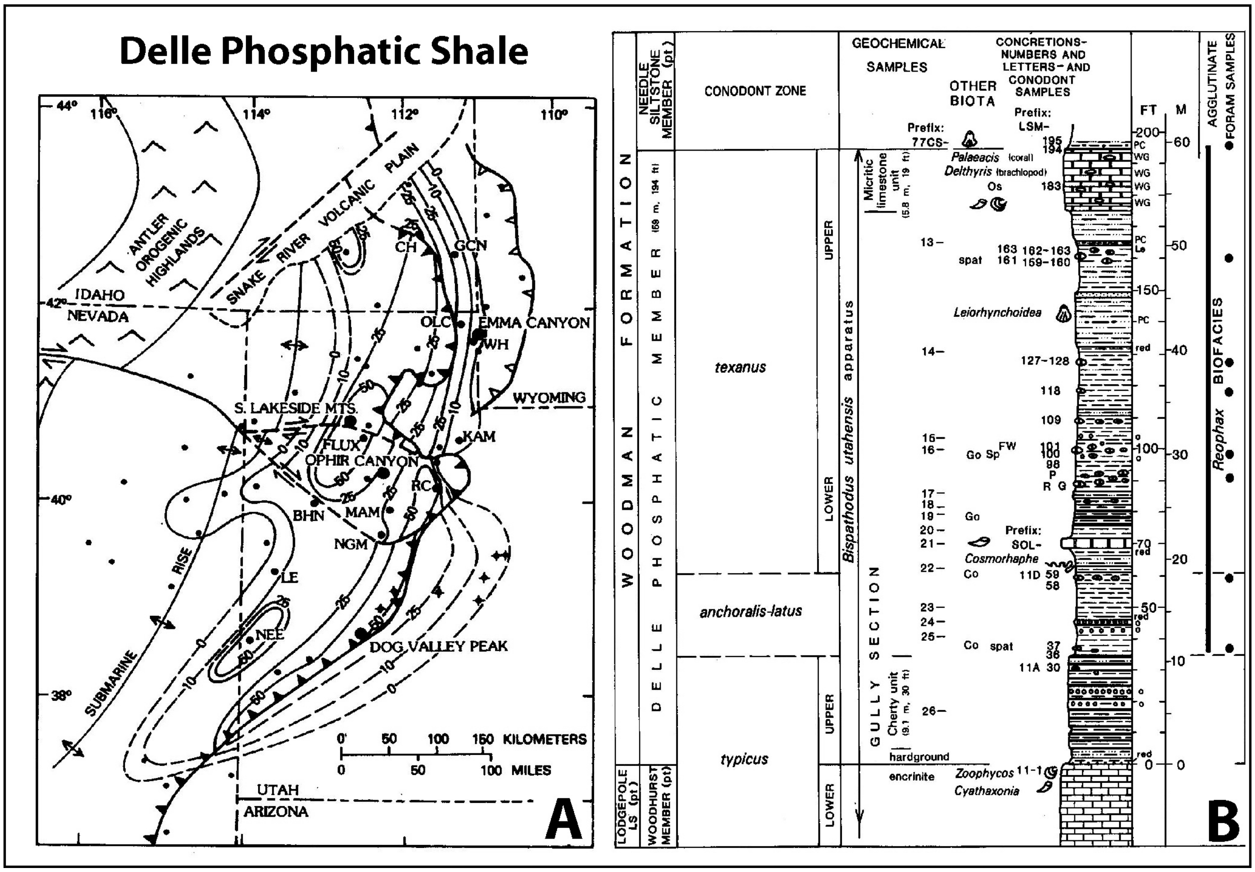

Figure 58: The Delle Phosphatic Shale Member in western Utah (Sandberg and Gutschick, 1984). A. Isopach thickness partly palenspastically restored. Thickness in meters; 25 m = 82 ft. The 'thicks' where thickness exceeds 50 m define the depositional axis of the Deseret basin during the mid-Mississippian. B. The 192 ft thick 'type' section in the South Lake Mountains, Tooele County, showing the relative abundance of the organic-rich shale lithofacies.

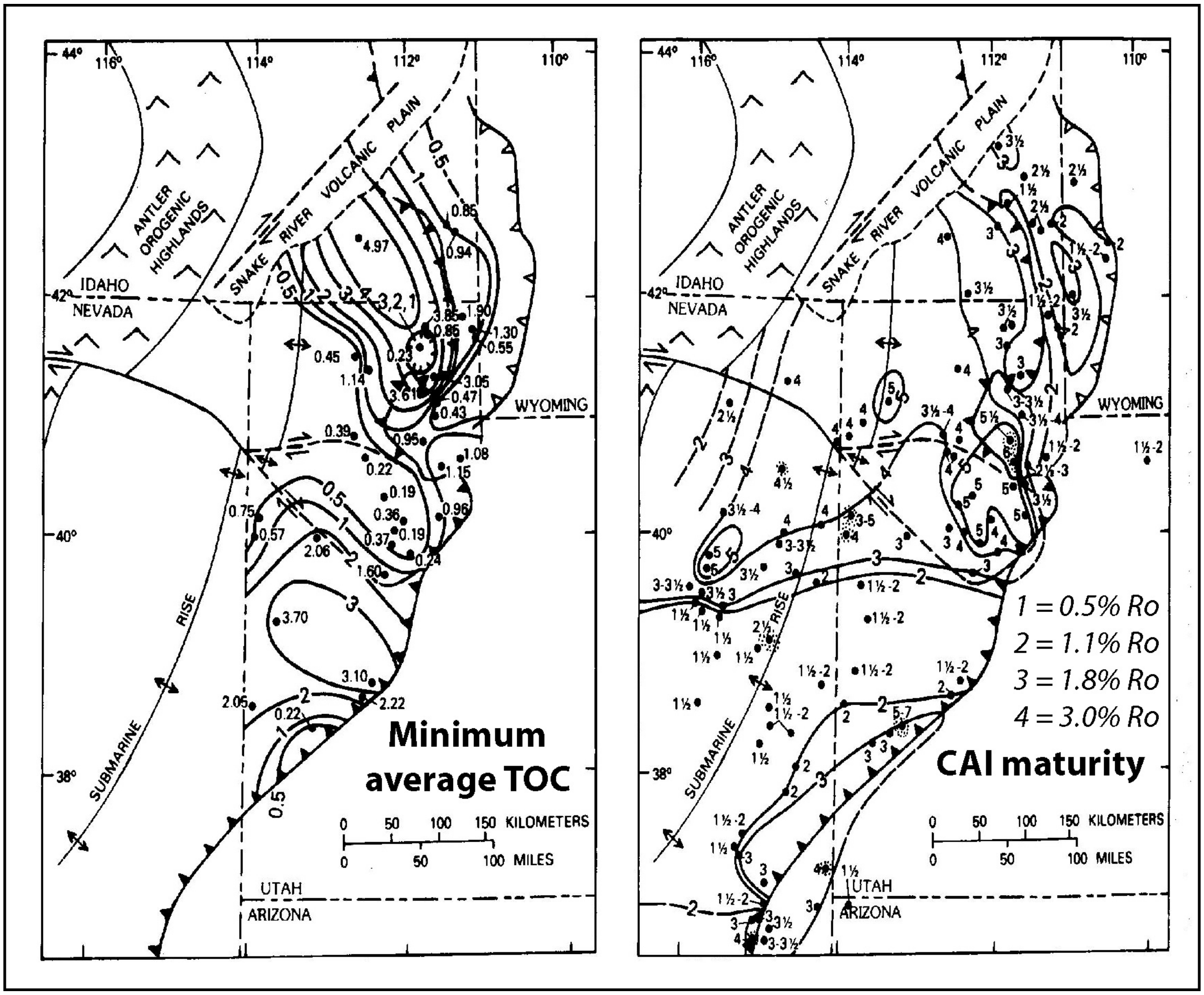

Figure 59: Organic richness and maturity of the Delle Phosphatic Shale Member in western Utah (Sandberg and Gutschick, 1984). A. Distribution of average TOC values at many localities. The values are considered to represent a minimum due to the effects of weathering on the surface samples. B. Thermal maturity as determined from conodont alteration index (CAI). The Ro equivalents are shown in the table on the figure.

Manning Canyon Shale

The Manning Canyon Shale was deposited in the proto-Oquirrh basin, a transtensional basin superposed on the Antler foredeep and related to the Ancestrial Rockies tectonic events (Fig. 60; Miller and others, 1992). As with other terrigeneous sediments filling the Oquirrh basin, the source of the sediments was the rising craton in northeast Utah (Welsh and Bissell, 1979) transported westward down the Doughnut trough in approximately the location of the present Uinta Mountains. Thereby, the Manning Canyon Shale shares most sedimentologic characteristics, except thickness, with the Doughnut Formation.

Thickness in excess of 1,500 ft is centered in the Oquirrh and Wasatch Mountains, principally in the hanging wall sheet of the Charleston-Nebo thrust (Fig.60). Near the 'type' location (Gilluly, 1932) in the southwest Oquirrh Mountains (Fig. 61), the Manning Canyon Shale is 1,559 ft thick (Moyle, 1959). The formation is predomantly dark gray, slightly calcareous, organic-rich claystone (Fig. 62, A) with interbedded limestone and sandstone (quartzarenite and subgraywacke). Beds of siltstone and mudstone, and rare arkose, also are present in most sections. In the Soldier Canyon section (Fig. 61) 61% of the section is silty claystone, 35% is limestone, 3% is sandstone, and just 2% is siltstone/mudstone. The lower 700 ft of the section has silt-free claystone, but in the upper 900 ft the claystone is silty. The Mississippian-Pennsylvanian systemic boundary is thought to be in the upper part of the section (Gilluly, 1932). The larger part of the section is late Chesterian (Welsh and Bissell, 1979).

The Manning Canyon Shale overlies with a gradational contact platy, dark blue-gray limestones of the upper Great Blue Limestone (2,500-2,800 ft; Rigby and Clark, 1962) of upper Mississippian age. It is conformably overlain by blue-gray limestones of the Hall Canyon Member of the Oquirrh Formation (Bissell, 1959).

The Manning Canyon Shale may be even thicker in Provo Canyon (Fig. 62, B), perhaps up to 2,600 ft thick (Moyle, 1959). However, due to its stratigraphic position between two massive carbonate-sandstone successions, the shale unit is deformed (thinned or thickened) structurally, perhaps significantly. The internal structuring can be observed in weathered exposures along the Provo River and is reported in the Oquirrh Mountains by Gilluly (1932).

The Doughnut Formation is a fissile, dark gray, carbonaceous shale containing scattered sandstone and limestone beds. In the western Uinta Mountains it is over 300 ft thick, but it thins eastward and is less than 100 ft thick at the Utah-Colorado state line (Foutz, 1966). Bryant (1990) describes the Doughnut Formation in the Wasatch Range as 425 ft of medium gray, thin bedded limestone containing pods of dark gray to black chert with up to 90 ft of black shale at the base. In the Uinta mountains it is over 200 ft of black shale containing thin dark gray limestone and sandstone beds.

Reported average TOC values (Swetland and others, 1978) for the Manning Canyon and Doughnut black shales are variable from less than 1% to over 8% (Fig. 63). There is little pattern of average TOC with the thickness of black shale at the section sampled, or between the Manning Canyon and Doughnut sites, except that the three Manning Canyon sections are thicker than 250 ft.

In the Mount Nebo-Nephi area (Witkind and Weiss, 1991) the Manning Canyon Shale lies beneath nearly 13,000 ft of Pennsylvanian-Lower Permian strata alone, as well as an undetermined Mesozoic section. The thickness of overburden to the north in the Provo and Oquirrh Mountains area is likely even greater. Due to the extreme burial, one can expect the Manning Canyon Shale in the Oquirrh basin to be at a very high thermal maturity, perhaps even beyond dry gas, and to have been generating significant quantities of gas perhaps even before the end of the Paleozoic. Outside of the Oquirrh basin, the maturity of the Manning Canyon-Doughnut black shales will be less, but there is only limited information in the literature to indicate actual maturity levels. Two samples of Manning Canyon Shale (Swetland and others,

1978) at Soldier Canyon (Fig. 61) have reported thermal alteration index (TAI) values of 3+ and 4- (Ro > 2.0%) and a single Doughnut shale sample at Sols Canyon, Daggett County (11-2N-18E) has a TAI of 2 (< 0.4% Ro).

Relevant to an assessment of the gas potential of the Manning Canyon Shale in west-central Utah is a geochemical report (UGS public files) for 'Chainman Shale' samples from the Equitable Resources Mamba Federal #31-22 well (22-16S-19W) drilled in Snake Valley, west of the Confusion Range, south of Grandy near the Nevada state line. The mudlog for the well describes a dark gray to black calcareous shale. This 230 ft thick shale interval has TOC values ranging from 0.60 to 2.53%, but a 30 ft segment corresponding to a gamma-ray kick has values of 2.48 to 2.53%. Pyrolysis Tmax is very high, 452-468°C, indicating an equivalent maturity of 1.0 to 1.3% Ro (late oil-wet gas). The shale is 3,000 ft deep in the well. The well was a dry hole.

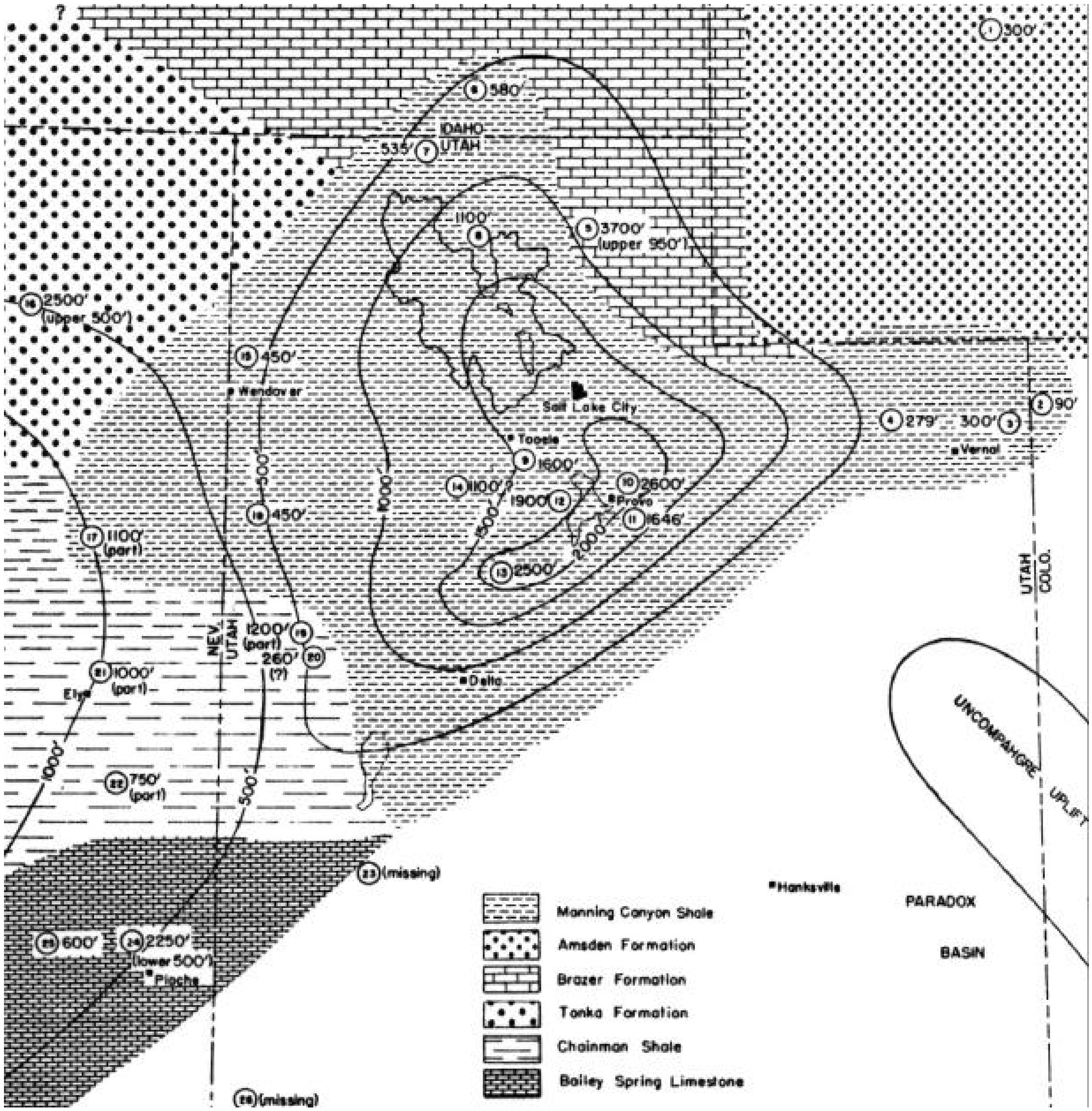

Figure 60: Thickness of the Manning Canyon Shale in northern Utah and correlative formations in adjacent areas (Moyle, 1959). The contour interval is 500 ft. The maximum thickness reported is 2,600 ft in Provo Canyon.

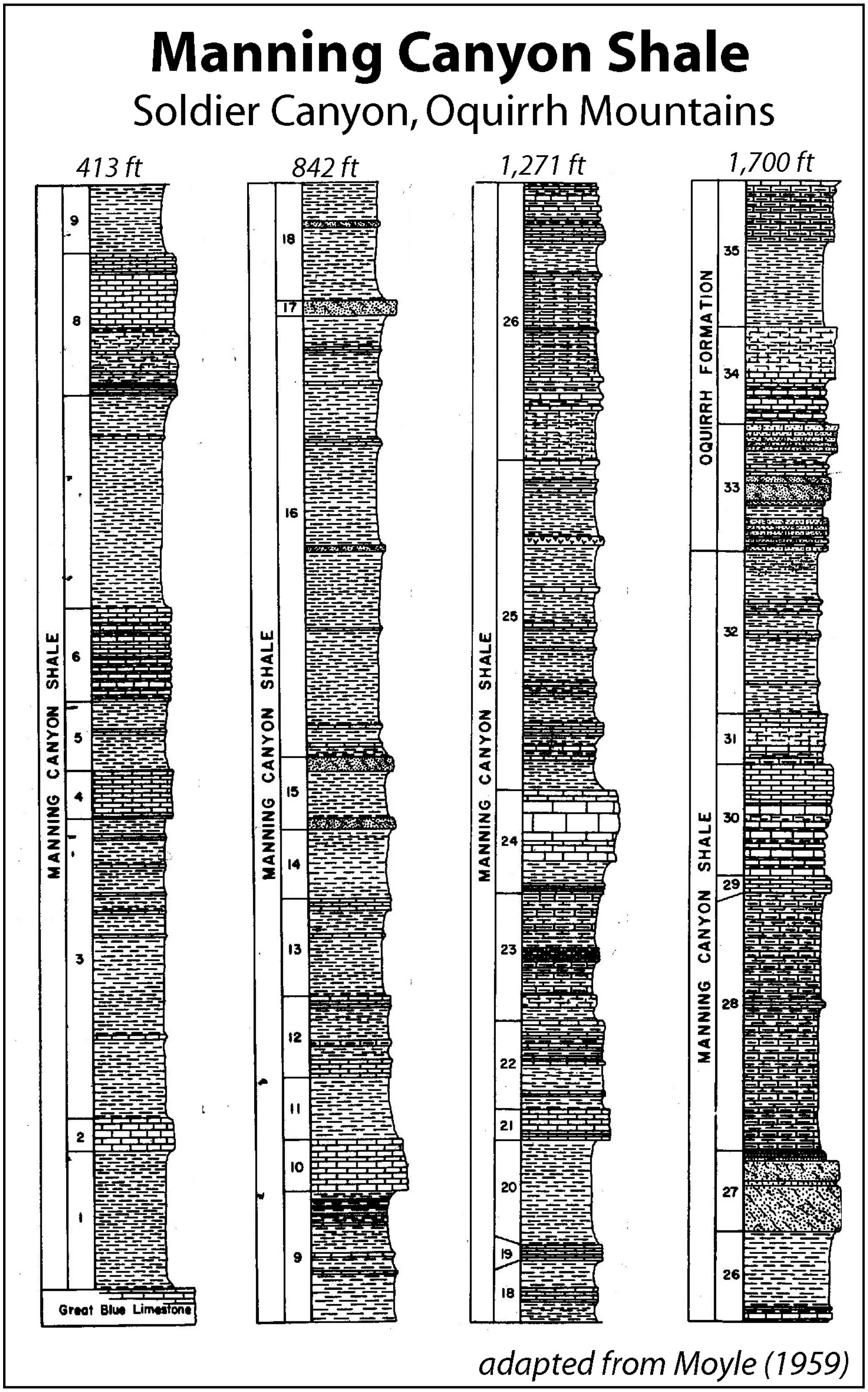

Figure 61: Manning Canyon Shale stratigraphic section measured at Soldier Canyon (33-4S-4W) in the southwestern Oquirrh Mountains, Tooele County. The section is reported to be 1,559 ft thick at this location (Moyle, 1959).

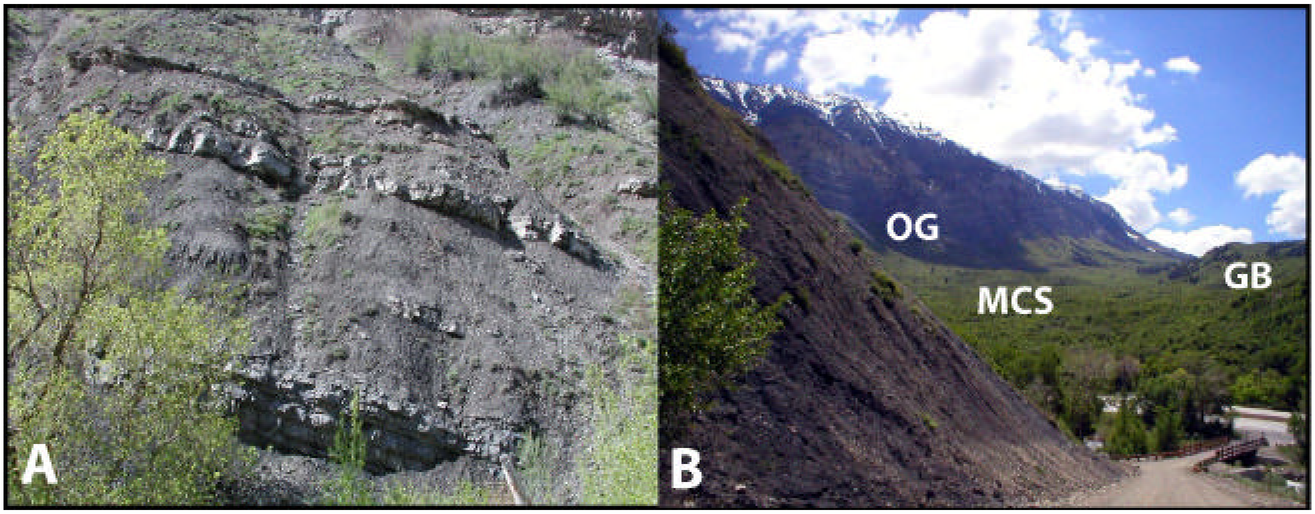

Figure 62: The Manning Canyon Shale in the western Provo Canyon, Utah County.
A. Outcrop of dark organic-rich shale interbedded with dark thin-bedded micritic limestone (photo courtesy of Thomas Chidsey, Jr., Utah Geological Survey); B. View southward across the Provo River into Pole Canyon, which is underlain by the Manning Canyon Shale (MCS and in foreground) dipping gently eastward above the Great Blue Limestone (GB) and beneath the Oquirrh Group (OG) forming the steep flanks of Cascade Mountain.

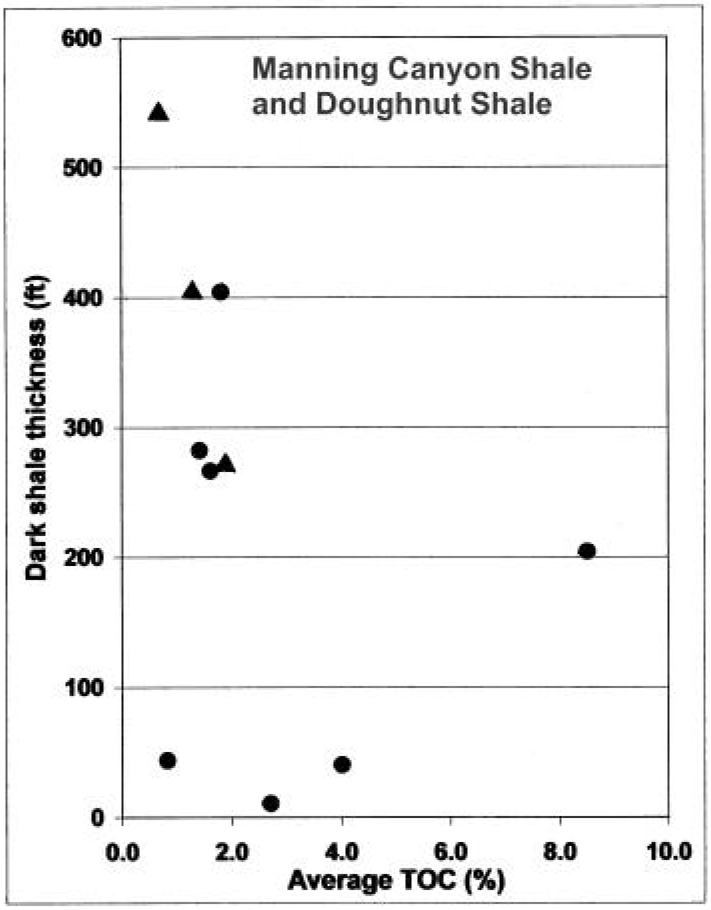

Figure 63: Average TOC for the Manning Canyon Shale (solid triangles) and Doughnut Formation (solid circles) plotted against the net thickness of dark gray shale in the section sampled. Data from Swetland and others (1978).

Hermosa Group Black Shales

The Paradox basin is a nearly elliptical depression (Fig. 64) formed in the Pennsylvanian by the transpressive rise of the northwest-trending Uncompaghre uplift (Stone, 1977). During the Pennsylvanian, the basin accumulated a thick evaporate succession (Fig. 65), including halite and potash, that soon deformed into a variety of domes and linear salt walls in the deeper northeast half of the basin, the fold and fault belt.

The Hermosa Group (Figs. 66, A) is the principal syn-orogenic sedimentary fill of the Paradox basin. This succession spans nearly the entire Pennsylvanian (Atokan through Virgilian; Welsh and Bissell, 1979). Beginning with the onset of basin subsidence, it was deposited on variegated paleosols (Molas Formation) up to 260 ft thick of Morrowan-Atokan age formed by chemical weathering at the karstified surface of underlying Mississippian shelf carbonates. The Hermosa

Group was deposited as a series of trangressive-regressive evaporate cycles dominated by restricted basin carbonates (Hite and others, 1984). It is divided into three formations with the middle unit, the Paradox Formation, differentiated by the presence of halite in each cycle. The lower and upper formations are salt-free. The Pinkerton Trail Formation consists of cyclically interbedded dark gray shale, anhydrites and dolostones. It is up to 400 ft thick around the basin margins, but thins towards the basin center where halite is co-deposited in with the other evaporate lithologies. The Paradox Formation contains 29 recognized cycles in a section up to 7,000 ft thick. The cycles (Fig. 66, B) are comprised of an alternation of halite through anhydrite, dolostone and limestone to a black shale, then reversing order back to halite. In most instances, the black shales, which are on the order of several tens of feet thick, are in the centers of the cycles as designated. Individual cycles may or may not include halite and in some the black shale may be quite thin. Honaker Trail Formation is a 1,000-1,700 ft thick shoaling upward succession of carbonates of late Desmoinesian to Virgilian age. It represents the final filling of the actively subsiding transpressional basin.

Palynomorphs from the evaporate-black shale cycles of the Paradox Formation indicate a climatic oscillation between warm-wet and cool-dry periods corresponding to glacio-eustatic sealevel rise and fall with an approximately 100,000 year periodicity (Rueger, 1996). During the interglacials, seawater flooded the Paradox basin from the west ending deposition of evaporites. During these warm-wet periods, mud and terrigenous plant remains were transported into the basin from the Silverton delta, which was situated to the southeast in southern Colorado (Fetzner, 1960). With the onset of the next glacial period, sealevel dropped restricting seawater flux into the basin. The corresponding cool-dry climate promoted evaporation and closed off influx from the Silverton delta.

The black shales of the Hermosa Group consist of nearly equal portions of clay-sized quartz, dolomite and other carbonate minerals, and various clay minerals. The clay is mainly illite with minor amounts of chlorite and mixed layer chlorite-smectite (Hite and others, 1984).

The Gibson Dome #1 well (21-30S-21E, San Juan County) was drilled by the U.S. Department of Energy as a stratigraphic test and cored continuously from 200 to 6,500 ft depth. This well provides valuable information on the distribution of organic richness in the black shales in the Hermosa Group (Fig. 67; also see Appendix A). The TOC is seen to increase regularly downward through the Honaker Trail Formation from less than 1% to about 2%. The two 'spikes' in this part of the profile are in coaly shales. TOC increases to just over 4% in the Ismay-Desert Creek interval (cycles 1-5). Values in excess of 6% are present in the Akah interval (cycle 6-9. In the Barker Creek interval (cycle 10-20) very high TOC values are observed in the relatively thin cycles 10 and 13. Also high values up to nearly 6% and 4% are found in the Alkali Gulch interval (cycles 21-29) and Pinkerton Trail Formation, respectively.

A compilation of TOC data for 39 wells scattered across the Paradox basin provides a more comprehensive assessment of organic richness from various stratigraphic intervals (see Appendix A). The data set is from Table 1 in Nuccio and Condon (1996a) and the DOE Gibson Dome #1 and DOE Elk Ridge #1 wells (Hite and others, 1984). The TOC values are displayed in Fig. 68 as frequency distributions. The median and maximum values for the five stratigraphic intervals are:

- Honaker Trail 0.97% and 2.97% (excluding coaly shales)
- Ismay-Desert Creek 1.93% and 10.98%
- Akah-Barker Creek 4.05% and 12.86%
- Cane Creek (cycle 21) 3.96% and 11.06%
- Pinkerton Trail 1.22% and 3.44%.

The kerogen (Fig. 69) is largely gas-prone humic type III and mixed type II-III (Nuccio and Condon, 1996b). As would be expected, the thermal maturities are higher in the deeper Cane Creek cycle near the base of the Paradox Formation than in the Ismay-Desert Creek interval at the top (Fig. 70). Across most of the Paradox basin, the Cane Creek cycle is well within the gas generative window (> 1.1% Ro), even for a more oil-prone kerogen than is generally present in these black shales. It is probable that the wells preferentially have sampled Paradox black shales in the structurally higher, and thereby 'cooler', parts of the basin. If true, a substantial part of the Paradox Formation in the interdome 'synclines' has been or is still in the gas generative window.

Nuccio and Condon (1996b) offer a somewhat unconventional view of thermal maturity in a map (Fig. 71) contouring production index (PI) values derived from RockEval pyrolysis data. Production index is the measure of the ratio of free hydrocarbons in the source rock to the total hydrocarbons that can be generated by thermal breakdown of kerogen. For oil-prone source rocks, values in the range 0.1-0.4 are attributed to the oil generative window, and values greater than 0.4 are placed in the gas generative window. Given that the kerogen is dominantly humic, the gas threshold might better be set at a PI of 0.2, in which case a large volume of the Paradox Formation in the fold and fault belt would have been, or now is, generating natural gas.

Numerous factors favor the possible development of shale gas in the black shale intervals of the Hermosa Group. First, the shales are very organic-rich, on the whole the most carbonaceous shales in Utah, and they are inherently gas-prone. Second, they have reached relatively high degrees of thermal maturity across much of the basin center as evidenced by their present Ro and PI values. Third and perhaps most significant, the shales are encased in halite and anhydrite which retard gas leakage, even by diffusion. Yet it is curious that the Paradox basin is largely an oil province (Morgan, 1992; Montgomery, 1992) in which gas production is historically secondary and associated. Perhaps this relates to the concentration of petroleum development in the shallower targets on the southwest basin margin and in the anticlines.

The salt structures in the Paradox basin were growing already in the Pennsylvanian as evidenced by the thinning of the Hermosa Group strata (Fig. 72, A) towards the structures (Doelling, 1988). This feature of early salt movement influencing stratal thickness and depositional patterns is known from other salt basins (Schamel and others, 1995). The consequence in the Paradox basin is that the interdome 'synclines' (Fig. 72, B) are likely sites for thicker accumulations of the black shale facies and less severe deformation of the Paradox Formation (Fig. 73). Here also the black shales are more likely to have generated and retained natural gas. Despite the greater depth for wells required to test the 'synclines', they should be tested for shale gas reservoirs, or gas accumulations in general.

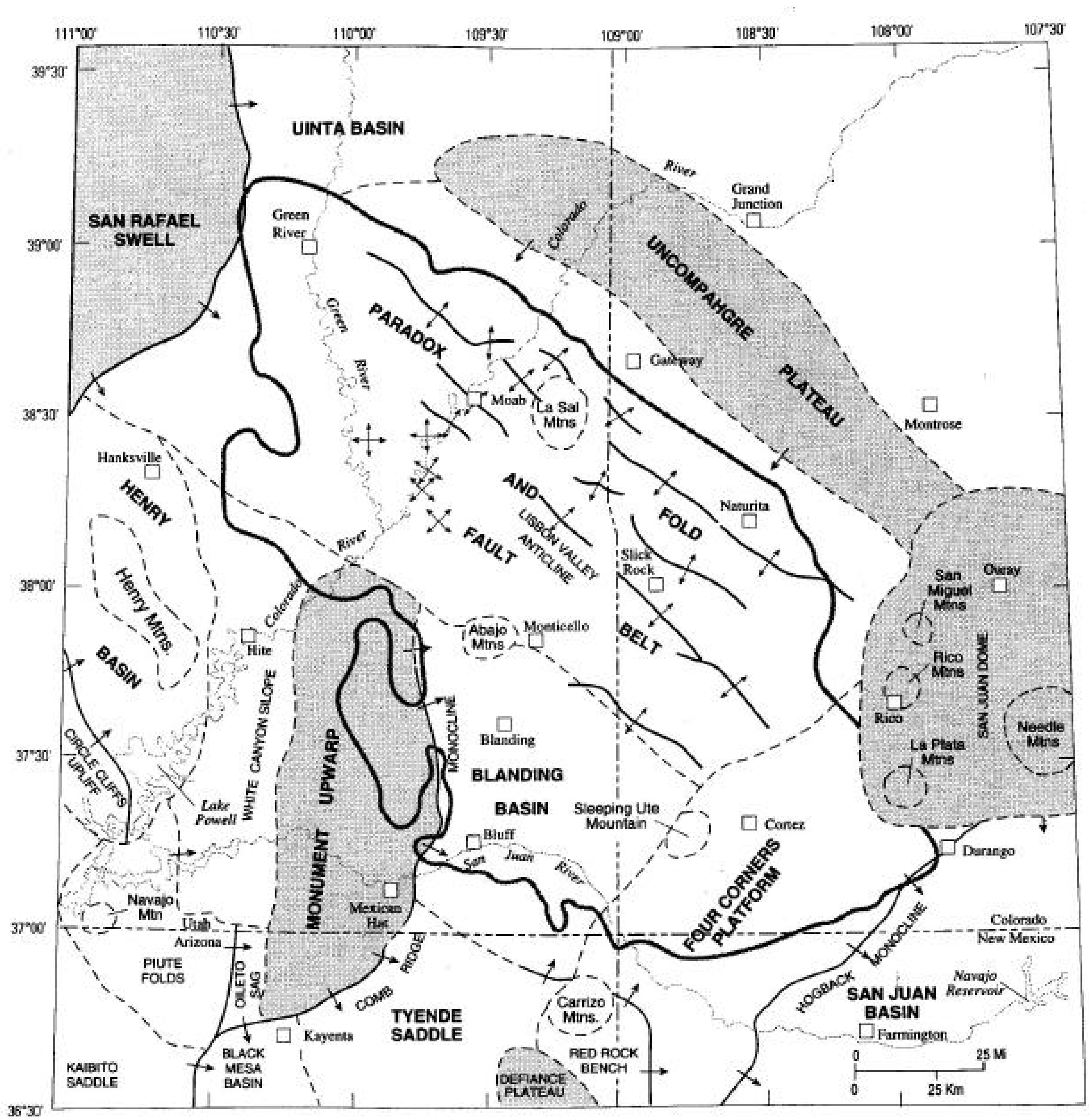

Figure 64: Sturctural elements of the Paradox basin and surrounding areas (Nuccio and Condon, 1996a).

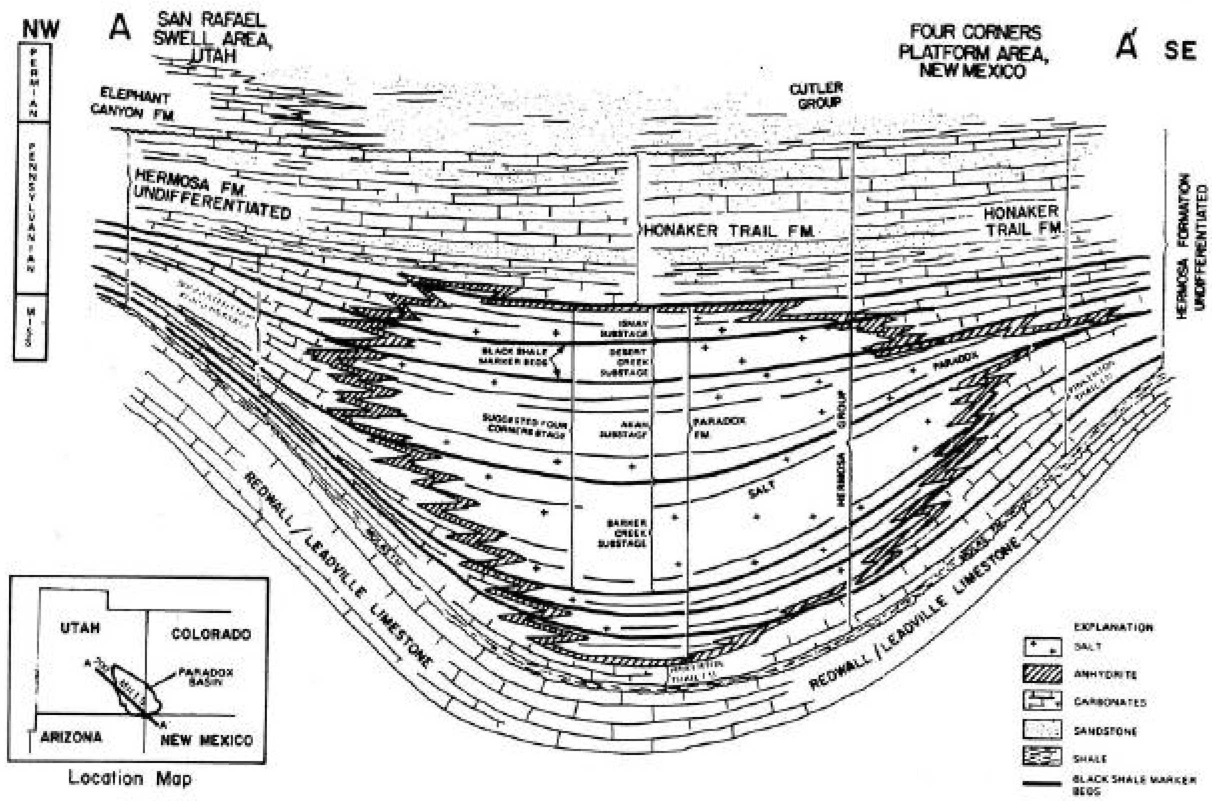

Figure 65: Generalized Pennsylvanian stratigraphy of the Paradox basin (Huntoon, 1988, redrawn after Baars and others, 1967).

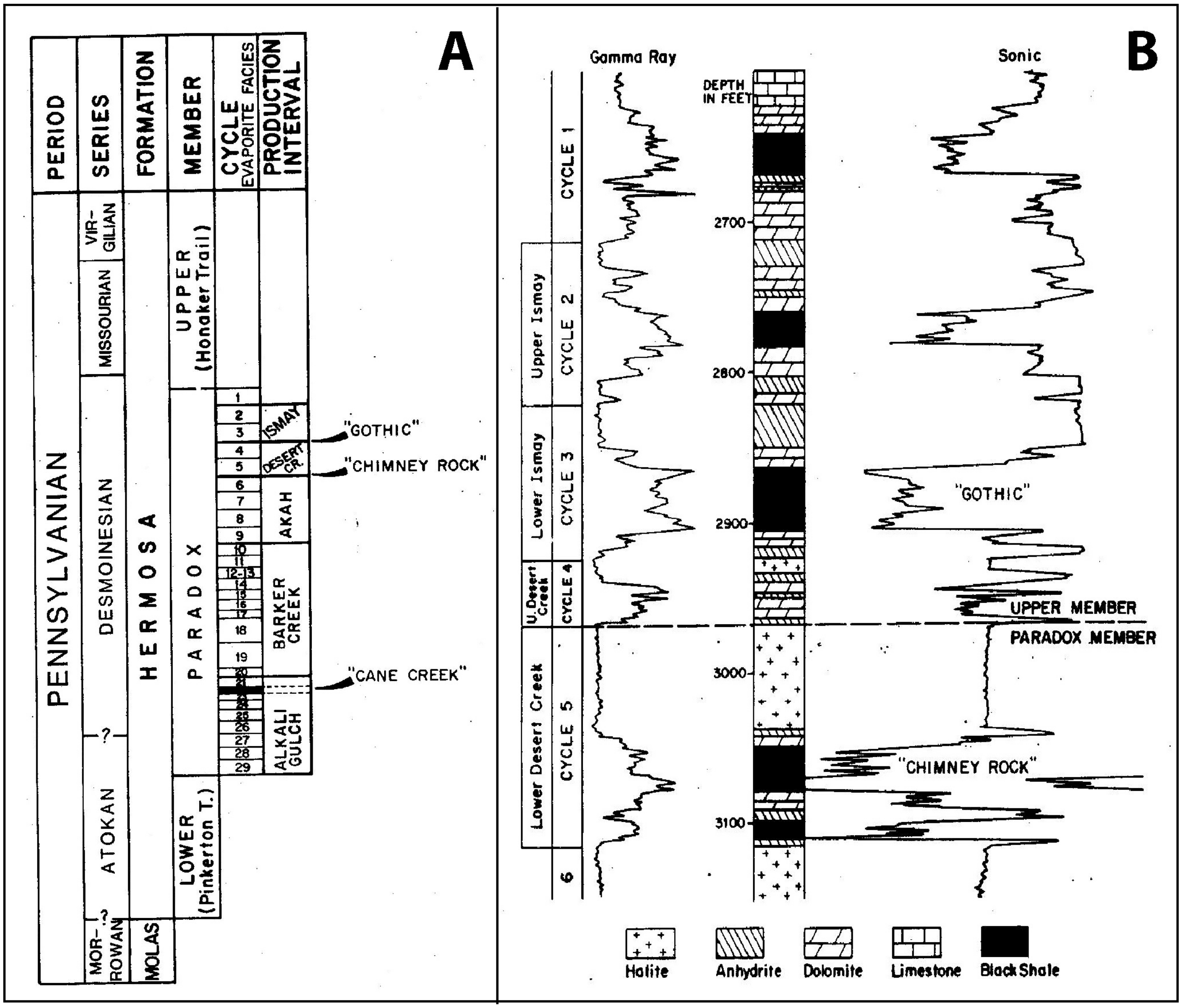

Figure 66: Stratigraphy of the Hermosa Group, Paradox basin (Hite and others, 1984).

A. Pennsylvanian stratigraphy of the Paradox basin showing the 'cycles' of the Paradox Formation, including the principal named black shale intervals. B. Detailed stratigraphy of the upper five cycles of the Paradox Formation, which include the Gothic and Chimney Rock black shale intervals.

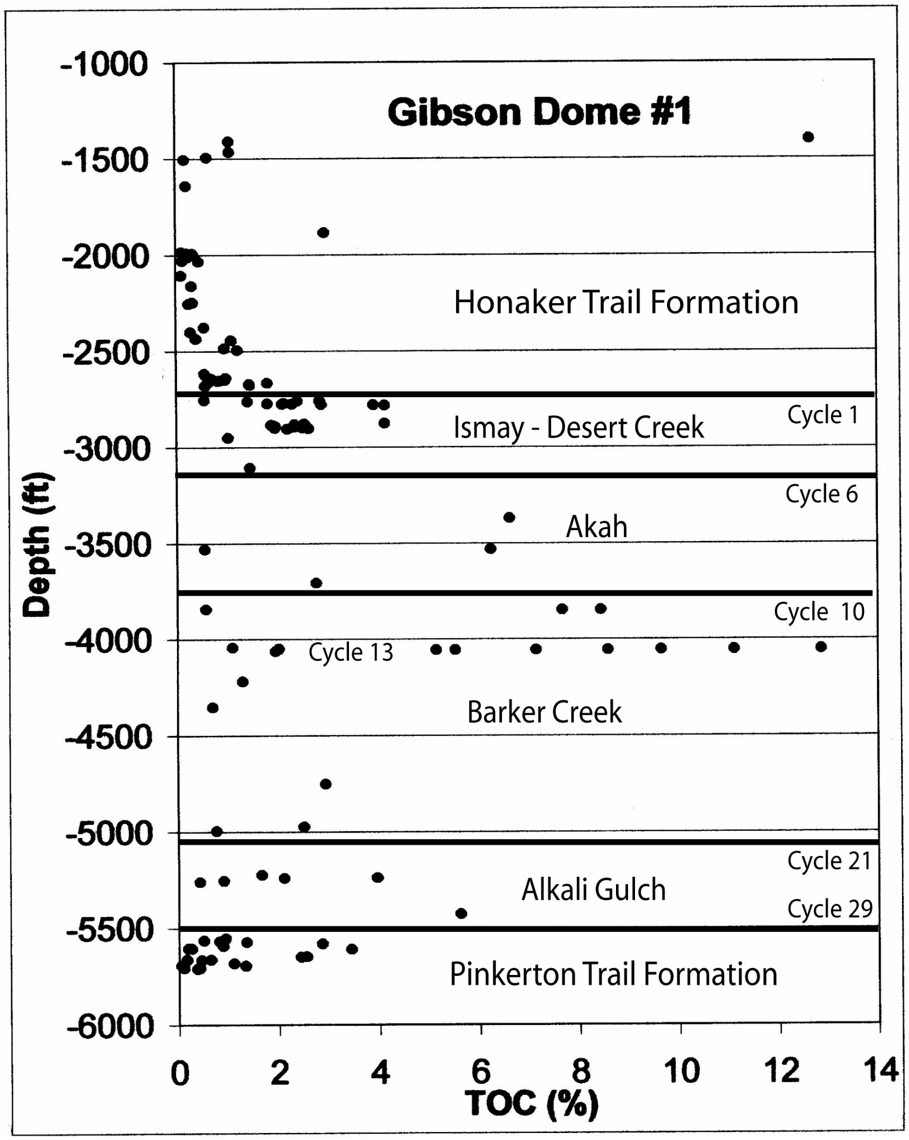

Figure 67: Distribution of TOC values with depth in the Gibson Dome #1 well (21-30S-21E, San Juan County). Data from Hite and others (1984).

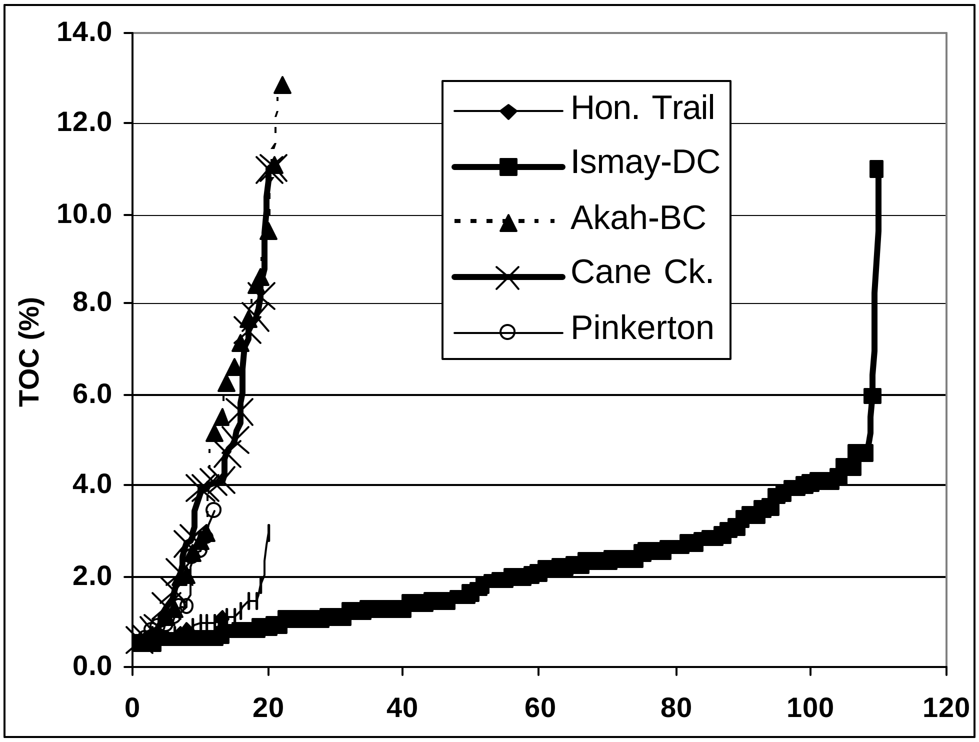

Figure 68: Distribution of TOC values measured in various stratigraphic intervals of the Hermosa Group, Paradox basin. Data from Nuccio and Condon (1996a) and Hite and others (1984).

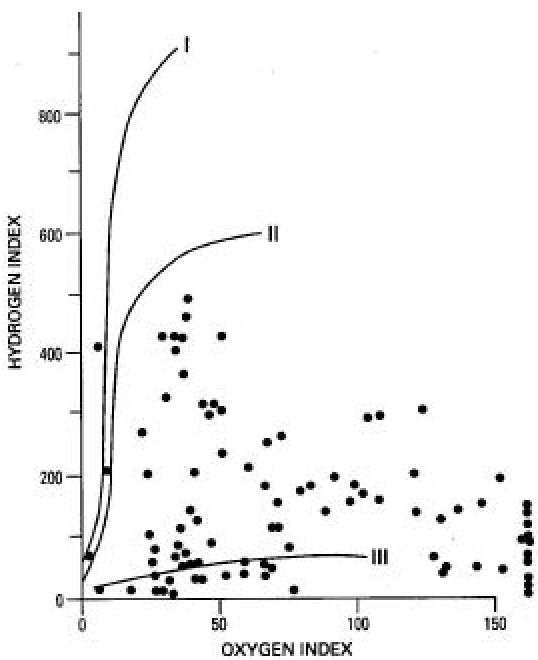

Figure 69: Modified van Krevelen plot of samples from the Ismay-Desert Creek interval showing that the kerogen is mainly type III and mixed type II-III (Nuccio and Condon, 1996b).

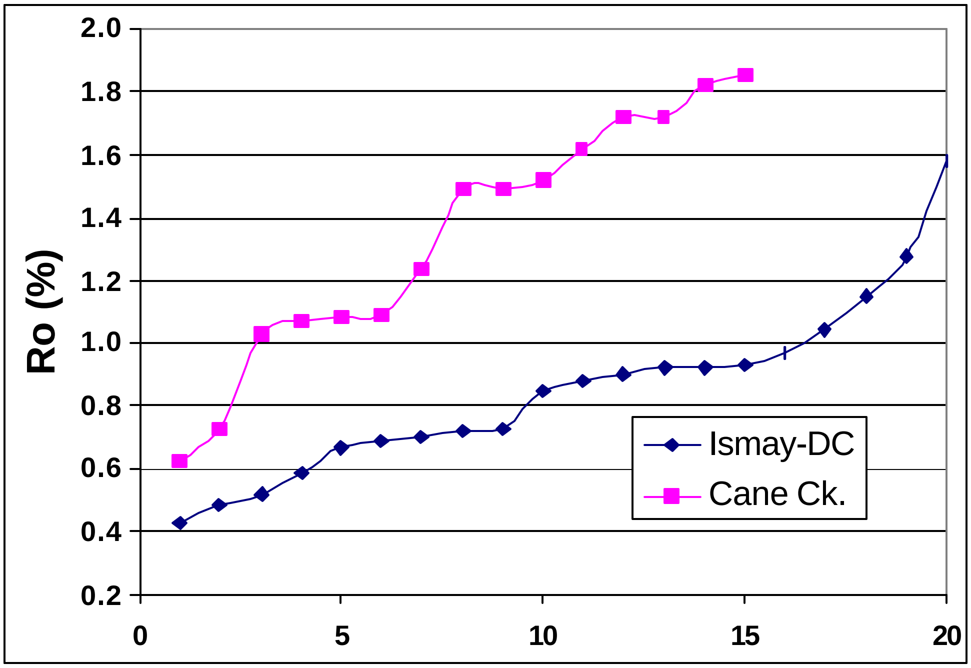

Figure 70: Distribution of Ro values measured in the Ismay-Desert Creek and Cane Creek intervals of the Paradox Formation. Data from Nuccio and Condon (1996a).

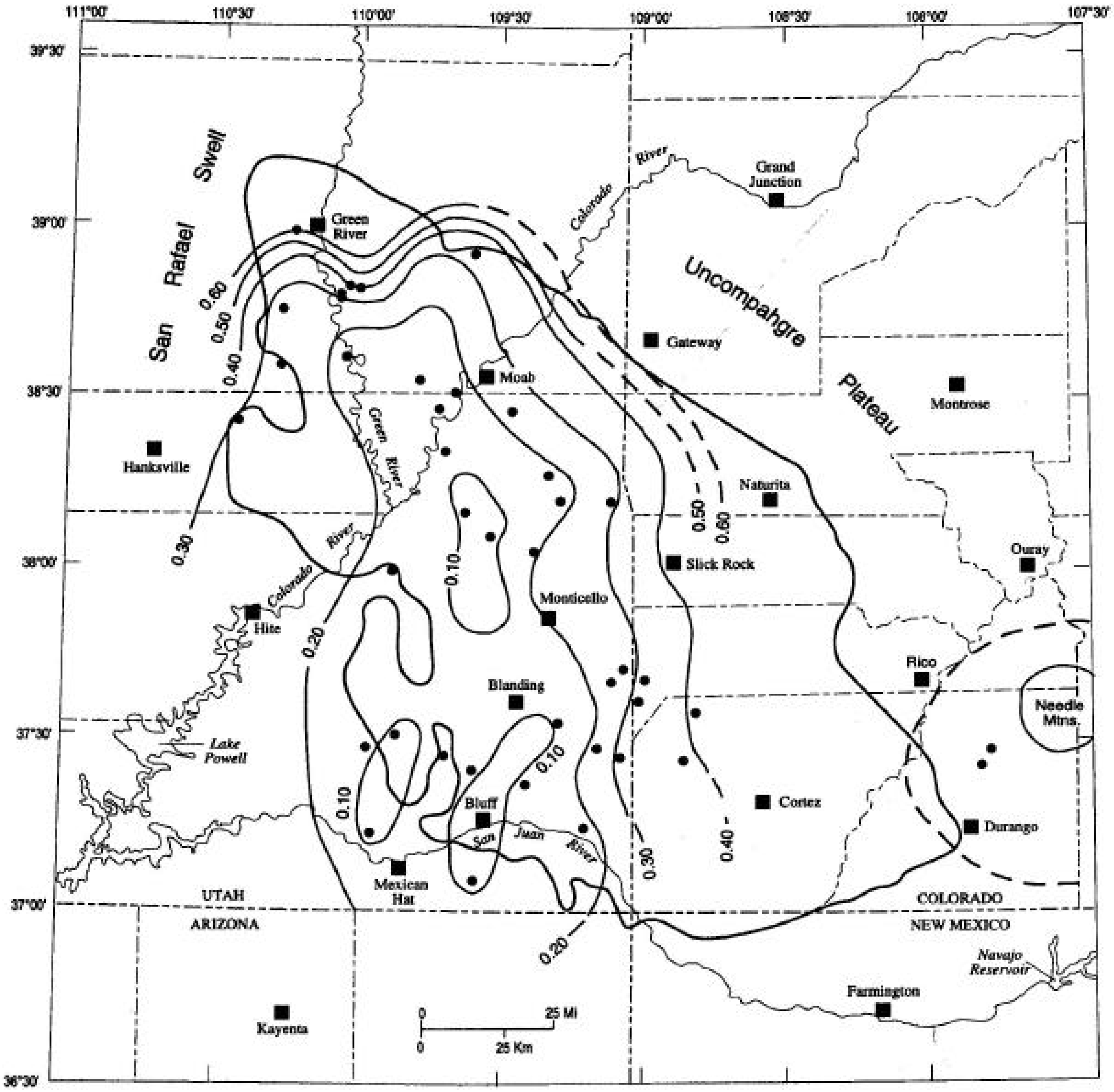

Figure 71: Thermal maturity map of the Paradox basin a the level of the Ismay-Desert Creek interval (Nuccio and Condon, 1996). Contoured is production index (PI) at 0.10 contour spacing.

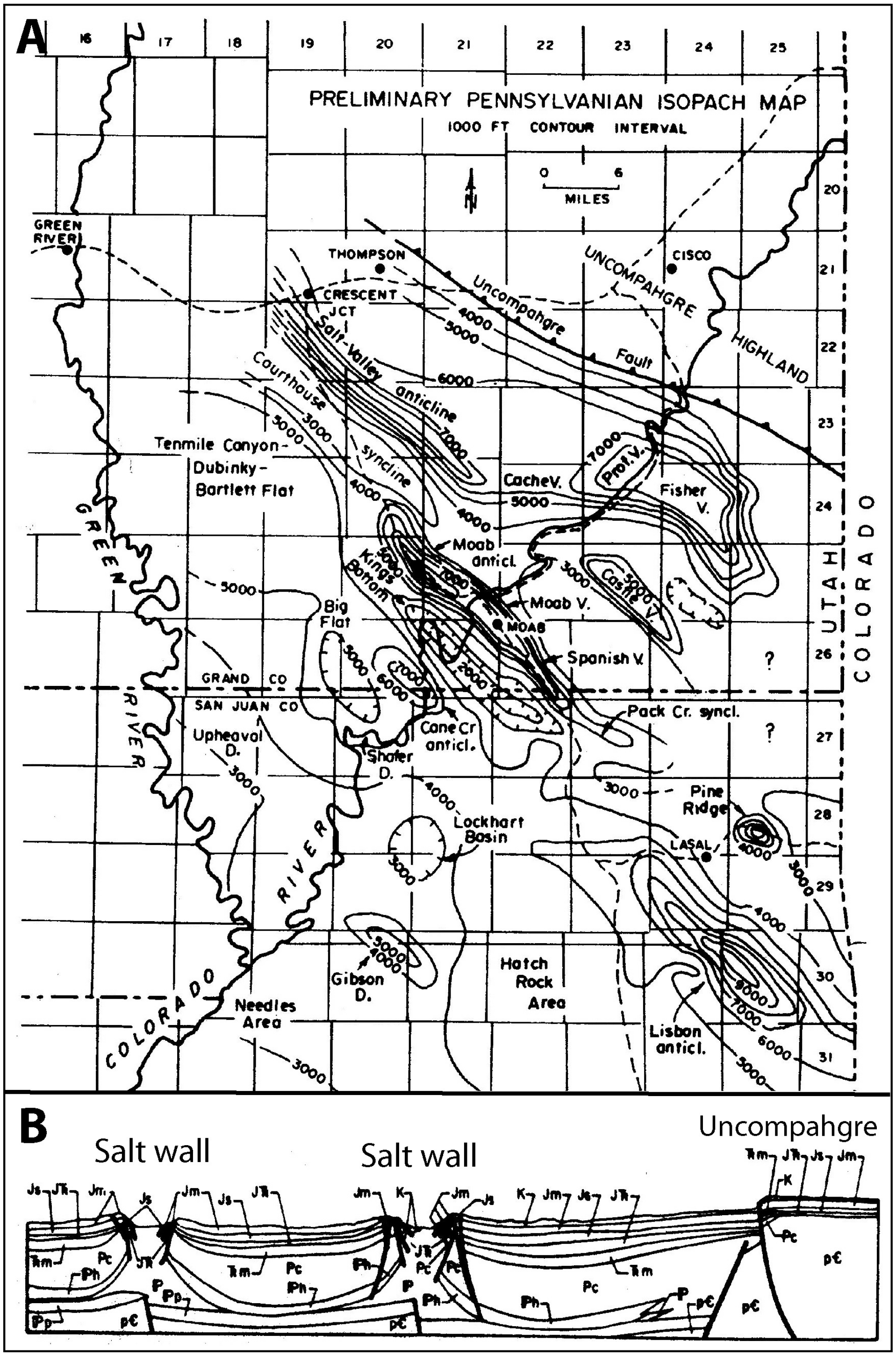

Figure 72: Salt walls in the fold and fault belt of the Paradox basin.

A. Pennslyvanian system isopach map delineates the salt walls, which began growing during or shortly after deposition of the Paradox Formation (Doelling, 1988). B. Structural cross section showing the broad, deep 'synclines' separating the salt walls (Huntoon, 1988).

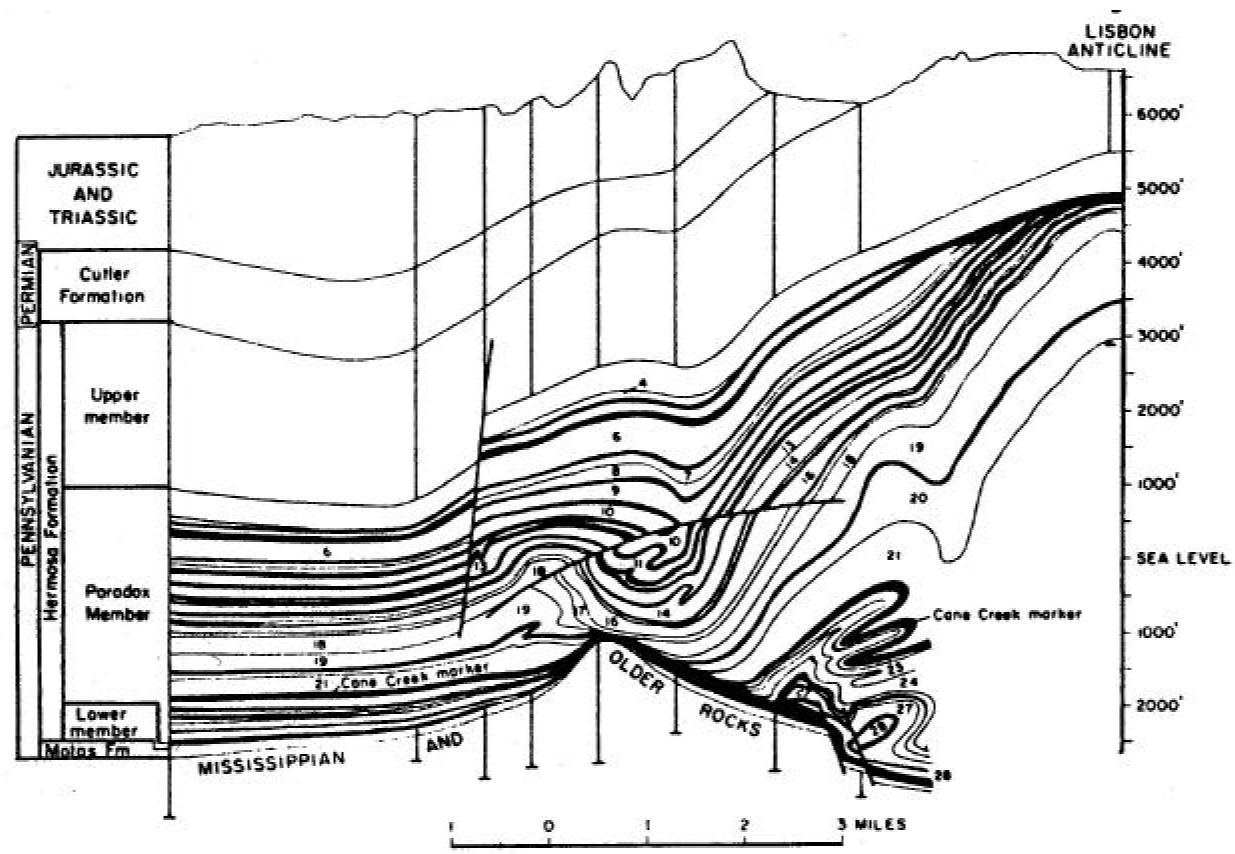

Figure 73: Structural cross section of the west limb of the Lisbon Valley anticline showing the deformed Paradox Formation cycles in the anticline and apparent absence of deformation beneath the adjacent 'syncline' (Hite, 1968).

Park City-Phosphoria Black Shales

The phosphatic black sha les of the Phosphoria Formation are demonstrated oil and gas source rocks of considerable regional significance in the northwest Rocky Mountains (Johnson, 2003; Johnson, 2005). The black shale facies is present in two members, the Meade Peak and the Retort, as a heterogeneous assembledge of limestones, cherts, black shales and bedded phosphorites (Maughan, 1984). The Phosphoria Formation was deposited in early Late Permian (Roadian and Wordian stages) time in a shallow marginal sea on the northwest margin of Pangea (Hein, 2004). This coastal depression, the Sublett basin in Idaho, was a remnant of the Antler fordeep (Fig. 74); the low islands bounding the basin to the west were remnants of the Antler orogen. Due to the low-lattitude paleo-position of this seaway and general arid conditions in the mid-Permian, prevailing off-shore winds resulted in moderate to intense upwelling that brought cold, nutrient-rich waters to the surface leading to high organic productivlty and accumulation of phosphatic, organic-rich sediments in the Sublet basin (Hein, 2004).

In Utah, south of the Sublet basin, lay a carbonate shelf, the site of deposition of the shallow marine carbonates of the Park City Formation (Fig. 74). The Park City and Phosphoria Formations of northeast Utah, southeast Idaho and southwest Wyoming are correlative with the Park City Group (Kaibab Limestone, Plympton Formation and Gerster Limestone) of west-central Utah and east-central Nevada. As was true through the Mississippian-Pennsylvanian, sedimentation rates were higher in the Antler foredeep, west of the 'hingeline' than on the craton to the east (Fig. 75). The foredeep deposits are now allochthonous, parts of the Sevier thrustbelt.

During the sealevel high-stand coinciding with the Meade Peak Member in the Sublett basin, nutrient-rich waters spilled out of the basin and across the adjacent shelf deposition phosphatic limestones and black shales (Fig. 76). In northern Utah, this transgression is marked by the Meade Peak Tongue of the Phosphoria Formation, which rests unconformably on the shallow marine limestones of the Grandeur Member of the Park City Formation in the foredeep or the Weber Sandstone on the craton (Fig. 75) and is conformably overlain by the Franson Member of the Park City Formation. The Meade Peak and Franson members are unconformity bounded and record a single major transgressive-regressive cycle (Hendrix and Byers, 2000). The Meade Peak Member is thickest in southern Idaho and southwest Wyoming (Fig. 77) and thins rapidly southward into Utah.

In the Wasatch Range near Salt Lake City, the Meade Peak Phosphatic Shale Member is about 100 ft of dark-gray, phosphatic shale occurring near the middle of the 650 to 1,970 ft thick Park City Formation, which is composed of cherty gray limestone, calcareous siltstone and cherty sandstone (Bryant, 1990). To the north in southern Weber County, the Meade Peak Member measured at Hardy Hollow (2-5N-2E), 14 miles east of Ogden, is 171 ft of interbedded silty phosphatic mudstone, dolomite, dolomitic siltstone, phosphorite and calcareous sandstone (Schell and Moore, 1970), but at this location the unit may be structurally thickened. At Devils Slide on the Weber River, Cheney and Sheldon (1959) report 225 ft of mainly black shale, pelletal phosphorite, and argillaceous cherty carbonate. Along the south flank of the Uinta Mountains and at Sheep Canyon on the northeast flank the Meade Peak Member is up to 65 ft of interbedded organic-rich fine-grained, laminated dolomite and granular phosphatic packstone with gray shale restricted to the transition into the Franson Member (Hendrix and Byers, 2000).

The average organic richness (Fig. 78) of the Meade Peak Member in Utah and adjacent areas is generally less than 2.0% (Maughan, 1979). Higher TOC values reported in Utah are 3.9% at Dry Bread Hollow, northern Wasatch Range (14-7N-3E, Weber County, loc. 50) and 4.5% at Terrance Mountains (3-8N-12W, Box Elder County, loc. 45); locations are shown on Figure 77. On the flanks of the Uinta Mountains the organic-rich dolomite of the Meade Peak Member has TOC in the range 0.29 to 2.04%; the associated phosphatite packstone is only 0.11 to 0.45% (Hendrix and Byers, 2000).

Published information on organic maturity (Figs. 79 and 80) is unconventional, but suggestive that Meade Peak Member in the Sevier thrustbelt is highly mature, perhaps even at or beyond the upper limit of dry gas (Maughan,1979; Claypool and others, 1978) . However, in the Wasatch Range (frontal Sevier thrusts) Mountains lower maturities are indicated (Fig. 79).

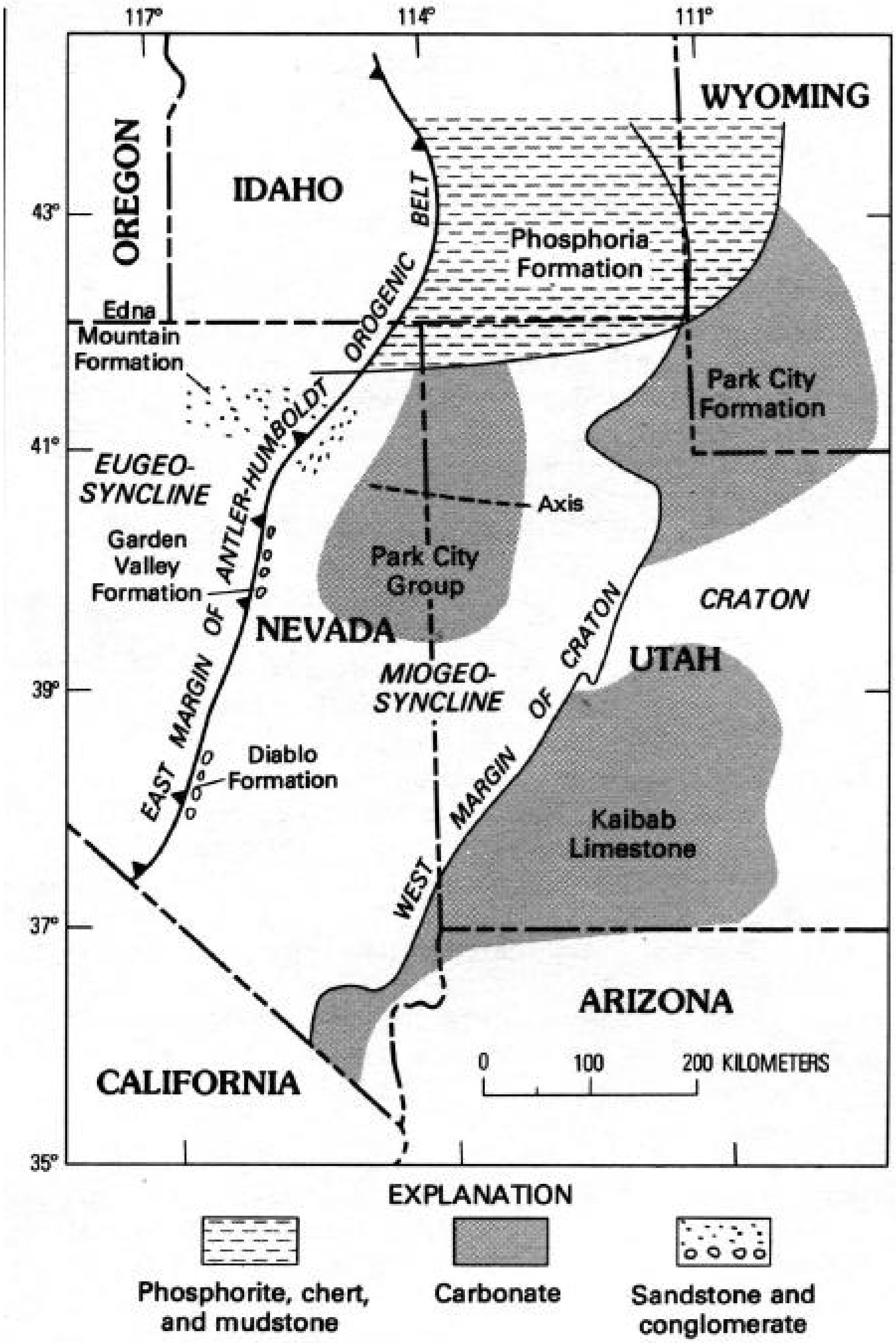

Figure 74: Distribution of the Park City Formation/Group in northern Utah, and its correlatives, the Phosphoria Formation in Idaho and the Kaibab Limestone in southern Utah (Wardlaw and others, 1979)

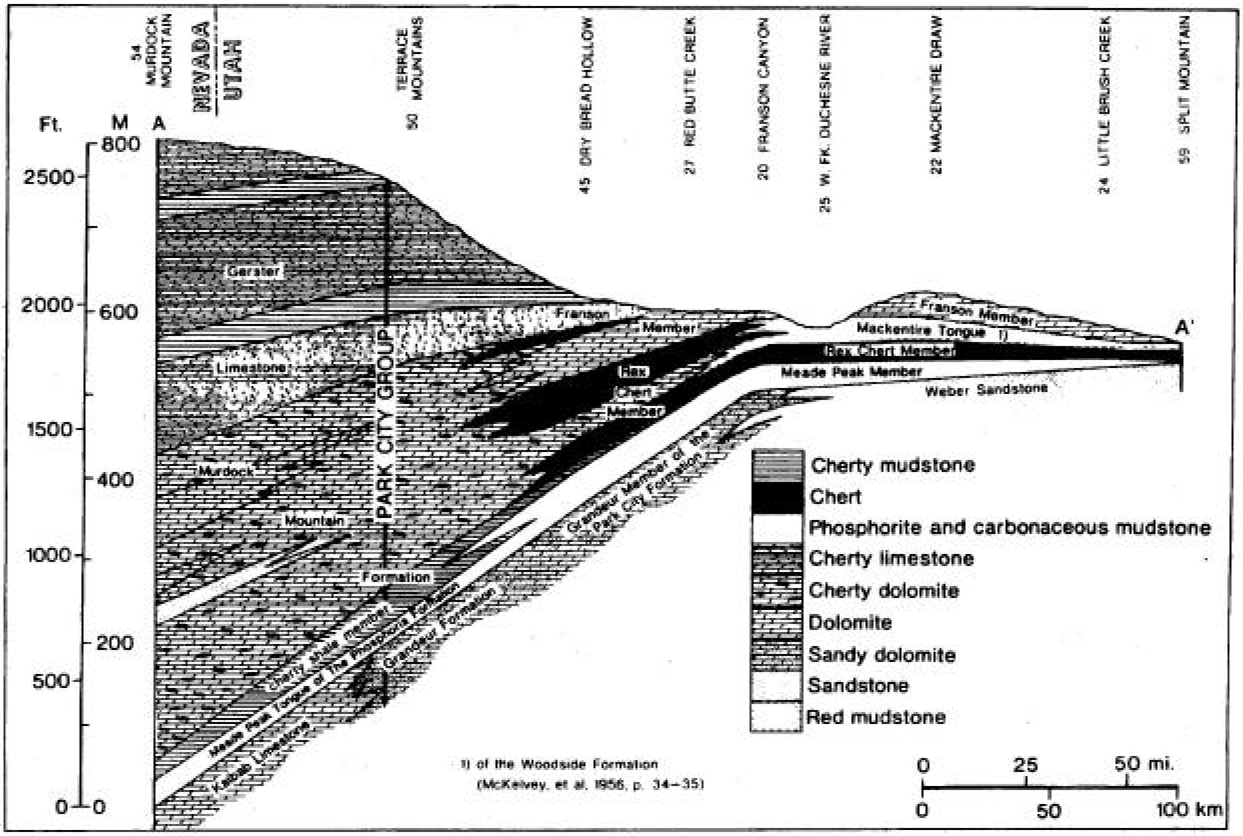

Figure 75: Stratigraphic section of the Park City Group from northwest Nevada east to Split Mountain in northeast Utah (Maughan, 1979). The Meade Peak Member is the only significant black shale unit within the Park City Group; it thins to both the east and the west. Refer to Figure 77 for the location of the stratigraphic section.

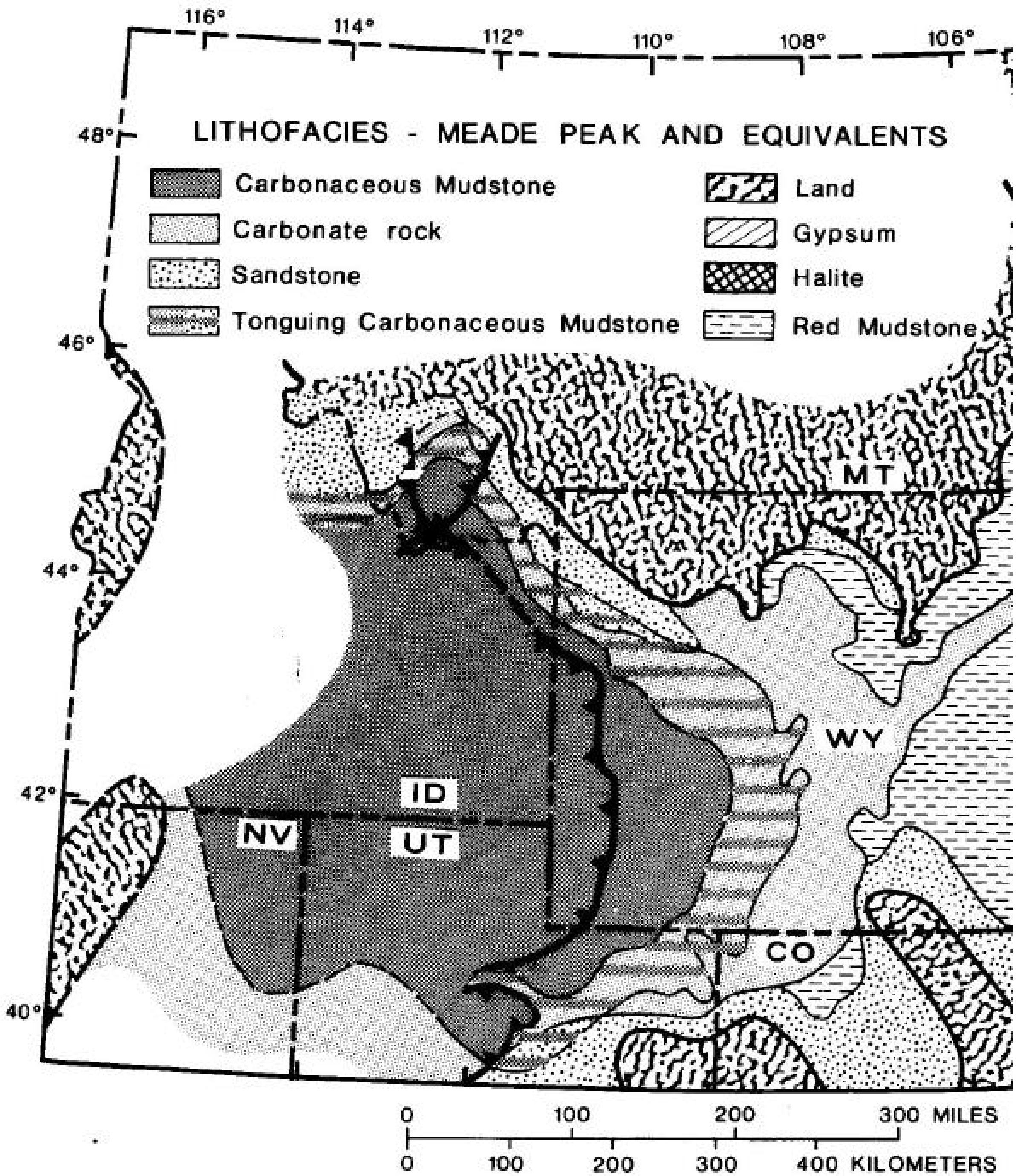

Figure 76: Map showing the maximum distribution of the Meade Peak Tongue of the Phosphoria Formation and its time-equivalent lithofacies. Modified from Maughan (1984).

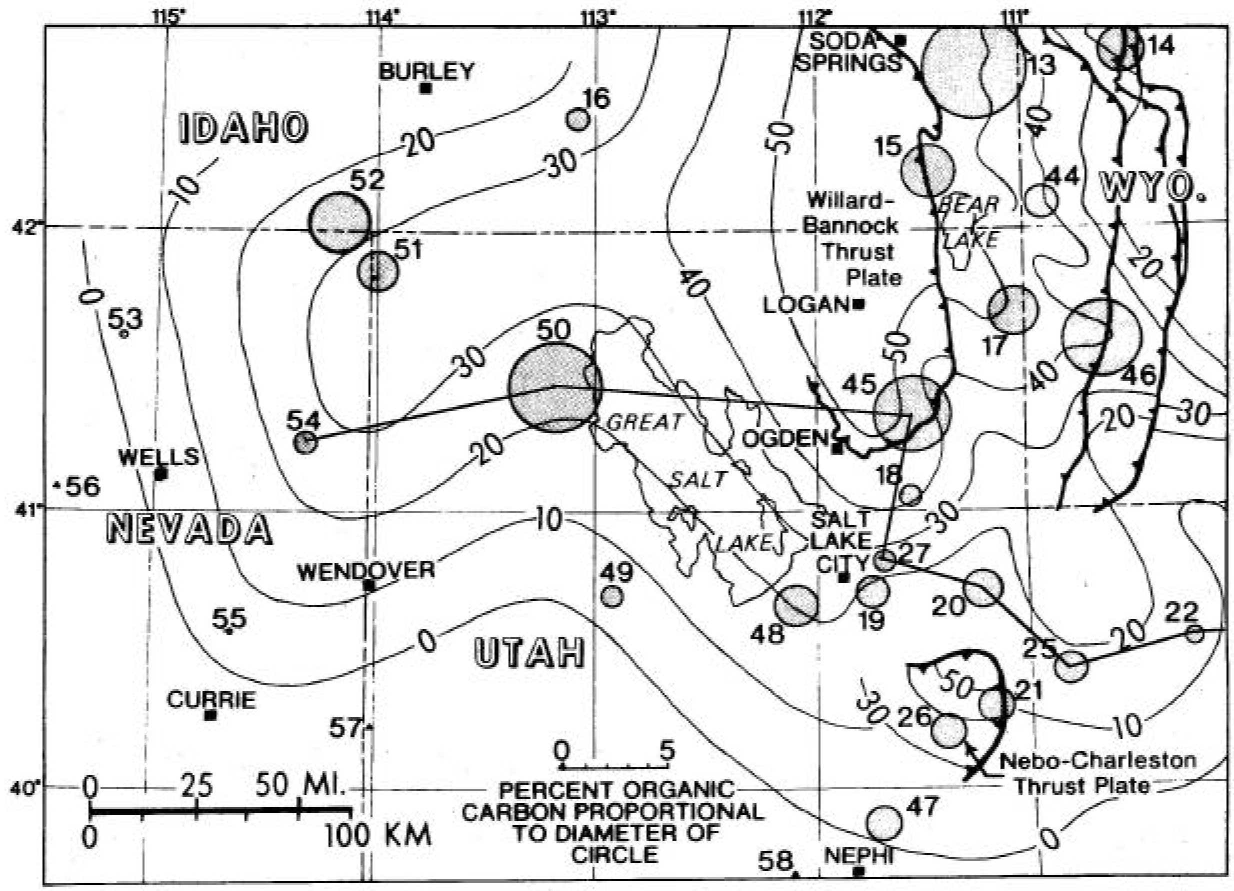

Figure 77: Thickness in meters of the Meade Peak Phosphatic Shale Member in northwest Utah and adjacent states. Modified after Maughan (1979). Ten meters is the equivalent of 32.8 ft; 50 meters is 164 ft. .

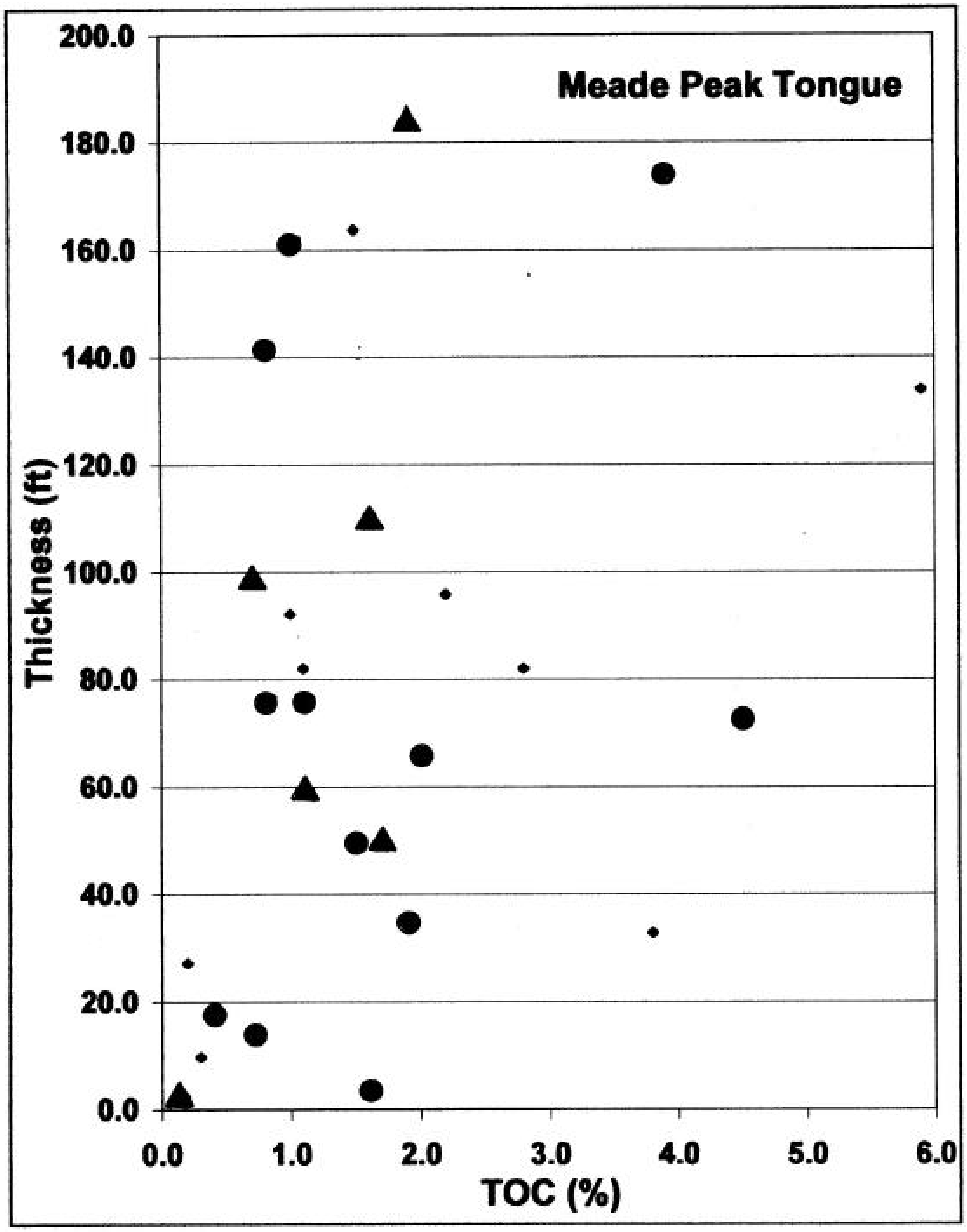

Figure 78: Organic richness (average wt. % TOC) of the Meade Peak Shale Member plotted against the thickness of the member at the sample location. Data are from Maughan (1979). Locations in the Uinta Mountains are shown in solid triangles; Utah locations in the Sevier thrustbelt are shown in solid circles; locations outside of Utah are shown as small dots. All locations are displayed in Figure 77.

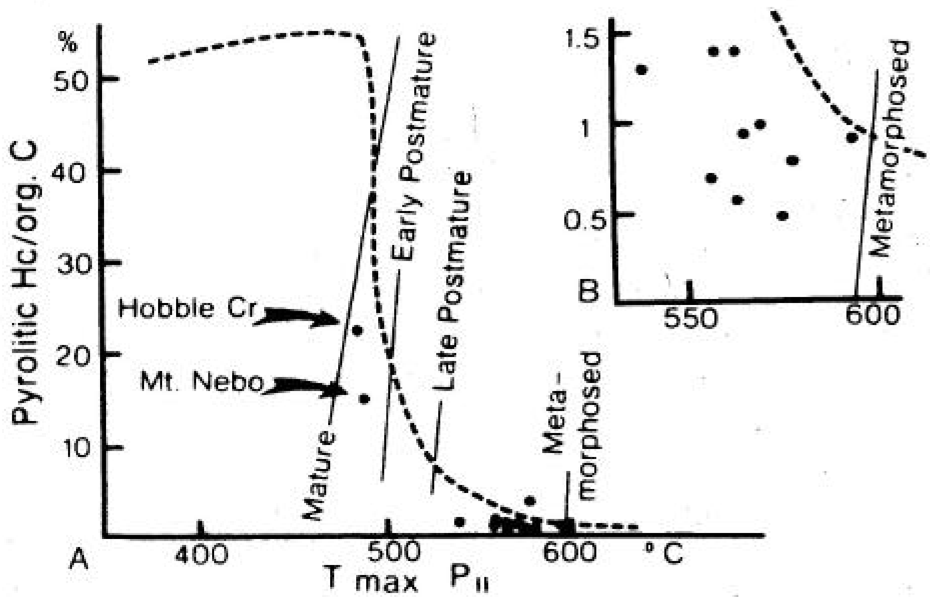

Figure 79: Diagram showing the high degree of maturity of Meade Peak Shale as determined by pyrolysis measurements (see Claypool and others, 1978), which normally has very high values of Tmax and low HC/TOC (Maughan, 1979). Hobble Creek and Mt. Nebo are locations 26 and 47 in Figure 77, respectively.

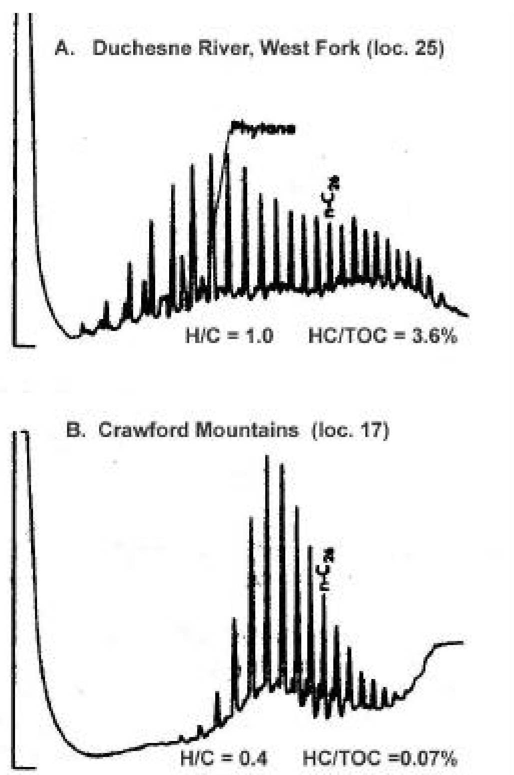

Figure 80: Representative gas chromatograms for saturate fractions of mature (A) versus highly mature (B) Meade Peak Shale samples in northern Utah. Modified after Claypool and others (1978).

Assessment and Recommendations

The two factors that are essential for successful development of shale gas reservoirs are *gas content* and *gas deliverability*. Gas content of a shale is determined by a combination of factors that influence storage of free, adsorbed and dissolved gas, but the most critical for a self-sourcing shale is the organic richness and maturity. As with coals, the gas content is strongly dependent on kerogen 'rank', the level of maturity. Complicating Ro as an approximate measure of gas content in shale is the degree to which gas readily migrates out of or into the shale. Due to smaller molecular size, methane migrates out of shales much faster and more completely than do the components of oil. In the absence of exceptional seals, recent gas generation (or influx of gas from external sources) may be a necessary factor for a shale gas reservoir. Due to the very low matrix permeability of most shales, fractures are essential to assure deliverability at commercial rates. Fracture treatments may merely create new conduits linking existing natural fractures, or they may create a dense network of fractures in an otherwise little fractured rock, as appears to be the case in the Barnett Shale. The possible response of the shale to hydraulic fracturing can serve, together with gas saturation, as an approximate guide to deliverability.

Ideally, satisfactory conditions for gas content and deliverability should exist over an area of at least several tens of square miles to permit the economies of scale that appear to be crucial to the commercial development of all resource plays, especially low-yield shale gas.

Given the very limited amount and scope of information in the literature relevant to Utah's black shales, the 'screening criteria' that could be applied in this project, in most instances, was limited to just (1) organic richness and maturity of the black shale, (2) thickness of the kerogen-rich interval, (3) likelihood of natural and induced fracturing, determined subjectively, and (4) potential barriers to hydraulic fracturing, or water-saturated zones, in adjacent strata. As a consequence, the assessments presented herein are subjective and should be considered preliminary, pending further data gathering and analysis.

This project has recognized five kerogen-rich shale units as having reasonable potential for commercial development as shale gas reservoirs. These are four members of the Mancos Shale in northeast Utah - the Prairie Canyon, the Juana Lopez, the Lower Blue Gate, and the Tununk. The fifth is the black shale facies within the Hermosa Group in southeast Utah.

The *Prairie Canyon* and *Juana Lopez* Members are both detached mudstone-siltstone-sandstone successions embedded within the Mancos Shale in northeast Utah. The Prairie Canyon Member is up to 1,200 ft thick, but the stratigraphically deeper Juana Lopez Member is less than 100 ft. Both are similar in lithology and basinal setting to the gas-productive Lewis Shale in the San Juan basin. As in the Lewis Shale, the lean, dominantly humic, kerogen is contained in the shale interlaminated with the siltstone-sandstone. The high quartz content is likely to result in a higher degree of natural fracturing than the enclosing claystone-mudstone rocks. Thus, they may respond well to hydraulic fracturing. Also the porosity of the sandstone interbeds averaging 5.4% can enhance gas storage. Both units extend beneath the southeast Uinta basin reaching depths sufficient for gas generation and retention from the gas-prone kerogen. Although not known to be producing natural gas at present, both units are worthy of testing for add-on gas, especially in wells that are programmed to target Lower Cretaceous or Jurassic objectives.

The *Lower Blue Gate* and *Tropic-Tununk* shales generally lack the abundant siltstone-sandstone interbeds that would promote natural and induced fracturing, but they do have zones of observed organic richness in excess of 2.0% that might prove to be 'sweet spots' for shale gas where the rocks are sufficiently buried beneath the southern Uinta basin and perhaps parts of the Wasatch Plateau. Directional drilling methods are likely required to exploit the high-TOC sweet spots, if they indeed prove to control gas content variations in the Mancos Shale.

The black shale facies in the *Hermosa Group* of the Paradox basin is enigmatic. These shales contain mixed type II-III kerogen that should favor gas generation, yet oil with associated gas dominate current production. They are relatively thin, just a few tens of feet thick on average, yet they are encased in excellent sealing rocks, salt and anhydrite. In the salt walls (anticlines) the shales are complexly deformed making them difficult to develop even with directional drilling methods, but where they are likely less deformed in the interdome areas (synclines) they are very deep. Yet in these deep areas one can expect peak gas generation. The shales are overpressured, which suggests generation currently or in the recent past. Prospects are good that shale gas reservoirs can be developed in the Paradox basin, but it may prove to be technically and economically challenging.

The *Mowry Shale* is kerogen-rich, gas-prone and siliceous, all factors that should favor development as a gas reservoir where sufficiently deep for gas generation and retention. It is possible that this black shale might be exploited somewhere in the Green River basin or other parts of southwest Wyoming, but the area for developing a play in Utah is too limited for a stand-alone project that does not cross the state line. It is only north of the Uinta Mountains that it is sufficiently thick to be considered an economically viable shale gas reservoir.

The black shale facies of the *Green River Formation* is extremely thick and widespread in the Uinta basin, and it is very rich in type I kerogen. The very fact that the kerogen is type I has retarded hydrocarbon generation. Much of the black shale facies is undermature and that that is mature has produced mainly oil and associated gas. The oil-saturated shales are poor candidates for development of non-associated thermogenic gas. A resource play might exist in some parts of the Uinta basin centered on non-associated biogenic methane from the black shale facies. But this would require the existence of a shallow seal that could be readily bypassed by meteoric waters without permitting the leakage of methane. Mats of congealed high pour point oils at shallow depths might serve this function, if they are sufficiently widespread. At this point, even their existence beyond a few small locations is conjecture.

The *Meade Peake Member*, the *Manning Canyon Shale* and the *Doughnut Formation* deserve a closer look due to their considerable thickness and organic richness, but, at present, too little is known about the units to pronounce them as possible shale gas reservoirs. The actual interval of kerogen-rich shale in each unit may prove to be either too mature, too thin and/or too structurally deformed to favor even exploratory drilling. The *Delle Phosphatic Shale Member* appears to be out of the question as a shale gas reservoir for the same reasons that might disqualify the other Paleozoic black shales.

There are several steps required to better understand and document the potential for shale gas development in Utah. These include:

- Systematic gathering, analysis and compilation of information on gas tests and shows in wells penetrating the Mancos Shale, the Hermosa Group and possibly other black shale units. It is likely that shale gas has been discovered throughout the state, but not adequately recognized as such. This study should be done together with examination of electric logs to look for possible kerogen-rich, silty or fractured intervals to compare to the gas test/shows data. Given the limitations with commercial databases, it would be advised to at least supplement this investigation using all types of records at the Utah Division of Oil, Gas and Mining and those available from operators. This exercise might be the easiest, least expensive, yet most effective way of building confidence for this resource play.
- Characterization of organic richness, kerogen type and thermal maturity of the Prairie Canyon Member using the cores available at the USGS Core Research Center. Curiously, no such data has been published on this set of cores, nor is any now available in the Center's files.
- Focused modeling of organic maturity of the Mancos Shale and the Hermosa Group shales using kinetic parameters tailored to the kerogen types actually present in the rocks.
- Examination and testing of the existing cores through the Mancos Shale for rock mechanics properties (elastic moduli) and propensity for fracturing. This would include doing triaxial stress tests on selected core samples, supplemented perhaps by 'scratch test' measurements using procedures developed by TerraTek Inc.

The most effective assessment of this resource will come from individual operators taking the trouble and expense to test the potential for add-on gas as they drill through the Mancos Shale, the Hermosa Group, or any of the other kerogen-rich shales in Utah. These shales should be seen as a potential reservoir for gas, not just a source rock charging distant traps.

Acknowledgements

The author wishes to acknowledge the contributions of many persons who generously offered advice and/or provided information to this project: S. Robert Bereskin (Bereskin and Associates); Thomas Chidsey, Jr. (Utah Geological Survey); Walter E. Dean (U.S. Geological Survey); Edmund R. "Gus" Gustason (EnCana Oil & Gas (USA) Inc.); Jeannine Honey (USGS Core Research Center); Michael Laine (Utah Core Research Center); Michael D. Lewan (U.S. Geological Survey); Craig D. Morgan (Utah Geological Survey); David Tabet (Utah Geological Survey).

Craig Morgan and Roger Bon supervised this project on behalf of the Utah Geologic Survey.

References Cited

Anders, D.E., and P.M. Gerrild, 1984, Hydrocarbon generation in lacustrine rocks of Tertiary age, Uinta Basin, Utah - organic carbon, pyrolysis yield, and light hydrocarbons, *in* J. Woodward, F.F. Meissner, and J.L. Clayton, eds., Hydrocarbon Source Rocks of the Greater Rocky Mountain Region: Denver, CO, Rocky Mountain Association of Geologists, p. 513-529.

Anders, D. E., J. G. Palacas, and R. C. Johnson, 1992, Thermal maturity of rocks and hydrocarbon deposits, Uinta basin, Utah, *in* T. D. Fouch, V. F. Nuccio, and T. C. Chidsey, eds., Hydrocarbon and mineral resources of the Uinta basin, Utah and Colorado: Salt Lake City, Guidebook 20, p. 53-76.

Baars, D.L., J.W. Parker, and J. Chronic, 1967, Revised stratigraphic nomenclature of Pennsylvanian System, Paradox basin: AAPG Bulletin, v. 51, p. 393-403.

Baars, D. L., 1988, Triassic and older stratigraphy; Southern Rocky Mountains and Colorado Plateau, *in* L. L. Sloss, ed., Sedimentary Cover - North American Craton: The Geological Society of America, The Geology of North America D-2, p. 53-64.

Berg, R. R., and A. F. Gangi, 1999, Primary migration by oil-generation microfracturing in low-permeability source rocks: Application to the Austin Chalk, Texas: AAPG Bulletin, v. 83, p. 727-756.

Bissell, H.J., 1959, Oquirrh Formation, *in* H.J. Bissell, ed., Guidebook to the Geology of Utah No. 14: p. 93-127.

Bojesen-Koefoed, J. A., and H. P. Nytoft, 2003, Petroleum geochemistry: Cenomanian-Turonian succession of three cores from the Cretaceous Western Interior Seaway, USA: Geologic Survey of Denmark and Greenland Report 2003/18.

Bowker, K. A., 2002, Recent developments of the Barnett Shale play, Fort Worth Basin, *in* B. E. Law, and M. Wilson, eds., Innovative Gas Exploration Concepts Symposium: Denver, CO, Rocky Mountain Association of Geologists, p. 16.

Broadhead, R. F., 1993, Petrography and reservoir geology of Upper Devonian shales, northern Ohio, *in* J. B. Roen, and R. C. Kepferle, eds., Petroleum Geology of the Devonian and Mississippian Black Shale of Eastern North America: U.S. Geological Survey Bulletin 1909, p. H1-H15.

Bredehoeft, J.D., J.B. Wesley, and T.D. Fouch, 1994, Simulation of he origin of fluid pressure, fracture generation, and the movement of fluids in the Uinta basin, Utah: AAPG Bulletin, v. 78, p. 1729-1747.

Bryant, B., 1990, Geologic map of he Salt Lake City 30' x 60' quadrangle, north-central Utah, and Uinta County, Wyoming: U.S. Geological Survey Miscellaneous Investigations Map I-1944, 1:100,000

Budai, B. M., A. M. Martini, L. M. Walter, and T. C. W. Ku, 2002, Fracture-filling calcite in the Antrim Shale: Applications foe the regional and temporal recognition of microbial methane: Geofluids, v. 2, p. 163-183.

Burruss, R. C., 1993, Stability and flux of methane in the deep crust - a review, *in* D. G. Howell, ed., The Future of Energy Gases: U.S. Geological Survey Professional Paper 1570, p. 21-29.

Burtner, R. L., and M. A. Warner, 1984, Hydrocarbon generation in Lower Cretaceous Mowry and Skull Creek Shales of the northern Rocky Mountain area, *in* J. Woodward, F. F. Meissner, and J. L. Clayton, eds., Hydrocarbon Source Rocks of the Greater Rocky

Mountain Region: Denver, Rocky Mountain Association of Geologists, p. 449-468.

Capuano, R. M., 1993, Evidence of fluid flow in microfractures in geopressured shales: AAPG Bulletin, v. 77, p. 1303-1314.

Carroll, A. R., and K. M. Bohacs, 2001, Lake-type controls on petroleum source rock potential in nonmarine basins: AAPG Bulletin, v. 85, p. 1033-1053.

Castle, J. W., 1990, Sedimentation in Eocene Lake Uinta (lower Green River Formation), northeastern Uinta basin, Utah, *in* B. J. Katz, ed., Lacustrine Basin Exploration - Case Studies and Modern Analogs: AAPG Memoir 50: Tulsa, AAPG, p. 243-263.

Chan, M.A., S.L. Newman, and F.E. May, 1991, Deltaic and shelf deposits in the Cretaceous Blackhawk Formation and Mancos Shale, Grand County, Utah: Utah Geological Survey Miscellaneous Publication 91-6, 83 p.

Cheney, T. M., and R. P. Sheldon, 1959, Permian stratigraphy and oil potential, Wyoming and Utah, *in* N. C. Williams, ed., Tenth Annual Field Conference, Intermountain Association of Petroleum Geologists, p. 90-100.

Claypool, G. E., A. H. Love, and E. K. Maughan, 1978, Organic geochemistry, incipient metamorphism, oil generation in black shale members of Phosphoria Formation, western interior United States: AAPG Bulletin, v. 62, p. 98-120.

Cluff, R. M., 1993, Source rocks and hydrocarbon generation in the New Albany Shale (Devonian-Mississippian) of the Illinois basin, *in* J. B. Roen, and R. C. Kepferle, eds., Petroleum Geology of the Devonian and Mississippian Black Shale of Eastern North America: U.S. Geological Survey Bulletin 1909, p. I1-I15.

Cole, R. D., and R. G. Young, 1991, Facies characterization and architecture of a muddy shelf-sandstone complex: Mancos B interval of the Mancos Shale, northwest Colorado - northeast Utah, *in* A. D. Miall, and N. Tyler, eds., The Three-dimentional Facies Architecture of Terrigeneous Clastic Sediments and its Implications for Hydrocarbon Discovery and Recovery: SEPM Concepts in Sedimentology and Paleontology, v. 3, p. 277-286.

Cole, R.D., R.G. Young, and G.C. Willis, 1997, The Prairie Canyon Member, a new unit of the Upper Cretaceous Mancos Shale, west-central Colorado and east-central Utah: Utah Geological Survey Miscellaneous Publication 97-4, 23 p.

Cosgrove, J.W., 2001, Hydraulic fracturing during the formation and deformation of a basin: a factor in the dewatering of low-permeability sediments: AAPG Bulletin, v. 85, p. 737-748.

Curtis, J.B., 2002, Fractured shale-gas systems: AAPG Bulletin, v. 86, p. 1921-1938.

Dane, C. H., W. A. Cobban, and E. G. Kauffman, 1966, Stratigraphy and regional relationships of a reference section for the Juana Lopez Member, Mancos Shale, in the San Juan Basin, New Mexico: U.S. Geological Survey Bulletin 1224-H, 15 p.

de Witt, W., Jr., J. B. Roen, and L. G. Wallace, 1993, Stratigraphy of Devonian black shales and associated rocks in the Appalachian basin, *in* J. B. Roen, and R. C. Kepferle, eds., Petroleum Geology of the Devonian and Mississippian Black Shale of Eastern North America: U.S. Geological Survey Bulletin 1909, p. B1-B47.

Dean, W. E., and M. A. Arthur, 1998, Cretaceous Western Interior Seaway Drilling Project: an overview, *in* W. E. Dean, and M. A. Arthur, eds., Stratigraphy and Paleoenvironments of the Cretaceous Western Interior Seaway, USA:. SEPM Concepts in Sedimentology and Paleontology No. 6, p. 1-10.

Doelling, H. H., 1968, Carcass Canyon coal area, Kaiparowits Plateau, Garfield and Kane

Counties, Utah: Utah Geological and Mineralogical Survey Special Studies 25, 23 p.
Doelling, H.H., 1988 , Geology of Salt Valley anticline and Arches National Park, Grand County, Utah, in Salt Deformation in the Paradox Region, Utah: Utah Geological and Mineral Survey Bulletin 122, p 1-58.
Doelling, H. H., and R. L. Graham, 1972, Southwestern Utah coal fields: Alton, Kaparowitz Plateau and Kolob-Harmony: Utah Geological and Mineralogical Survey Monograph Series No. 1, 533 p.
Dube, H. G., G.E. Christiansen, J.H. Frantz, Jr., and N.R. Fairchild, Jr., 2000, The Lewis Shale, San Juan Basin: What we know now: SPE Paper 63091, 24 p.
Durand, B., 1988, Understanding of HC migration in sedimentary basins (present state of knowledge): Organic Geochemistry, v. 13, p. 445-459.
Eckels, M. T., D. H. Suck, and P. J. Harrison, 2005, New, oild plays in southern Uinta basin get fresh look with 3D seismic technology: Oil & Gas Journal, v. 103, p. 32-40.
England, W. A., A. S. Mackenzie, D. M. Mann, and T. M. Quigley, 1987, The movement and entrapment of petroleum fluids in the subsurface: Journal of the Geological Society of London, v. 144, p. 327-347.
Epstein, A.G., J.B. Epstein, and L.D. Harris, 1977, Conodont color alteration - an index to organic metamorphism: U.S. Geological Survey Professional Paper 995, 27 p.
Fetzner, R. W., 1960, Pennsylvanian paleotectonics of Colorado Plateau: AAPG Bulletin, v. 44, p. 1371-1413.
Fisher, M. K., C. A. Wright, B. A. Davidson, A. K. Goodwin, E. O. Fielder, W. S. Buckler, and N. P. Steinsberger, 2002, Integrating fracture mapping technologies to optimize stimulations in the Barnett Shale: SPE Paper 77441, Annual Technical Conference and Exhibition, San Antonio, Texas, p. 1-7.
Fletcher, S., 2005, Unconventional gas vital to US supply: Oil & Gas Journal, v. 103, no. 8, p. 20-25.
Fouch, T. D., 1975, Lithofacies and related hydrocarbon accumulations in Tertiary strata of the western and central Uinta Basin, Utah, *in* D. W. Bolyard, ed., Deep Drilling Frontiers of he Central Rocky Mountains: Denver, Rocky Mountain Association of Geologists, p. 163-174.
Fouch, T. D., V. F. Nuccio, D. E. Anders, D. D. Rice, J. K. Pitman, and R. F. Mast, 1994, Green River (!) petroleum system, Uinta basin, Utah, U.S.A., *in* L. B. Magoon, and W. G. Dow, eds., The Petroleum System - From Source to Trap: AAPG Memoir 60, p. 399-421.
Foutz, D. R., 1966, Stratigraphy of the Mississippian system in northeastern Utah and adjacent states: PhD thesis, Washington State University, 107 p.
Frantz, J. H., Jr., J. N.R. Fairchild, H. G. Dube, S. M. Campbell, G. E. Christiansen, and A. J. Olszewski, 1999, Evaluating reservoir production mechanisms and hydralic fracture geometry in the Lewis Shale, San Juan Basin, p. 8.
Gautier, D.L., 1983, Chapter 8: Marine shales, in D.D. Rice and D.L. Gautier, eds., Patterns of Sedimentation, Diagenesis, and Hydrocarbon Accumulations in Cretaceous Rocks of the Rocky Mountains: SEPM Short Course Notes No. 11, 41 p.
Gloyn, R. W., D. E. Tabet, B. T. Tripp, C. E. Bishop, C. D. Morgan, J. W. Gwynn, and R. E. Blackett, 2003, Energy, Mineral, and Ground-water Resources of Carbon and Emery Counties, Utah: Utah Geological Survey Bulletin 132, 161 p.
Gualtieri, J.L., 1988, Geologic map of the Westwater 30' x 60' quadrangle, Grand and Uintah Counties, Utah and Garfield and Mesa Counties, Colorado: U.S. Geological Survey

Miscellaneous Investigations Map I-1765, 1:100,000.
Hampson, G. J., J. A. Howell, and S. S. Flint, 1999, A sedimentological and sequence stratigraphic re-interpretation of the upper Cretaceous Prairie Canyon Member ("Mancos B") and associated strata, Book Cliffs area, Utah, USA: Journal of Sedimentary Research, v. 69, p. 414-433.
Hasenmueller, R., 1993, New Albany Shale (Devonian and Mississippian) of the Illinois basin, *in* J. B. Roen, and R. C. Kepferle, eds., Petroleum Geology of the Devonian and Mississippian Black Shale of Eastern North America: U.S. Geological Survey Bulletin 1909, p. C1-C19.
Hein, J. R., 2004, Evolution of thought concerning the origin of the Phosphoria Formation, Western US Phosphate Field, *in* J. R. Hein, ed., Life Cycle of the Phosphoria Formation: From Deposition to the Post-Mining Environment, v. 8: Amsterdam, Elsevier, p. 19-42.
Hendrix, M. S., and C. W. Byers, 2000, Stratigraphy and sedimentology of Permian strata, Uinta Mountains: allostratigraphic controls on the accumulation of economic phosphate, *in* C. R. Glenn, ed., Marine authigenesis from global to microbial: Society of Economic Petrologists and Mineralogists Special Publication No. 66, p. 349-367.
Hill, D. G., and C. R. Nelson, 2000, Gas productive fractured shales - an overview and update: GasTIPS, v. 6, p. 4-13.
Hite, R.J., 1968, Salt deposits of the Paradox basin, southeast Utah and southwest Colorado, in Saline Deposits: Geological Society of America Special Paper 68, p. 319-330.
Hite, R. J., D. E. Anders, and T. G. Ging, 1984, Organic-rich source rocks of Pennsylvanian age in the Paradox basin of Utah and Colorado, *in* J. Woodward, F. F. Meissner, and J. L. Clayton, eds., Hydrocarbon Source Rocks of the Greater Rocky Mountain Region: Rocky Mountain Association of Geologists Guidebook, p. 255-274.
Hook, S. C., and W. A. Cobban, 1980, Reinterpretation of type section of Juana Lopez Member of Mancos Shale: New Mexico Geology, v. 2, p. 17-22.
Hunt, J. M., 1979, Petroleum Geochemistry and Geology: San Francisco, W.H. Freeman, 617 p.
Huntoon, P.W., 1968, Late Cenozoic gravity tectonic deformation related to the Paradox salts in the Canyonlands area of Utah, in Salt Deformation in the Paradox Region, Utah: Utah Geological and Mineral Survey Bulletin 122, p 79-93.
Isaacson, A., 2003, The structure of Utah's natural gas industry: Utah Economic and Business Review, v. 63, p. 1-15.
Jarvie, D. M., and B. L. Claxton, 2002, Barnett Shale oil and gas as an analog for other black shales: extended abstract, AAPG Midcontinent meeting, New Mexico, 2 p.
Jennings, G. L., K. H. Greaves, and S. R. Bereskin, 1997, Natural gas resource potential of the Lewis Shale, San Juan Basin, New Mexico and Colorado: SPE Paper 9766, 8 p.
Johnson, E.A., 2003, Geologic assessment of the Phosphoria Total Petroleum System, Uinta-Piceance Province, Utah and Colorado, Petroleum Systems and Geologic Assessment of Oil and Gas in the Uinta-Piceance Province, Utah and Colorado: U.S. Geological Survey Digital Data Series DDS-69-B, Chapter 9, 42 p.
Johnson, E.A., 2005, Geologic assessment of undiscovered oil and gas resources in the Phosphoria Total Petroleum System, southwestern Wyoming province, Wyoming, Colorado, and Utah: U.S. Geological Survey Digital Data Series 69-D, Chapter 4, 46 p.
Johnson, S. Y., M. A. Chan, and E. A. Konopka, 1992, Pennsylvanian and early Permian paleogeography of the Uinta-Piceance basin region, northwestern Colorado and northeastern Utah: U.S. Geological Survey Bulletin 1787-CC, 35 p.

Johnson, S. Y., 1992, Phanerozoic evolution of sedimentary basins in the Uinta-Piceance basin region, northwestern Colorado and northeastern Utah: U.S. Geological Survey 1787-FF, 38 p.

Johnson, E. A., 2003, Geologic assessment of the Phosphoria Total Petroleum System, Uinta-Piceance Province, Utah and Colorado, Petroleum Systems and Geologic Assessment of Oil and Gas in the Uinta-Piceance Province, Utah and Colorado: U.S. Geological Survey Digital Data Series DDS-69-B, Chapter 9, p. 42.

Johnson, D., 2004a, Technology advances expand potential pay. Barnett Shale - 1: Oil & Gas Journal, v. 102, p. 51-59.

Johnson, D., 2004b, Reservoir characterization improves stimulation, completion practices. Barnett Shale - 2: Oil & Gas Journal, v. 102, p. 60-63.

Katz, B. J., 1995, The Green River Shale: an Eocene carbonate lacustrine source rock, *in* B. J. Katz, ed., Petroleum Source Rocks: p. 309-324.

Kellogg, H. E., 1977, Geology and petroleum of the Mancos B Formation, Douglas Creek arch area, Colorado and Utah, *in* H. K. Veal, ed., Exploration Frontiers of the central and southern Rockies: Denver, Rocky Mountain Association of Geologists, p. 167-179.

Kepferle, R. C., 1993, A depositional model and basin analysis for the gas-bearing black shale (Devonian and Mississippian) in the Appalachian basin, *in* J. B. Roen, and R. C. Kepferle, eds., Petroleum Geology of the Devonian and Mississippian Black Shale of Eastern North America: U.S. Geological Survey Bulletin 1909, p. F1-F23.

Kirschbaum, M. A., 2003, Geologic assessment of undiscovered oil and gas resources of the Mancos/Mowry Total Petroleum System, Uinta-Piceance Province, Utah and Colorado, *in* Petroleum Systems and Geologic Assessment of Oil and Gas in the Uinta-Piceance Province, Utah and Colorado: U.S. Geological Survey Digital Data Series DDS-69-B, Chapter 6, 29 p.

Kirschbaum, M. A., and L.N.R. Roberts, 2005, Geologic assessment of undiscovered oil and gas resources in the Mowry Composite Total Petroleum System, Southwestern Wyoming Province, Wyoming, Colorado, and Utah *in* Petroleum Systems and Geologic Assessment of Oil and Gas in the Southwestern Wyoming Province, Wyoming, Colorado, and Utah: U.S. Geological Survey Digital Data Series 69-D, Chapter 5, 22 p.

Kuuskraa, V. A., G. Koperna, J. W. Schmoker, and J. C. Quinn, 1998, Barnett shale rising star in Fort Worth basin, Oil & Gas Journal, p. 67-76.

Lammerson, P.R.., 1982, The Fossil Basin area and its relationship to the Absaroka thrust fault system, *in* R.B. Powers, ed., Geologic Studies of the Cordilleran Thrust Belt: Rocky Mountain Association of Geologists, p. 279-340.

Law, B. E., and C. W. Spencer, 1993, Gas in tight reservoirs - an emerging major source of energy, *in* D. G. Howell, ed., The Future of Energy Gases: U.S. Geological Survey Professional Paper 1570, p. 233-252.

Lawrence, J. C., 1965, Stratigraphy of the Dakota and Tropic Formations of Cretaceous age in southern Utah, *in* H. D. Goode, and R. A. Robinson, eds., Guidebook to the Geology of Utah, v. 19: Salt Lake City, UT, Utah Geological and Mineralogical Survey, p. 71-91.

Lee, Y., and D. Deming, 2002, Overpressures in the Anadarko basin, southwestern Oklahoma: Static or dynamic?: AAPG Bulletin, v. 86, p. 145-160.

Leithold, E. L., and W. E. Dean, 1998, Depositional processes and carbon burial on a Turonian prodelta at the margin of the Western Interior Seaway, *in* W. E. Dean, and M. A. Arthur, eds., Stratigraphy and Paleoenvironments of the Cretaceous Western Interior Seaway,

USA: SEPM Concepts in Sedimentology and Paleontology No. 6, p. 189-200.
Lewan, M. D., and A. A. Henry, 2001, Gas:oil ratios for source rocks containing type-I, -II, -IIS, and -III kerogens as determined by hydrous pyrolysis, *in* T. S. Dyman, and V. A. Kuuskraa, eds., Geologic Studies of Deep Natural Gas Resources, v. U.S. Geological Survey Digital Data Series 67, p. E1-E9.
Lewan, M. D., 2002, Fundamental issues on thermogenic gas generation from source-rock maturation and reservoir-oil cracking, *in* B. E. Law, and M. Wilson, eds., Innovative Gas Exploration Concepts Symposium: Denver, CO, Rocky Mountain Association of Geologists, 4. p.
Mackenzie, A. S., and T. M. Quigley, 1988, Principles of geochemical prospect appraisal: AAPG Bulletin, v. 72, p. 399-415.
Mann, U., 1994, An integrated approach to the study of primary petroleum migration, *in* J. Parnell, ed., Geofluids: Origin, migration and evolution of fluids in sedimentary basins: Geological Society Special Publication no. 78: London, The Geological Society, p. 233-260.
Martini, A. M., J. M. Budai, L. M. Walter, and M.Schoell, 1996, Microbial generation of economic accumulation of methane within a shallow organic-rich shale: Nature, v. 383, p. 155-158.
Martini, A. M., L. M. Walter, J. M. Budai, T. C. W. Ku, C. J. Kaiser, and M. Schoell, 1998, Genetic and temporal relations between formation waters and biogenic mathane: Upper Devonian Antrium Shale, Michigan basin, USA: Geochemica et Cosmochemica Acta, v. 62, p. 1699-1720.
Martini, A. M., L. M. Walter, T. C. W. Ku, J. M. Budai, J. C. McIntosh, and M. Schoell, 2003, Microbial production and modification of gases in sedimentary basins: A geochemical case study from a Devonian shale gas play, Michigan basin: AAPG Bulletin, v. 87, p. 1355-1375.
Mattavelli, L., and L. Novelli, 1988, Geochemistry and habitat of natural gases in Italy: Organic Geochemistry, v. 13, p. 1-13.
Matthews, R. D., 1993, Review and revision of the Devonian-Mississippian stratigraphy in the Michigan basin, *in* J. B. Roen, and R. C. Kepferle, eds., Petroleum Geology of the Devonian and Mississippian Black Shale of Eastern North America: U.S. Geological Survey Bulletin 1909, p. D1-D41.
Maughan, E. K., 1979, Petroleum source rock evaluation of the Permian Park City Group in the northeasern Great Basin, Utah, Nevada, and Idaho, *in* G. W. Newman, and H. D. Goode, eds., 1979 Basin and Range Symposium: Denver, CO, Rocky Mountain Association of Geologists, p. 523-530.
Maughan, E. K., 1984, Geological setting and some geochemistry of petroleum source rocks in the Permian Phosphoria Formation, *in* J. Woodward, F. F. Meissner, and J. L. Clayton, eds., Hydrocarbon Source Rocks of the Greater Rocky Mountain Region: Denver, Rocky Mountain Association of Geologists, p. 281-294.
Mavor, M.J., S.R. Bereskin, J.R. Robinson, and T.J. Pratt, 2003, Lewis Shale Gas Resource and Production Potential: Gas Research Institute, GRI-03/0037.
McIntosh, J., L. M. Walter, and A. M. Martini, 2002, Pleistocene recharge to mid-continent basins: effects on salinity sturcture and microbial gas generation: Geochemica et Cosmochemica Acta, v. 66, p. 1681-1700.
Merewether, E. A., 1983, The Frontier Formation and mid-Cretaceous orogeny in the foreland of

southwestern Wyoming: The Mountain Geologist, v. 20, p. 121-138.
Merewether, E. A., and W. A. Cobban, 1986, Biostratigraphic units and tectonism in the mid-Cretaceous foreland of Wyoming,Colorado and sdjacent areas, *in* J. A. Peterson, ed., Paleotectonics and sedimentation in the Rocky Mountain region, United States, Part III, Middle Rocky Mountains: AAPG Memoir 41, p. 443-467.
Milici, R. C., 1993, Autogenic gas (self sourced) from shales - an example from the Appalachian basin, *in* D. G. Howell, ed., The Future of Energy Gases: U.S. Geological Survey Professional Paper 1570, p. 253-278.
Milici, R. C., and R. T. Ryder, 2004, Petroleum systems succeed play basis in Appalachian basin resource estimate: Oil & Gas Journal, v. 102, p. 40-43.
Miller, E.L., M.M. Miller, C.H. Stevens, J.E. Wright, and R. Madrid, 1992, Late Paleozoic paleogeographic and tectonic evolution of the western U.S. Cordillera, in B.C. Burchfiel, P.W. Lipman, and M.L. Zoback, eds., The Cordilleran Orogen: Conterminous U.S.: The Geological Society of America, The Geology of North America, v. G-3, p. 57-106.
Molenaar, C. M., 1983, Major depositional cycles and regional correlations of Upper Cretaceous rocks, southern Colorado Plateau and adjacent areas, *in* M. W. Reynolds, and E. D. Dolly, eds., Mesozoic Paleogeography of West-central United States: Denver, CO, Rocky Mountain Section-SEPM, p. 201-223.
Molenaar, C. M., and B. W. Wilson, 1990, The Frontier Fromation and associated rocks of northeastern Utah and northwestern Colorado: U.S. Geological Survey Bulletin 1787-M, 21 p.
Molenaar, C. M., and W. A. Cobban, 1991, Middle Cretaceous stratigraphy on the south and east sides of the Uinta basin, northeastern Utah and northwestern Colorado: U.S. Geological Survey Bulletin 1787-P, 34 p.
Montgomery, S., 1992, Paradox basin: Cane Creek play: Petroleum Frontiers, v. 9, 66 p.
Montgomery, S. L., D. M. Jarvie, K. A. Bowker, and R. M. Pollastro, 2005, Mississippian Barnett Shale, Fort Worth basin, north-central Texas: Gas-shale play with multi-trillion cubic foot potential: AAPG Bulletin, v. 89, p. 155-175.
Morgan, C. D., 1992, Horizontal drilling potential of the Cane Creek Shale, Paradox Formation, Utah, *in* J. W. Schmoker, E. B. Coalson, and C. A. Brown, eds., Geological Studies Relevant to Horizontal Drilling: Examples from Western North America: Denver, CO, Rocky Mountain Association of Geologists, p. 257-265.
Morgan, C. D., 2003, The Bluebell Oil Field, Unita Basin, Duchesne and Uintah Counties, Utah: Characterization and Oil Well Demonstration: Utah Geological Survey Special Study 106, 95 p.
Nelson, P. H., 2002, Subsurface fluid pressures from drill-stem tests, Uinta basin, Utah: The Mountain Geologist, v. 39, p. 17-26.
Nichols, K. M., and N. J. Silberling, 1991, Petrology and significance of a Mississippian (Osagean-Meramecian) anoxic event, Lakeside Mountains, Utah: U.S. Geological Survey Bulletin 1787-T, 12 p.
Noe, D.C., 1993, PC-3. Mancos marine sandstones, *in* C.A. Hjellming, ed., Atlas of Major Rocky Mountain Gas Reservoirs: New Mexico Bureau of Mines & Mineral Resources, p. 99-100.
Nuccio, V.F., J.W. Schmoker, and T.D. Fouch, 1992, Thermal maturity, porosity, and lithofacies relationships applied to gas generation and production in Cretaceous and Tertiary low-permeability (tight) sandstone, Uintas basin, Utah, *in* T.D. Fouch, V.F. Nuccio, and T.C.

Chidsey, Jr., eds., Hydrocarbon and Mineral Resources of the Uinta Basin, Utah and Colorado: Utah Geological Association Guidebook 20, p. 77-93.

Nuccio, V. F., and S. M. Condon, 1996a, Burial and thermal history of the Paradox basin, Utah and Colorado, and petroleum potential of the Middle Pennsylvanian Paradox Formation: U.S. Geological Survey Bulletin 2000-O, 41 p.

Nuccio, V. F., and S. M. Condon, 1996b, Burial and thermal history of the Paradox basin, Utah and Colorado, and petroleum potential of the Middle Pennsylvanian Paradox Formation, *in* A. C. Huffman, Jr., W. R. Lund, and L. H. Godwin, eds., Geology and Resources of the Paradox Basin: Utah Geological Association Guidebook 25, p. 57-76.

Nummendal, D., and C.M. Molenaar, 1995, Sequence stratigraphy of ramp-setting strand plain successions: The Gallup Sandstone, New Mexico, in J.C. Van Wagoner and G.T. Bertram, eds., Sequence Stratigraphy of Foreland Basin Deposits: AAPG Memoir 64, p. 277-310.

Osborne, M. J., and R. E. Swarbrick, 1997, Mechanisms for generating overpressure in sedimentary basins: a reevaluation: AAPG Bulletin, v. 81, p. 1023-1041.

Pachen, D. G., and M. E. Hohn, 1993, Production and production controls in Devonian shales, West Virginia, *in* J. B. Roen, and R. C. Kepferle, eds., Petroleum Geology of the Devonian and Mississippian Black Shale of Eastern North America: U.S. Geological Survey Bulletin 1909, p. F1-F23.

Pepper, A. S., 1991, Estimating the petroleum expulsion behavior of source rocks: a novel quantitative approach, *in* W. A. England, and A. J. Fleet, eds., Petroleum Migration, v. Special Publication No. 59: London, Geological Society, p. 9-31.

Pepper, A. S., and P. J. Corvi, 1995, Simple kinetic models of petroleum formation. Part 1: oil and gas generation from kerogen: Marine and Petroleum Geology, v. 12, p. 291-319.

Pepper, A. S., and T. A. Dodd, 1995, Simple kinetic models of petroleum formation. Part II: oil-gas cracking: Marine and Petroleum Geology, v. 12, p. 321-340.

Petzet, A., 2002, Devon pressing Barnett shale exploitation, expanding search: Oil & Gas Journal, v. 100, no. 28, p. 18-20.

Petzet, A., 2005, Resource plays, CBM to fuel drilling upturns in US, Canada: Oil & Gas Journal, v. 103, p. 32-34.

Pollastro, R. M., R. J. Hill, D. M. Jarvie, and M. E. Henry, 2003, Assessing undiscovered resources of the Barnett-Paleozoic total petroleum system, Bend Arch-Fort Worth basin province, Texas: AAPG Southwest Section meeting, Forth Worth, Texas.

Poole, F. G., and G. E. Claypool, 1984, Petroleum source-rock potential and crude-oil correlation in the Great Basin, *in* J. Woodward, F. F. Meissner, and J. L. Clayton, eds., Hydrocarbon Source Rocks of the Greater Rocky Mountain Region: Denver, Rocky Mountain Association of Geologists, p. 179-229.

Quigley, T. M., and A. S. Mackenzie, 1988, The temperatures of oil and gas formation in the subsurface: Nature, v. 333, p. 549-552.

Rach, N. M., 2004, Drilling expands in Texas' largest gas field: Oil & Gas Journal, v. 102, p. 45-50.

Reeside, J. B., Jr., and W. A. Cobban, 1960, Studies of the Mowry Shale (Cretaceous) and contemporary formations in the United States and Canada: U.S. Geological Survey Professional Paper 355, p. 126.

Remy, R. R., 1992, Stratigraphy of the Eocene part of the Green River Formation in the south-central part of the Uinta basin, Utah: U.S. Geological Survey Bulletin 1787-BB, 79 p.

Rice, D. D., T. D. Fouch, and R. C. Johnson, 1992, Influence of source-rock type, thermal maturity, and migration on composition and distribution of natural gases, Uinta basin, Utah, *in* T. D. Fouch, V. F. Nuccio, and T. C. Chidsey, eds., Hydrocarbon and mineral resources of the Uinta basin, Utah and Colorado: Utah Geological Association Guidebook 20, p. 95-109.

Rice, D. D., 1993, Biogenic gas: Controls, habitats, and resource potential, *in* D. G. Howell, ed., The Future of Energy Gases: U.S. Geological Survey Professional Paper 1570, p. 583-606.

Rigby, J. K., and D. L. Clark, 1962, Devonian and Mississippian Systems in central Utah, Brigham Young University Geology Studies, v. 9, part 1, p. 17-25.

Roberts, L. N. R., and M. A. Kirschbaum, 1995, Paleogeography of the Late Cretaceous of the Western Interior of middle North America - coal distribution and sediment accumulation: U.S. Geological Survey Professional Paper 1561, 115 p.

Roen, J. B., 1984, Geology of Devonian black shales of the Appalachian basin: Organic Chemistry, v. 5, p. 241-254.

Ross, C. A., and J. R. P. Ross, 1985, Late Paleozoic depositional sequences are synchronous and worldwide: Geology, v. 13, p. 194-197.

Ruble, T. E., A. J. Bakel, and R. P. Philp, 1994, Compound-specific isotopic variability in Uinta Basin native bitumens: paleoenvironmental implications: Organic Chemistry, v. 21, p. 661-671.

Ruble, T. E., and R. P. Philp, 1998, Stratigraphy, depositional environments and organic geochemistry of source-rocks in the Green River petroleum system, Uinta basin, Utah, *in* J. K. Pitman, and A. R. Carroll, eds., Modern and Ancient Lake Systems - New Problems and Perspectives: Utah Geological Association Guidebook 26, p. 289-328.

Ruble, T. E., M. D. Lewan, and R. P. Philp, 2001, New insights on the Green River petroleum system in the Uinta basin from hydrous pyrolysis experiments: AAPG Bulletin, v. 85, p. 1333-1371.

Rueger, B. F., 1996, Palynology and its relationship to climatically induced depositional cycles in the Middle Pennsylvanian (Desmoinesian) Paradox Formation of southeastern Utah: U.S. Geological Survey Bulletin 2000-K, U.S. Geological Survey, 22 p.

Ryder, R. T., T. D. Fouch, and J. H. Elison, 1976, Early Tertiary sedimentation in the western Uinta Basin, Utah: Geological Society of America Bulletin, v. 87, p. 496-512.

Ryder, R. T., R. C. Burruss, and J. R. Hatch, 1998, Black shale source rocks and oil generation in the Cambrian and Ordovician of the central Appalachian basin, USA: AAPG Bulletin, v. 82, p. 412-441.

Ryer, T. A., 1976, Cretaceous stratigraphy of the Coalville and Rockport areas, Utah: Utah Geology, v. 3, p. 71-83.

Ryer, T. A., 1977, Patterns of Cretaceous shallow-marine sedimentation, Coalville and Rockport areas, Utah: Geological Society of America Bulletin, v. 88, p. 177-188.

Ryer, T. A., and M. McPhillips, 1983, Early Late Cretaceous paleogeography of east-central Utah, *in* M. W. Reynolds, and E. D. Dolly, eds., Mesozoic Paleogeography of West-central United States: Denver, CO, Rocky Mountain Section-SEPM, p. 253-272.

Ryer, T. A., 1984, Transgressive-regressive cycles and the occurrence of coal in some Upper Cretaceous strata of Utah, U.S.A., *in* R. A. Rahmani, and R. M. Flores, eds., Sedimentology of Coal and Coal-bearing Sequences: Oxford, Blackwell Scientific, International Association of Sedimentologists Special Publication 77:, p. 217-227.

Sandberg, C. A., D. R. Grogan, and T. J. Clisham, 1979, Mississippian source rocks in Utah and Idaho: U.S. Geological Survey Professional Paper 1150, p. 28-29.

Sandberg, C. A., R. C. Gutschick, J. G. Johnson, F. G. Poole, and W. J. Sando, 1982, Middle Devonian to Late Mississippian geologic history of the overthrust belt region, western United States, *in* R. B. Powers, ed., Geologic Studies of the Cordilleran Thrust Belt, v. 2: Denver, CO, Rocky Mountain Association of Geologists, p. 691-719.

Sandberg, C. A., and R. C. Gutschick, 1984, Distribution, microfauna, and source-rock potential of Mississippian Delle Phosphatic Member of Woodman Formation and equivalents, Utah and adjacent states, *in* J. Woodward, F. F. Meissner, and J. L. Clayton, eds., Hydrocarbon Source Rocks of the Greater Rocky Mountain Region: Denver, Rocky Mountain Association of Geologists, p. 135-178.

Schamel, S., V.M. Pilifossov, and E.S. Votsalevsky, 1995, Geologic controls on style of salt piercements in the Pricaspian basin, Kazakhstan: contrasts with the Gulf of Mexico, *in* Salt, Sediment and Hydrocarbons: Gulf Coast Section SEPM, 16th Annual Research Conference, p. 253-255.

Schell, E. M., and K. P. Moore, 1970, Stratigraphic sections and chemical analysis of Phosphatic analyses of phosphatic rocks of Permian and Mississippian age in Weber County, Utah: U.S. Geological Survey Circular 635, 11 p.

Schenk, H. J., and B. Horsfield, 1998, Using natural maturation series to evaluate the utility of parallel reaction kinetics models: an investigation of Toarcian shales and Carboniferous coals, Germany: Organic Geochemistry, v. 29, p. 137-134.

Seewald, J. S., B. C. Benitez-Nelson, and J. K. Whelan, 1998, Laboratory and theoretical constraints on the generation and composition of natural gas: Geochemica et Cosmochimica Acta, v. 62, p. 1599-1617.

Schoell, M., 1980, The hydrogen and carbon isotopic composition of methane from natural gases of various origins: Geochemica et Cosmochemica Acta, v. 44, p. 649-661.

Shumaker, R. C., 1993, Structural parameters that affect Devonian shale gas production in West Virginia and eastern Kentucky, *in* J. B. Roen, and R. C. Kepferle, eds., Petroleum Geology of the Devonian and Mississippian Black Shale of Eastern North America: U.S. Geological Survey Bulletin 1909, p. K1-K38.

Sloss, L. L., 1988, Tectonic evolution of the craton in Phanerozoic time, *in* L. L. Sloss, ed., Sedimentary Cover - North American Craton: Boulder, CO, The Geological Society of America, The Geology of North America D-2 , p. 25-51.

Smith, D. L., and E. L. Miller, 1990, Late Paleozoic extension in the Great Basin, western United States: Geology, v. 18, p. 712-715.

Speed, R. C., and N. H. Sleep, 1982, Antler orogeny and foreland basin: a model: Geological Society of America Bulletin, v. 93, p. 815-828.

Spreng, W. C., 1979, Upper Devonian and Lower Mississippian strata on the flanks of the western Uinta Mountains, Utah: Bringham Young University Geology Studies, v. 26, part 2, p. 67-79.

Stone, D.S., 1977, Tectonic history of the Uncompahgre uplift, *in* H.K, Veal, ed., Exploration Frontiers of eht Central and Southern Rockies: Denver, CO, Rocky Mountain Association of Geologists, p. 23-30.

Sweeney, J. J., and A. K. Burnham, 1990, Evaluation of a simple model of vitrinite reflectance based on chemical kinetics: AAPG Bulletin, v. 74, p. 1559-1570.

Swetland, P. J., J. L. Clayton, and E. G. Sable, 1978, Petroleum source-bed potential of

Mississippian-Pennsylvanian rocks in parts of Montana, Idaho, Utah, and Colorado: Mountain Geologist, v. 14, p. 79-87.

Tabet, D.E., and J.C. Quick, 1999, Extension of the Hams Fork coal region, Summit County, Utah - Potential for coalbed gas, *in* L.E. Spangler and C.J. Allen, eds., Geology of Northern Utah and Vicinity: Utah Geological Association Publication 27, p. 257-266.

Ulmishek, G. F., and H. D. Klemme, 1990, Depositional controls, distribution, and effectiveness of world's petroleum source rocks: U.S. Geological Survey Bulletin 1931, 59 p.

Van Tyne, A. M., 1993, Detailed study of Devonian black shales encountered in nine wells in western New York State, *in* J. B. Roen, and R. C. Kepferle, eds., Petroleum Geology of the Devonian and Mississippian Black Shale of Eastern North America: U.S. Geological Survey Bulletin 1909, p. M1-M16.

Walter, L. M., J. C. McIntosh, J. M. Budai, and A. M. Martini, 2000, Hydrogeochemical controls on gas occurrence and production in the New Albany Shale: GasTIPS, v. 6, p. 14-20.

Wardlaw, B. R., J. W. Collinson, and E. K. Maughan, 1979, Stratigraphy of Park City Group equivalents (Permian) in southern Idaho, northeastern Nevada, and northwest Utah: U.S. Geological Survey Professional Paper 1163-C, 16 p.

Warner, M.A., 1982, Source and time of generation of hydrocarbons in the Fossil Basin, western Wyoming Thrust Belt, in R.B. Powers, ed., Geologic Studies of the Cordilleran Thrust Belt: Rocky Mountain Association of Geologists, p. 805-815.

Weise, K., and K. A. Kuenvolden, 1993, Introduction to microbial and thermal methane, *in* D. G. Howell, ed., The Future of Energy Gases: U.S. Geological Survey Professional Paper 1570, p. 13-20.

Weiss, M.P., I.J. Witkind, and W.B. Cashion, 1990, Geologic map of the Price 30' x 60' quadrangle, Carbon, Duchesne, Uintah, Utah, and Wasatch Counties, Utah: U.S. Geological Survey Miscellaneous Investigations Map I-1981, 1:100,000.

Welsh, J. E., and H. J. Bissell, 1979, The Mississippian and Pennsylvanian (Carboniferous) Systems in the United States -- Utah: U.S. Geological Survey Professional Paper 1110-Y, 8 p.

Whitaker, R. M., 1975, Upper Pennsylvanian and permian strata of northeast Utah and northwest Colorado, *in* D. W. Bolyard, ed., Deep Drilling Frontiers of he Central Rocky Mountains: Denver, CO, Rocky Mountain Association of Geologists, p. 75-85.

Whiticar, M. J., E. Faber, and M. Schoell, 1986, Biogenic methane formation in marine and freshwater environments: CO_2 reduction vs. acetate fermentation - isotopic evidence: Geochemica et Cosmochemica Acta, v. 50, p. 693-709.

Whiticar, M. J., 1994, Correlation of natural gases with their sources, *in* L. B. Magoon, and W. G. Dow, eds., The Petroleum System - From Source to Trap, v. AAPG Memoir 60: Tulsa, American Association of Petroleum Geologists, p. 261-283.

Wiggins, W. D., and P. M. Harris, 1994, Lithofacies, depositional cycles, and stratigraphy of the lower Green River Formation, southwestern Uinta Basin, Utah, Notes for SEPM Core Workshop: Lacustrine Source-Rock Depositional Environments,AAPG Annual Meeting, Denver, June 11, 1994: Tulsa, SEPM.

Witkind, I.J., 1988, Geologic map of the Huntington 30' x 60' quadrangle, Carbon, Emery, Grand, and Uintah Counties, Utah: U.S. Geological Survey Miscellaneous Investigations Map I-1764, 1:100,000.

Witkind, I.J., and M.P. Weiss, 1991, Geologic map of the Nephi 30' x 60' quadrangle, Carbon, Emery, Juab, Sanpete, Utah, and Wasatch Counties, Utah: U.S. Geological Survey

Miscellaneous Investigations Map I-1937, 1:100,000.
Zhao, H., 2004, Thermal maturation and physical properties of Barnett Shale in Forth Worth basin, north Texas: abstract, AAPG Annual Meeting, Dallas, Texas.

Appendix A: Database CD-ROM

List of folders holding data files gathered for the project.

Blue Gate Shale	RGU#1	Core photos	(.jpg)
		Log text	
		Geochem data	(.xls)
Hermosa Group		Paradox geochem wells	(.doc)
		Paradox geochem	(.xls)
Marsing 16		Core photos	(.jpg)
Prairie Canyon		Core photos	(.jpg)
		Por-perm	(.jpg, .xls)
		Outcrop photos	(.jpg)
Tropic Shale		Core photos	(.jpg)
		Escalante-Denmark	report files
		Escalante-Geochem	(.xls)
		Escalante-USGS	(.xls)
U.Paleozoic		Geochem	(.xls, .tif, .pdf)